SCIONIX

9

HARSHAW RADIATION DETECTORS

CONTENTS

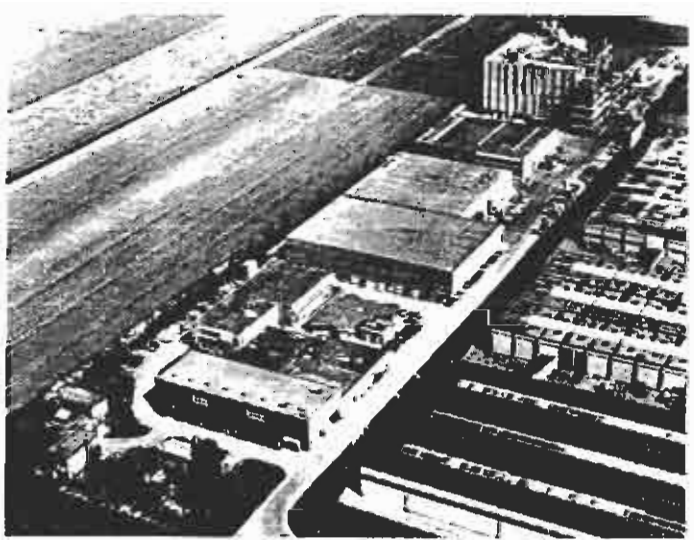

Harshaw Chemie B.V., De Meern, Holland.

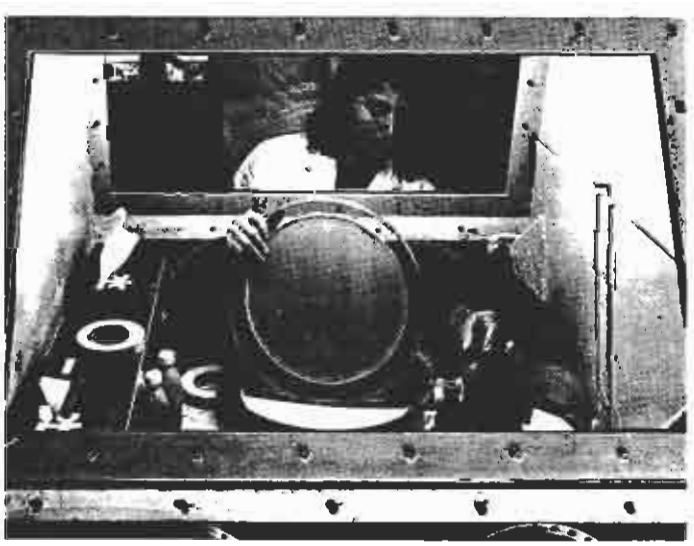

Processing a NaI(Tl) ingot suitable for Jumbo Gamma Camera's.

I. SCINTILLATION COUNTING PRINCIPLES

Contents:

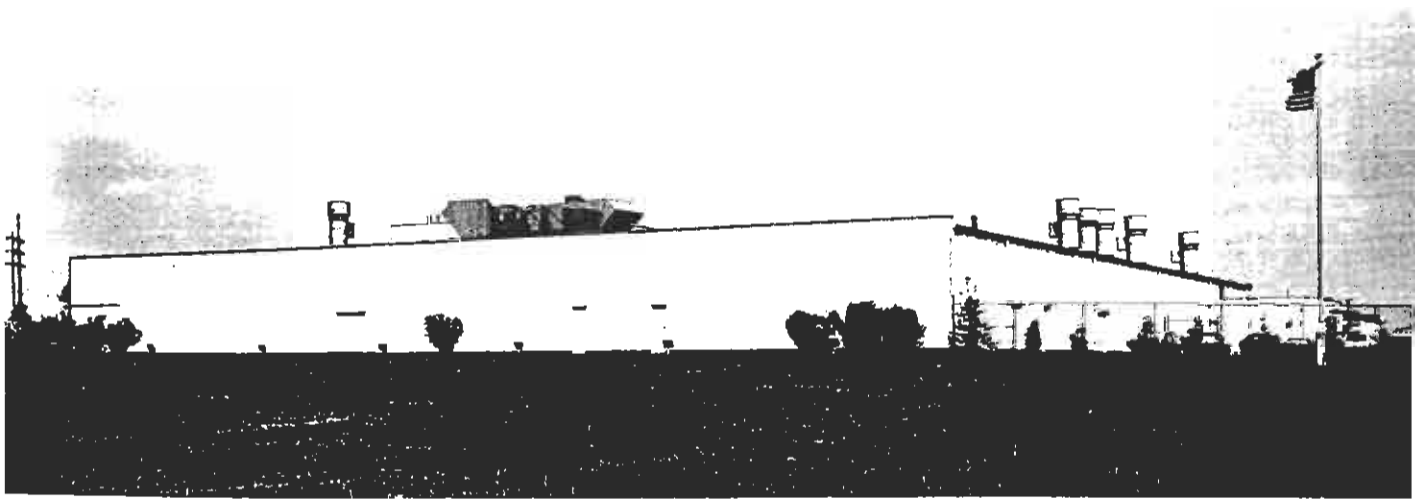

Harshaw/Filtrol Partnership facilities, Solon, Ohio, U.S.A.

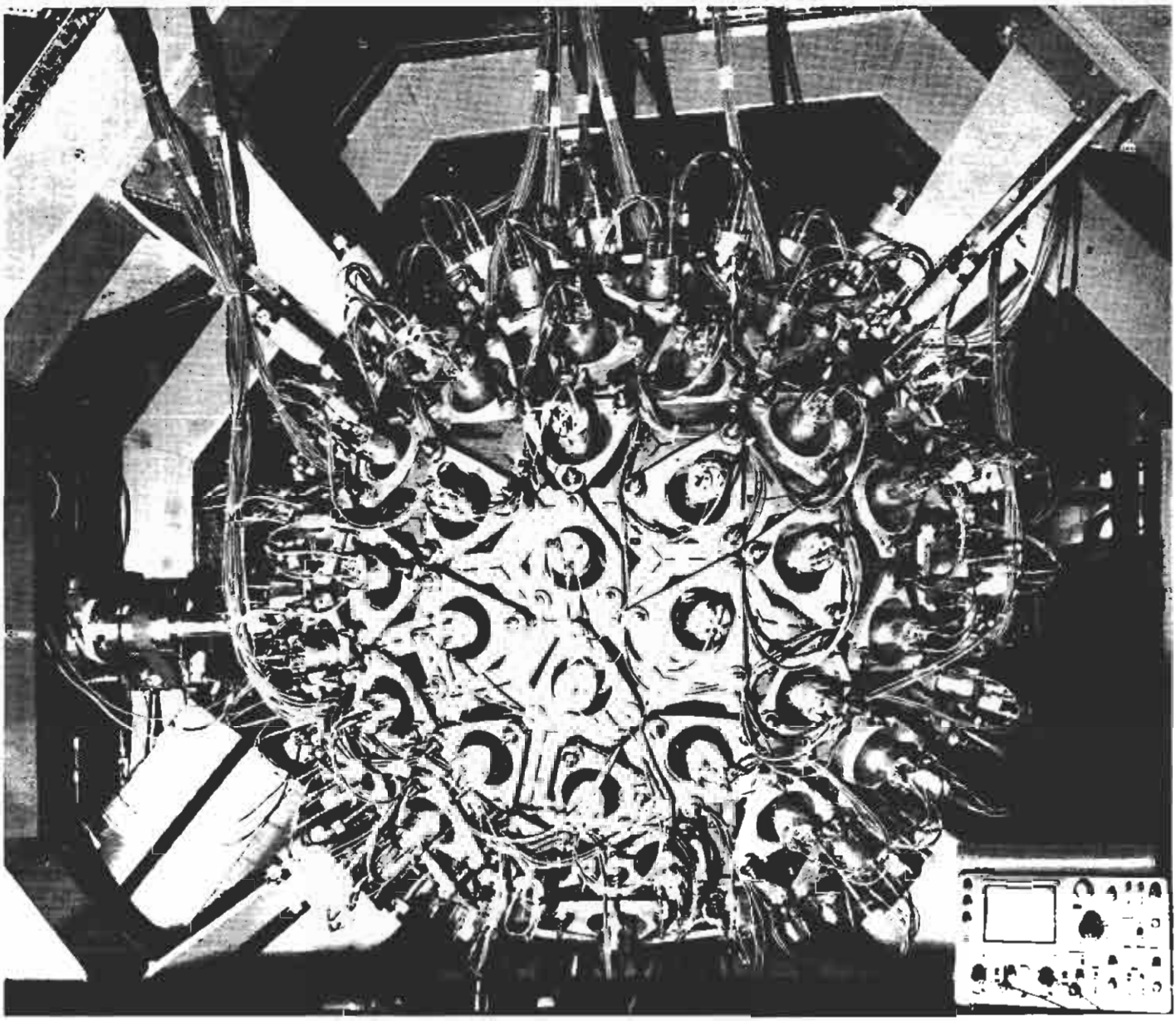

NaI(Tl) crystal ball at MPI Heidelberg, Germany. The ball has a diameter of 140 cm and consists of 162 pentagonal and hexagonal Polyscin Na(Tl) detectors.
(Photograph courtesy of MPI Heidelberg.)

I. SCINTILLATION COUNTING PRINCIPLES

A scintillation phosphor is a material able to convert energy lost by ionizing radiation into pulses of light. In most scintillation counting applications, the ionizing radiation of interest is in the form of X-rays, gamma rays and alpha or beta particles ranging from a few thousand electron volts to several million electron volts (from keV's to MeV's).

Pulses of light emitted during scintillation are detected by the sensitive photocathode of a photomultiplier tube. This current pulse is a result of the energy deposited in the crystal, and may be amplified and used to activate a scaler or rate-meter. It is for the latter application that scintillators are widely used as gamma ray and charged particle spectrometers.

1. Characteristics of various scintillation phosphors

A list of selected characteristics of a large number of inorganic scintillation phosphors is given in table I.1.

Some desirable characteristics of scintillators are:
- high density for greater gamma ray stopping power
- large pulse height for detection of low energy interactions
- short decay time for fast counting applications
- mechanical durability for fabrication purposes.

The primary advantages of the inorganic crystals are:
high gamma stopping power and high light output.
Of these materials, NaI(Tl) crystals are among the best available and are widely used for a variety of gamma counting applications.

For beta detection, plastic scintillators and gas filled counters are commonly employed. In some instances, inorganic crystals can be substituted where advantageous. CaF_2(Eu) in particular is an inorganic crystal that has replaced organic crystals in most beta counting applications. For high energy physics applications high Z materials such as BGO and barium fluoride are very suitable. The short radiation length of these crystals improves the lateral confinement of a shower.

Neutrons do not produce ionization directly in scintillation crystals, but can be detected through their interaction with the nuclei of the scintillator.

Neutrons interact with ^{6}Li nuclei to produce an alpha particle and a triton, which may in turn be detected by the scintillation they produce in LiI(Eu). LiI(Eu) and ^{6}LiI(Eu) are readily available inorganic crystals useful for neutron counting.

For timing applications a fast plastic scintillator is often used. Due to its extreme high light output, NaI(Tl) can also provide a good timing signal within a fraction of its decay time. Moreover its high absorption probability and its superior energy resolution dictates in many cases the use of a NaI(Tl) scintillator.

To follow fast changes in high intensity X-ray beams (like in CT scanners), Harshaw/Filtrol has developed crystals exhibiting extremely low afterglow. This afterglow is defined as the fraction of scintillation light still present 3 ms after the Röntgen interaction takes place. Bismuth germanate and cadmium tungstate are specially suited for these applications.

2. Photomultiplier tubes and photodiodes

The energy resolution and stability of a scintillation detector depends to a great extent upon the photomultiplier tube. The selection of a proper type is fundamental to good detector design.

Venetian blind, linear circular cage teacup and box-and-grid type dynode structures are widely used for scintillation counting. Typical venetian blind tubes are available with 12 and 14 stage dynode construction, allowing high gain. Although these tubes are noted for relatively slow response, they are well suited for use with NaI(Tl) crystals in most applications. The stability of venetian blind tubes is the result of their lower sensitivity to magnetic fields and inter-dynode voltage variations than in other tube types. Linear structures are noted for high gain and fast response, making them ideally suited for fast timing applications. Circular cage tubes are the least expensive structures and will perform satisfactorily in most applications. The gain of these tubes is limited by 10-stage (maximum) dynode construction. They are susceptible to magnetic fields and their gain characteristics are subject to dynode-to-dynode voltage variations. Box-and-grid types have easy electrode design and good uniformity. In some cases time response may become a problem.

The performance quality of a crystal-photomultiplier tube assembly depends upon the spectral sensitivity of the tube to the light emitted

TABLE 1. 1. Scintillation Phosphor Characteristics. INORGANICI

Material	Wavelength of Maximum Emission (nm)	Decay Constant (μs)*	Scintillation Cutoff Wavelength (nm)	Index of Refraction**	Density (g/cm^3)	Hygroscopic	Scintillation Conversion Efficiency (%)***
NaI(Tl)	415	0.23	320	1.85	3.67	yes	100
CsI(Na)	420	0.63	300	1.84	4.51	yes	85
CsI(Tl)	565	1.0	330	1.80	4.51	no	45
CaF_2(Eu)	435	0.94	405	1.44	3.19	no	50
BaF_2	325	0.63	134	1.49	4.88	no	20
CsF	390	0.005	320	1.48	4.64	yes	3-5
$Bi_4Ge_3O_{12}$	480	0.30	350	2.15	7.13	no	12
$ZnWO_4$	480	5.0	N/a	2.2	7.87	no	26
$CdWO_4$	540	5.0	450	2.3	7.90	no	40
^{6}LiI(Eu)[1]	470-485[1]	1.4	450	1.96	4.08	yes	35
Plastic[2]	350-450	0.002-0.020	varies	varies	1.06	no	30

* Room temperature, best single exponential decay constant.
** At wavelength of maximum emission.
*** Referred to NaI(Tl) with S-11 photocathode response

1. Primarily used for neutron detection
2. Not manufactured by Harshaw/Filtrol

by the scintillator. The emission spectra of four readily available inorganic crystals are plotted in figure I.1.

Table I.2. gives pertinent data for several photomultiplier tube types frequently used in scintillation counting. The stability, gain and spectral sensitivity of these tubes are adequate for NaI(Tl) and most other scintillation crystals described in this catalogue.

Photomultiplier gain stability and pulse height resolution are important parameters influencing the performance of a gamma ray spectrometer. Tube related pulse height resolution depends upon photocathode uniformity, photocathode sensitivity and first dynode secondary emission ratio. Collectively, these parameters largely determine the resolution performance and stability of a scintillation detector. Tube manufacturers' literature should be consulted for complete descriptions of tube types and characteristics.
When space is a serious constraint, silicon photodiodes are used instead of photomultipliers. Having much higher noise they can be used either in the current mode or for pulse counting at higher energy.

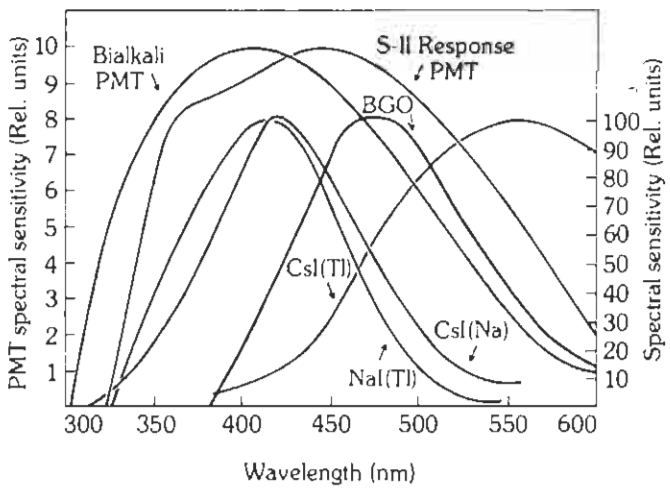

Fig. I.1. NaI(Tl), CsI(Tl) and CsI(Na) and BGO emission spectra. The emission curves have been normalized to 100% for illustrative purposes.
Harshaw/Filtrol Research Laboratory Report.

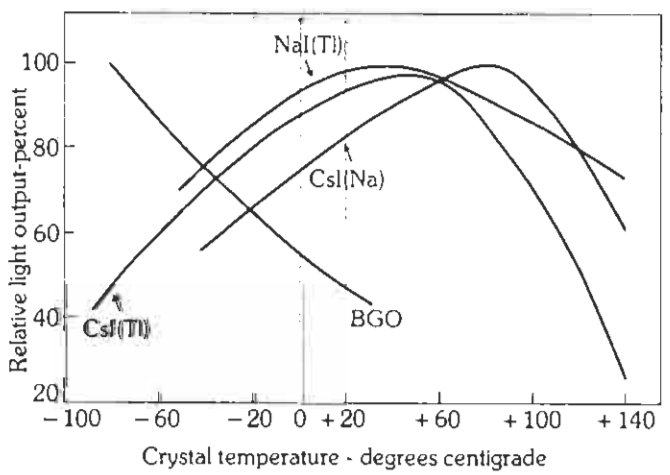

Fig. I.2. Temperature response of various scintillation phosphors.

3. Temperature response

The relative light output of all scintillators is a function of temperature. The inorganic crystals and the alkali halides in particular exhibit similar response to temperature as illustrated in figure I.2. This effect is significant in a number of applications such as oil well logging, space exploration and environmental surveillance.
The effect of temperature on light output is small for NaI(Tl) in the temperature range from $-10°C$ up to $100°C$, while a rather flat maximum occurs near room temperature.

4. Basic interactions in scintillation crystals

A knowledge of the basic processes by which a photon interacts with matter is essential to an understanding of the response of a scintillation detector.

TABLE I.2. Characteristics of representative photomultiplier tubes and photodiodes (normally supplied with Harshaw scintillators).

Photomultipliertubes

Manufacturer	Type	Diameter	Dynode system
Hamamatsu	R 1635	10 mm (3/8")	linear focused
Hamamatsu	R 647	13 mm (1/2")	linear focused
Hamamatsu	R 750	19 mm (3/4")	linear focused
RCA	4516	19 mm (3/4")	linear focused
Hamamatsu	R 434	28 mm (1 1/8")	box-and-grid
EMI	9734	30 mm (1 1/8")	box-and-grid
Hamamatsu	R 2060	38 mm (1 1/2")	circular cage
RCA	2060	38 mm (1 1/2")	circular cage
Philips	XP 2012	39 mm (1 1/2")	linear focused
Hamamatsu	R 1306	51 mm (2")	box-and-grid
RCA	6342 A	51 mm (2")	circular cage
RCA	4902	51 mm (2")	tea cup cage
EMI	9856 L	52 mm (2")	venetian blind
Philips	XP 2020	53 mm (2")	linear focused
EMI	9758 L	75 mm (3")	venetian blind
Hamamatsu	R 1307	76 mm (3")	box-and-grid
RCA	4900	76 mm (3")	tea cup cage
EMI	9732	101 mm (4")	venetian blind
EMI	9791 B	130 mm (5")	venetian blind
RCA	83006 E	130 mm (5")	tea cup cage
Philips	XP 2040	130 mm (5")	linear focused
Hamamatsu	R 1250	130 mm (5")	linear focused

Silicon photodiodes

Manufacturer	Type	Photosensitive area (mm^2)
EMI	S 30520	2 × 38
EMI	S 30530	3 × 4
Hamamatsu	S 1723	10 × 10
Hamamatsu	S 1337-16	1 × 6
Hamamatsu	S 1337-66	6 × 6
Hamamatsu	S 1337-1010	10 × 10

The intensity I_0 of a monoenergetic gamma beam entering a detector of thickness d is reduced to the transmitted intensity I according to:
$I(E) = I_0(E)e^{-\mu(E)d}$,
where the total linear attenuation coefficient $\mu(E)$ is the sum of all interaction cross sections like photo effect, compton scattering and pair production. In fig. I.3. cross section data for NaI are given.

4a. Photo effect

In the photo-electric process all of the energy of the incident photon is absorbed by a bound electron of an atom. As a result the atom is left with an electron vacancy resulting in the emission of X-rays or Auger electrons. The X-rays are generally absorbed in a second photo-electric event and the total energy is absorbed within the detector.

4b. Compton scattering

In this process incident photons are scattered by the electrons with a partial energy loss. The energy of the scattered photon and electron are given by:

$$E\gamma' = \frac{E\gamma}{1 + \frac{E\gamma}{0.511}(1 - \cos\Theta)} \quad \text{and} \quad E_e = E\gamma - E\gamma', \text{ with } E\gamma \text{ in MeV.}$$

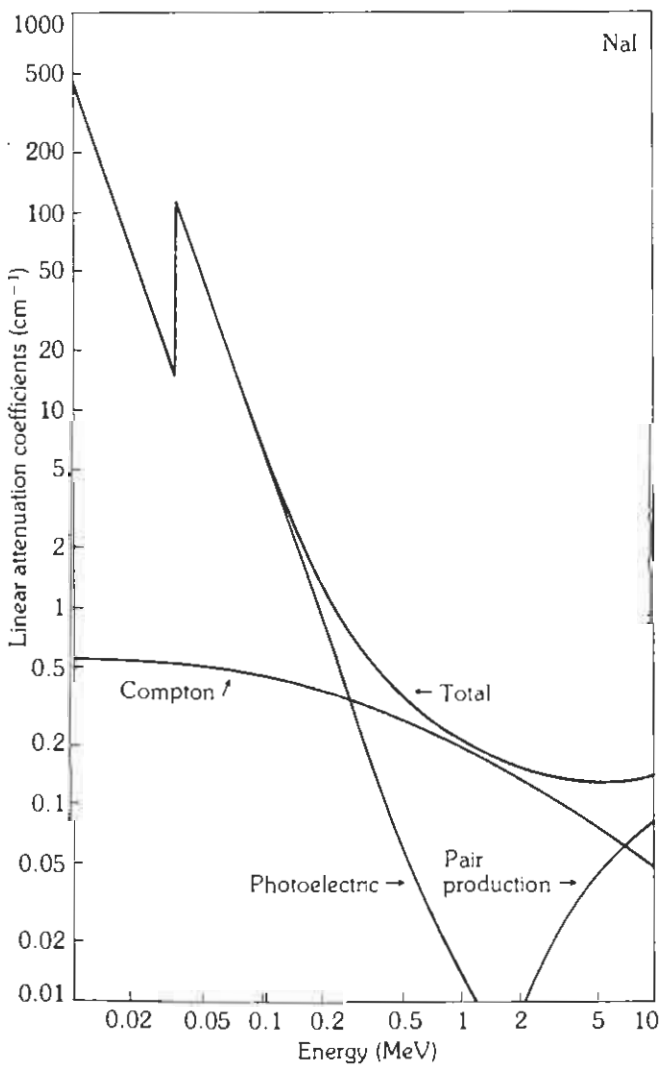

Fig. I.3. Complete cross section of NaI showing different contributions.

From these it may be deduced that a Compton electron energy spectrum will result which extends from zero energy ($\Theta = 0°$) up to a maximum energy ($\Theta = 180°$). See also fig. V.1.

4c. Pair production

If the incident photon has an energy in excess of 1.02 MeV then pair production is possible. In this process a positron electron pair is created from which the positron annihilates with an other electron by emission of two photons of 0.511 MeV. One or both of these annihilation quanta can escape from the crystal resulting in a rather complex spectrum.

A summary of various processes contributing to the response of a detector to a gamma-ray source is given in fig. I.4.
Absorption coefficient data for a large variety of materials are given in chapter 4.

5. Scintillator response on gamma-ray excitation

5a. Pulse height spectrometry

A basic principle of scintillation counting is that light output is essentially proportional to the energy deposited within a crystal. This feature is particularly important when selecting a crystal for use as a charged particle or gamma ray spectrometer. To be useful as a spectrometer, a scintillation material must exhibit a high probability for complete absorption of the incident radiation. NaI(Tl) crystals are widely used for gamma ray spectrometry. (Special features of other inorganic scintillation phosphors are described in chapter II).

The basic components of a spectrometer include the detector crystal, a photomultiplier tube, a preamplifier, a main amplifier and a single or multichannel analyzer. Each of these components should exhibit a response proportional to the energy of the incident radiation. Figure I.5. illustrates a spectrum obtained with a selected 3" × 3" (76 mm × 76 mm) NaI(Tl) detector and a multichannel analyzer. The prominent peak represents events in which the full energy of the 662 keV gamma ray was deposited within the crystal. Counts in lower channel numbers indicate events in which partial energy escape was produced by Compton scattering.

5b. Energy resolution

An important capability of any spectrometer is the ability to distinguish between gamma rays of slightly different energy. This parameter is termed resolution and is measured by counting the **number of channels between the half maximum point in the full energy peak, dividing by the channel number of the peak mid-point and multiplying the result by 100%.**

Typical resolutions for 662 keV gamma rays are 7% or better in small NaI(Tl) detectors.
If there were a 100% correlation between the release of a certain amount of energy in a crystal and conversion of this energy into a pulse of specific size, the pulse height resolution would approach zero. In practice this is not the case.
Statistical fluctuations in light productions, variations in light reflection and internal light absorption may all result in differing numbers of photons incident upon the photocathode.
Additionally, non-uniformity of the photocathode emission will result in different pulse sizes depending upon the distribution of light on the photocathode.

Finally, the number of photo electrons emitted at the cathode and dynodes will show variations caused by statistical fluctuations.
For radiation interactions below 3 MeV the absorption of detected energy usually occurs in a small region of the total crystal.
Light collection efficiency limits are imposed by crystal geometry and contribute to variations in the light incident upon the photocathode. It is possible to compensate largely for these effects through a patented Harshaw/Filtrol process that suitably alters the surface reflectivity of the crystal. For example, it is possible for crystals measuring 40 mm diameter by 760 mm length to exhibit an

essentially uniform response along their entire length. This in turn permits such crystals to be used as pulse height spectrometers even though the incident radiation may be from a diffuse source.

5c. Timing resolution

The best timing resolution of a scintillation detector is obtained with a fast linear focussed photomultiplier. The size and the geometry also clearly influences this timing.
When good energy resolution is required there must be a compromise for a careful selection of a photomultiplier.
Small NaI(Tl) detectors have typical timing resolutions of 2 – 3 ns for ^{60}Co measured against a fast scintillator, e.g. a CsF detector.

6. Characteristics of a gamma ray spectrum

The details of a gamma ray spectrum depend on the energy and intensity of the gamma radiation as well as the composition and geometry of the detector crystal. The following spectra are typical of several common gamma ray emitters and were obtained with Harshaw NaI(Tl) detectors of varying sizes.

Figure I.5. is a ^{137}Cs spectrum representative of those used for evaluating the performance of scintillators. The prominent peak is the full energy peak indicating events completely absorbed by the crystal. Compton events in which a scattered gamma ray travels

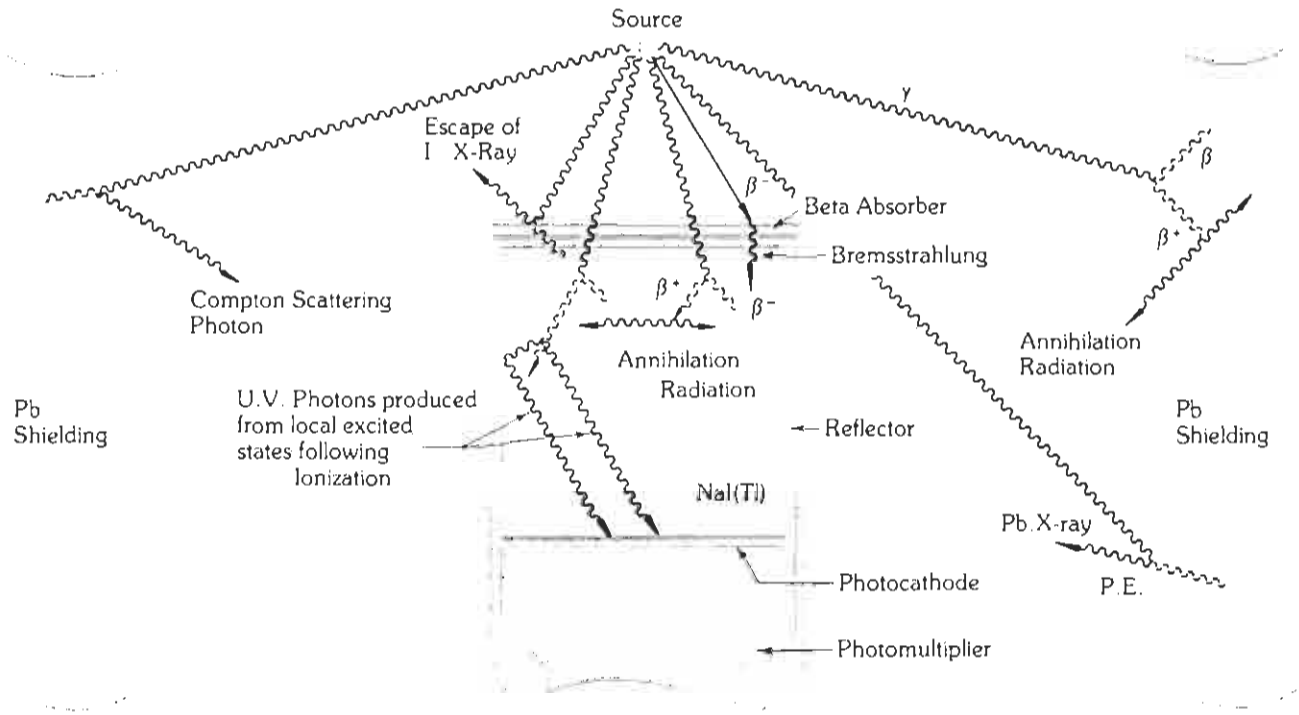

Fig. I.4. Illustration of various processes which contribute to the response of a detector to a gamma ray source.

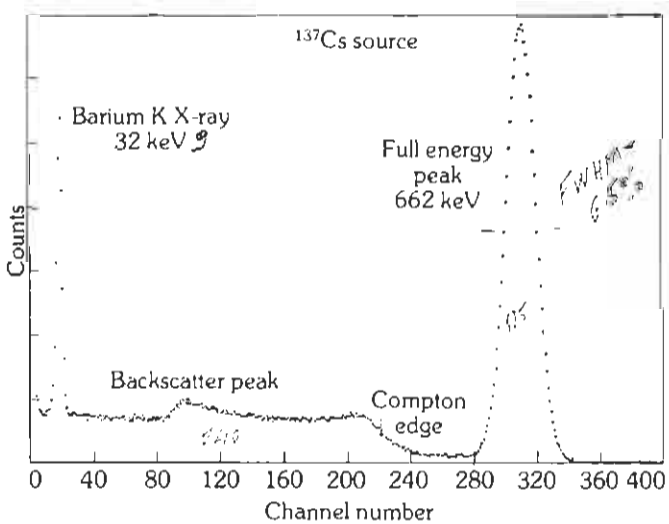

Fig. I.5. ^{137}Cs pulse height spectrum obtained with a selected Harshaw type 12S12 NaI(Tl) detector.
Harshaw/Filtrol Research Laboratory Report.

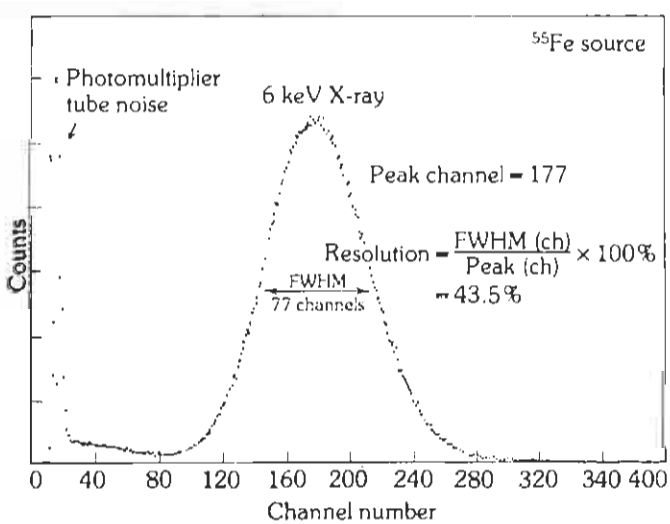

Fig. I.6. A low energy spectrum obtained with a Harshaw type SH NaI(Tl) detector.
Harshaw/Filtrol Research Laboratory Report.

180° opposite to the incident radiation produces electrons of 477 keV in the crystal. These events produce the Compton edge noted in the illustration. Other scattering events at lesser angles produce the characteristic counts to the low energy side of the Compton edge.

The backscatter peak results from Compton scattering into the detector from the surroundings under large angles.

Figure I.6. shows a 6 keV spectrum for ^{55}Fe. A Harshaw type SH assembly was used to obtain the data. This type of detector incorporates a selected photomultiplier tube and a thin, cleaved NaI(Tl) crystal. The use of thinly cleaved crystals is particularly desirable for good detector resolution at energies near 10 keV and lower.

6a. Energy resolution

The energy resolution defined in the preceeding section shows a dependence on the gamma ray energy. An example of the energy dependence measured for a long NaI(Tl) crystal is shown in fig. I.7.

As a standard Harshaw scintillation detectors are manufactured with a resolution at least as good as the figures listed in table I.3.

These figures depend strongly on the size and shape of the crystals.

If desired, the energy resolution can be guaranteed within the limits listed in the same table.
Presently, detectors with a resolution better than 6.5% for 662 keV can also be supplied. However, these are available in a limited number of sizes and usually require a longer delivery period.

TABLE I.3. Typical NaI(Tl) energy resolution values and values guaranteed upon request.

		Resolution		
Isotope as standard	Energy	Typical value	Guaranteed upon request	Type
^{55}Fe	5.9 keV	60%	45%	8SHB2.5M
^{129}I	30 keV	40%	30%	5S5
^{241}Am	60 keV	30%	15%	8SHB1.5
^{57}Co	122 keV	25%	15%	8S4
^{137}Cs	662 keV	9%	7%	12S12

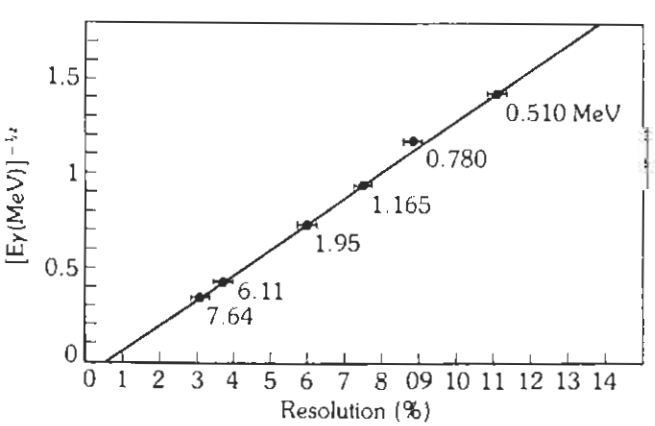

Fig. I.7. Example of energy resolution variation with gamma ray energy for a Harshaw NaI(Tl) crystal, type 10S24.

6b. Peak valley ratios

Scintillation detectors intended for measuring ^{60}Co sources (1170 and 1331 keV) can be specified on peak valley ratios. This peak valley ratio depends strongly on detector size and detector resolution. As an example a 3" dia × 3" height detector with 7% ^{137}Cs resolution can be supplied with 10 : 1 ^{60}Co peak valley ratio.

^{55}Fe Peak-valley ratio in a thin window cleaved crystal low energy detector is limited by the PM tube noise (standard values are 10 : 1). For extreme specifications PM tubes may be selected yielding peak-valley ratios better than 30 : 1 for ^{55}Fe.

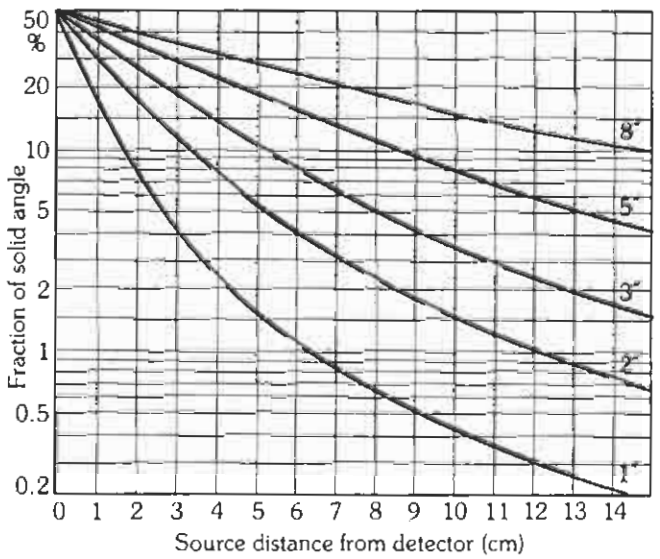

Fig. I.8

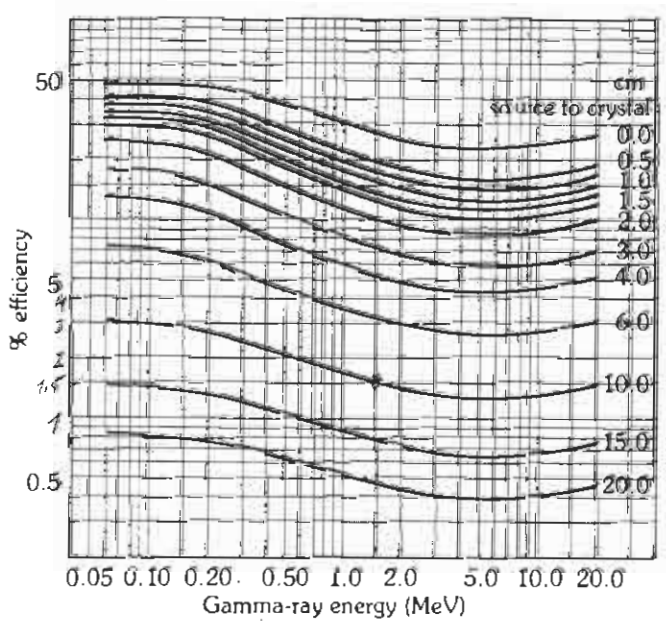

Fig. I.9. Calculated efficiencies of a NaI(Tl) crystal of 3 inches diameter × 3 inches thick.

6c. Detection efficiency

For a point gamma ray source and a detector shielded from spurious events, the number of events in the observed spectrum will be related to the disintegration rate of the source. As the distance of the source to the detector increases, the solid angle under which the source is viewed by the crystal decreases. This decrease in counting efficiency depends on the detector size as indicated in fig. I.8.

The absorption probability of a gamma ray entering the detector depends also on the gamma ray energy. In fig. I.9. both the efficiency dependence on gamma ray energy and on source to crystal distance are shown for a 3" × 3" (76 mm × 76 mm) NaI(Tl) crystal. Data for other crystal dimensions can also be supplied.

In applications where the source is contained within a small volume and where counting efficiency is more important than energy resolution, **well type** detectors are particularly useful. Almost 100% efficiency can be achieved by placing the source inside the NaI(Tl) crystal.
In fig. I.10. calculated detection efficiencies are displayed for different detector sizes as a function of energy. (Well diameters used in the calculation are 25 mm for the 5" × 5" detector, 20 mm for the 4" × 4" detector, 15 mm for the 3" × 3" detector and 10 mm for the 2" × 2" detector).
The spectra shown in fig. I.11. give a clear demonstration of the powerful possibilities of a well type counting detector. Both sets of data were compiled with the same Harshaw well type detector using equal live time counting.

6d. Photopeak counting efficiency

In many applications it is desirable to discriminate against background radiation or other spurious events. In these instances, it is necessary to count only full energy or photopeak counts. Photopeak efficiency can be obtained by multiplying the efficiencies given in fig. I.8., I.9. or I.10. by the photofraction at a particular energy, crystal dimension and crystal to source distance. In fig. I.12. an example is given of such a photofraction (peak total ratio). Data of other source distances are also available.

In table I.4. a few examples of efficiencies and count rates are listed.

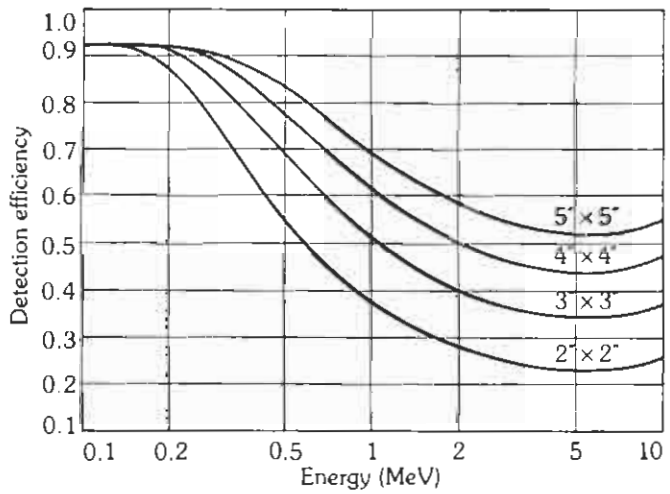

Fig. I.10. Calculated detection efficiency for **well** type NaI(Tl) crystals.

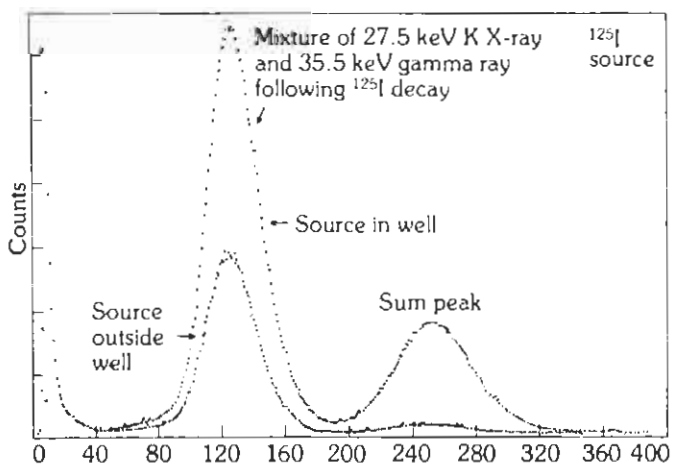

Fig. I.11. Effect of source placement with respect to a well type detector.
Harshaw/Filtrol Research Laboratory Report.

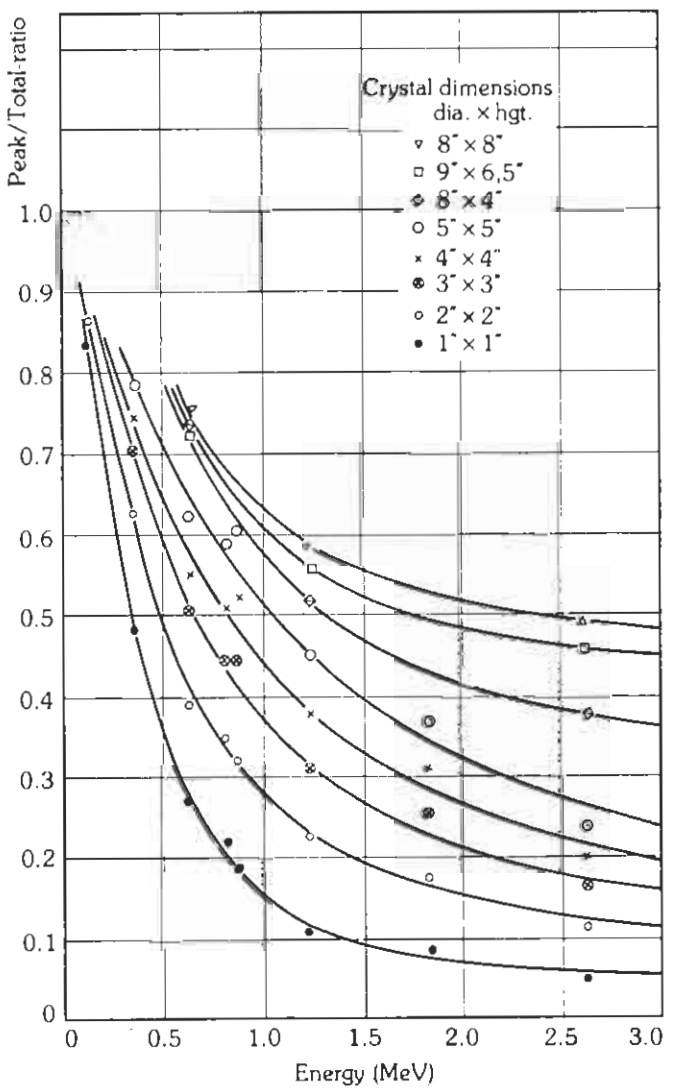

Fig. I.12. Experimental peak/total ratio for various crystal dimensions. Source distance is 10 cm.

7. Spectrum stabilization

Extreme countrate changes, temperature variations and instable electronics may cause a peak position change in the spectrum. As a reference pulser, an Americium doped NaI(Tl) crystal is advised. The counts of this pulser arise at e.g. 3 MeV and do not interfere with the gamma ray spectrum.
For environmental this is an excellent way to obtain a stable system.

For occasionally monitoring system gain stability, nuclear physicists may also use LED pulsers or a laser reference light source. Further information is contained in the next chapter.

TABLE I.4. Total counting efficiencies and photopeak efficiencies for different NaI(Tl) detector dimensions. Source intensity 37 kBq (1μCi), source distance 10 cm.

Crystal dimensions	Total eff. (%)		Photopeak eff. (%)		Photopeak counts (cpm)	
	0.5 MeV	2 MeV	0.5 MeV	2 MeV	0.5 MeV	2 MeV
1" × 1"	0.17	0.09	0.06	0.0007	1.3×10^3	1.5×10^2
2" × 2"	0.75	0.45	0.4	0.07	9.0×10^3	1.5×10^3
3" × 3"	2.0	1.3	1.2	0.30	2.6×10^4	6.6×10^3
5" × 5"	6.1	4.4	4.5	1.45	1.0×10^5	3.2×10^4
8" × 8"	15.0	12.5	12.6	6.40	2.8×10^5	1.4×10^5

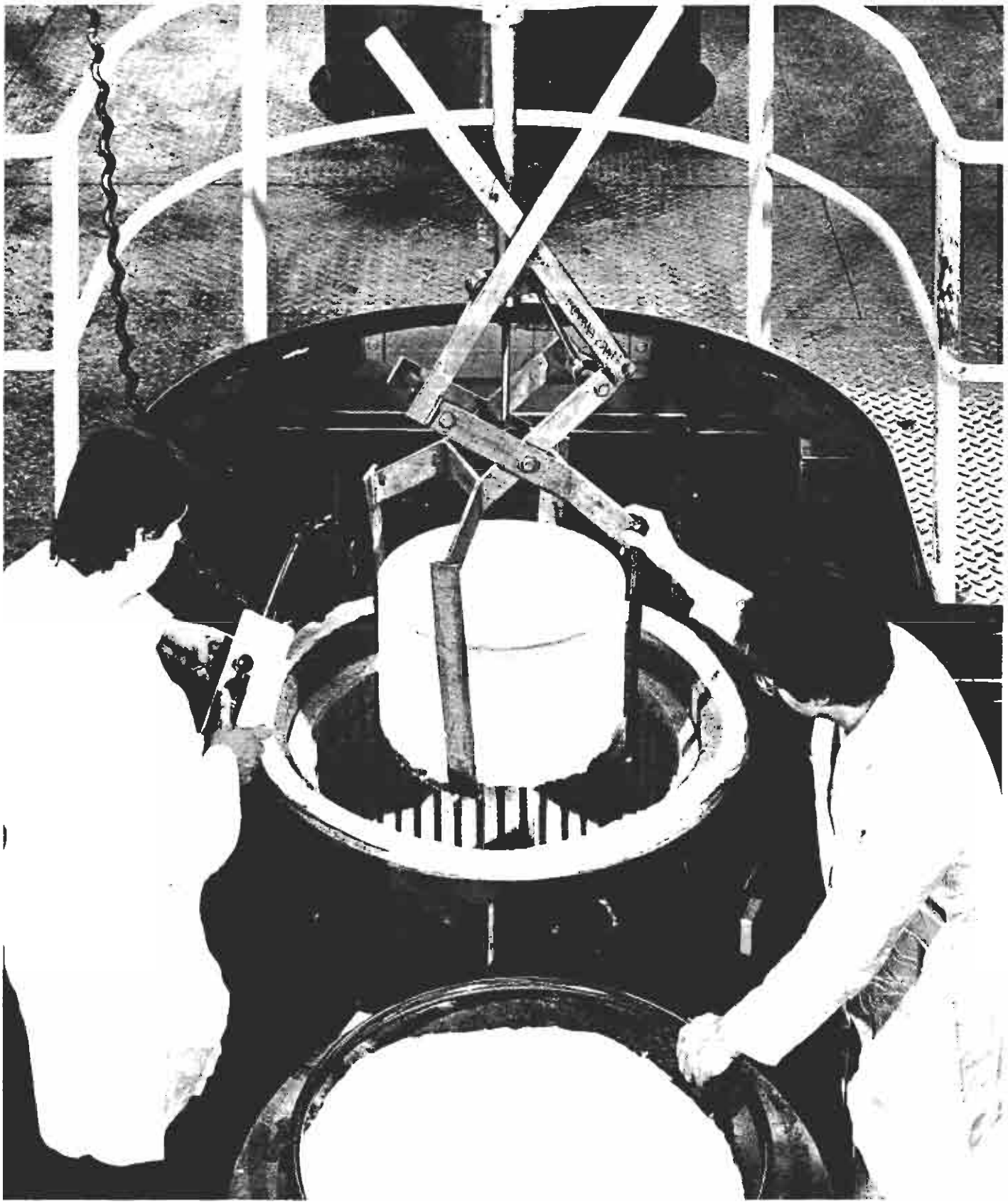

First view of a complete NaI(Tl) ingot.

II. HARSHAW SCINTILLATION PHOSPORS

Contents:

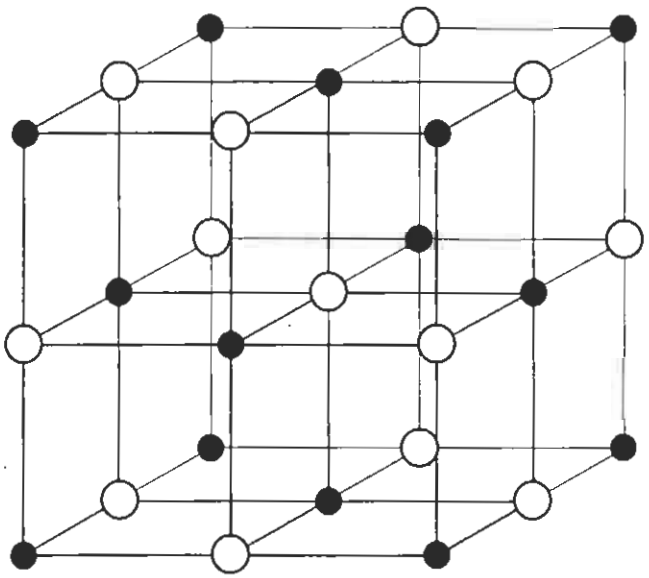

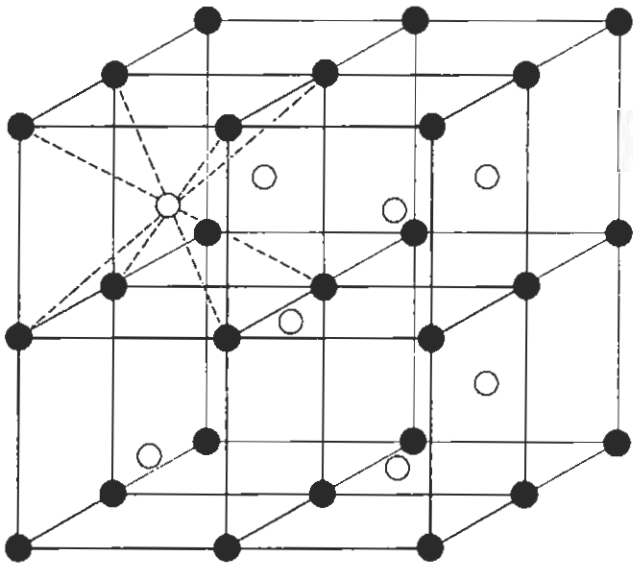

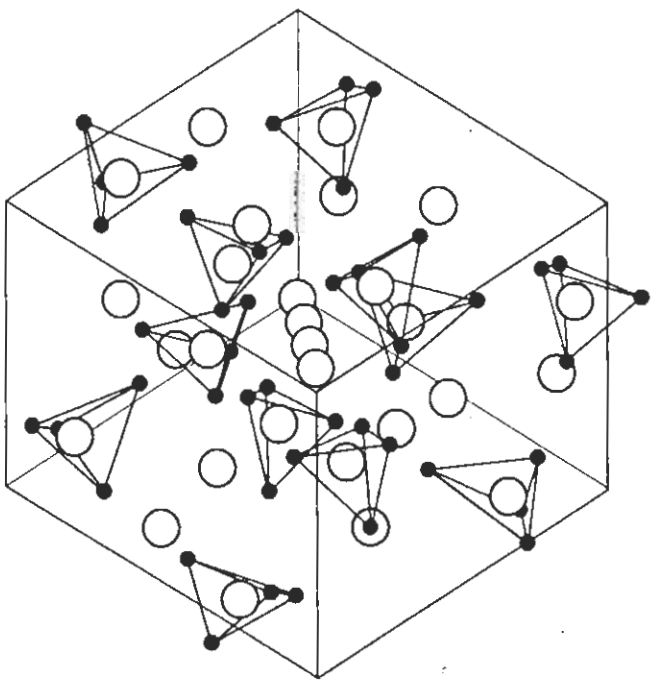

II. HARSHAW SCINTILLATION PHOSPHORS

1a. NaI(Tl)

Among all available scintillators NaI(Tl) is the most extensively used material. NaI(Tl) has a very high luminescent efficiency and is available in single crystal or polycrystalline forms in a wide variety of sizes and geometries. The NaI(Tl) exhibits no self absorption of the scintillation light making it possible to use very large scintillators.

These very large NaI(Tl) crystals are widely used in high-energy gamma ray physics, electron-positron physics, as anti-compton shields and as total gamma absorption devices in nuclear spectroscopy.

NaI(Tl) exhibits several decay constants. The primary single exponential decay constant is 230 ns and the amount of light emitted after 3 ms (the so called "afterglow") varies between 0.5 to 5%. In cases where the dc output of a photomultiplier should follow fast changes of the detected signals (for example in computed tomography scanners for medical X-ray applications) scintillators with less afterglow like BGO, $CdWO_4$ or CaF_2 (Eu) might be preferable.

The company's experience in making very large crystals with uniform light output is illustrated in the quality of gamma camera plates. These are thin crystals of large diameter which are compensated to provide a uniform response across the diameter.

Useful data can be found in table I.1. and II.1.

1b. POLYSCIN™ NaI(Tl)

POLYSCIN™ NaI(Tl) crystals are widely recognized as suitable alternatives to single crystal scintillators in many applications where thermal and mechanical shock are encountered. Detectors fabricated from POLYSCIN™ crystals offer ruggedness combined with scintillation performance identical to single crystal NaI(Tl). Current applications utilizing POLYSCIN™ NaI(Tl) detectors include aerospace research, well logging, geophysical survey, and environmental radiation monitoring.

The polycrystalline structure of POLYSCIN™ NaI(Tl) is derived from a unique manufacturing process developed by Harshaw/Filtrol in which single crystal ingots are recrystallized under heat and pressure.

The resulting material (POLYSCIN™) may be defined as a metamorphic alteration of a single crystal in which the angular spread in alignment between mosaic volumes has been increased and made random. This characteristic improves mechanical strength by inhibiting yield or cleavage fracture, but has no effect upon scintillation performance. POLYSCIN™ NaI(Tl) is fully equivalent to single material in optical and scintillation performance.

Table II.1. NaI(Tl) and POLYSCIN™ NaI(Tl) data.

Wavelength of maximum emission	415 nm
Decay constant	0.23 μs
Afterglow (after 3 ms)	0.3-5%
Index of refraction at 415 nm	1.85
Temperature coefficient of the light output at 300K (negative)	0.22-0.95%/K
Thermal coefficient of linear expansion	47.4×10^{-6}/K
Cleavage Plane	<100>
Hardness (Mho)	2
Density	3.67 g/cm³
Melting point	924 K
Hygroscopic	yes

Any fractures produced by thermal or mechanical shock in POLYSCIN™ NaI(Tl) are normally blocked or confined to small local volumes. In contrast, single crystals will cleave along (100) planes under similar shock conditions. In a detector assembly fabricated from single crystal material, even a small crack may propagate across the entire crystal, interfering with the uniformity of light collection and degrading pulse height resolution. In a POLYSCIN™ detector, it is unlikely a fracture will propagate enough to trap scintillation light or degrade resolution performance.

The widespread availability of POLYSCIN™ NaI(Tl) has released the detector designer from the physical and geometric constraints imposed by the limited size and cylindrical shape of single crystal ingots. Unique detector geometries can be fabricated directly from POLYSCIN™ NaI(Tl) ingots without extensive machining. Special geometries currently offered by Harshaw/Filtrol include hexagonal detectors, square and rectangular assemblies, and large diameter plates and slabs. In each case the detector crystal is obtained directly from a POLYSCIN™ NaI(Tl) ingot of the corresponding geometry.

Fig. II.1. These special matched window line detectors were fabricated from hexagonal POLYSCIN ™ NaI(Tl) ingots.

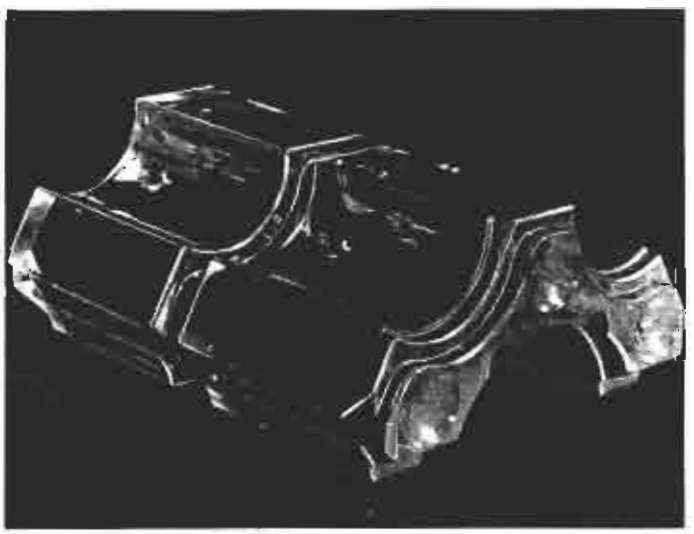

Fig. II.2. A machined and polished CsI(Na) crystal measuring 35 cm long × 23 cm high × 30 cm wide. This crystal was manufactured by Harshaw/Filtrol for use in an orbiting satellite study of gamma radiation.

1c. NaI(Tl + ^{241}Am)

NaI(Tl) crystals with ^{241}Am grown into the crystal lattice are widely used as constant amplitude light pulsers in a variety of gain stabilization techniques. These assemblies exhibit pulse shapes similar to those produced by gamma absorption within the NaI(Tl) crystal.

Pulser crystals are incorporated into the detector by optically coupling a small NaI(Tl + ^{241}Am) crystal to a primary (host) scintillation crystal. The pulser thus becomes an integral part of the detector assembly.

Alpha particles produced by the americium decay are absorbed in the pulser crystal and the resulting light is transmitted to the photomultiplier tube through the host crystal.

The position of the alpha peak in the gamma spectrum of the host crystal is known as Gamma Equivalent Energy (GEE) and is determined by the light output of the pulser crystal and the optical coupling to the host crystal.

However at these countrates the resolution may degrade.

A GEE range of 0.1 to 4 MeV is available depending upon the particular type of crystal assembly. Pulser count rates of 10 to 10,000 cps are possible. In the Harshaw system for environmental gamma ray monitoring a NaI(Tl + ^{241}Am) light pulser provides constant, high energy, reference pulses.

Harshaw/Filtrol has developed a stabilized amplifier/analyzer (the Harshaw NA-23), especially for this system to compensate for gain shifts. As an additional advantage the constant count rate of the pulser can be used for continuous verification of system performance.

In figure II.3 an example of a NaI(Tl) spectrum recorded for a ^{137}Cs gamma ray source is given with a NaI(Tl + ^{241}Am) pulser optically coupled to the NaI(Tl) crystal.

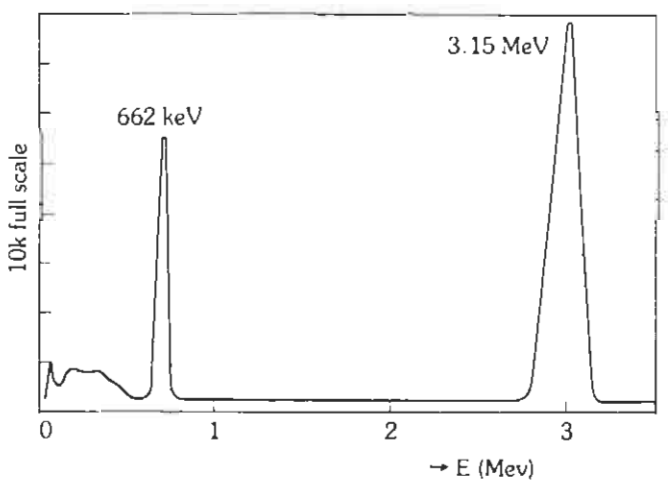

Fig. II.3. A typical spectrum for a NaI(Tl + ^{241}Am) light pulser optically coupled to a NaI(Tl) scintillator, which is irradiated with a ^{137}Cs source. Harshaw/Filtrol Research Laboratory Report.

Table II.2. NaI(Tl + ^{241}Am) light pulser data.

Half life of ^{241}Am alpha source	458 years
Alpha particle energy	5.48 MeV
Gamma Equivalent Energy (GEE)	0.1—4 MeV
Typical pulser count rate	50—2000 cps
Spectral line width	4—8%

2. CsI(Tl) and CsI(Na)

When activated with sodium or thallium, CsI is a rugged scintillator noted for high gamma stopping power and resistance to thermal and mechanical shock. Selected characteristics of CsI(Tl) and CsI(Na) are given in Table II.3.

Most physical characteristics of CsI are independent of the activator used. It is comparatively soft and plastic compared with NaI(Tl) and is easily fabricated into a variety of useful detector geometries (see figure II.2.). Because of its rugged character, CsI has been extensively applied to well logging, space exploration and military science where severe environmental conditions are frequently encountered.

The emission maximum of both materials is suitable for use with S-11 and bialkali photocathode response (refer to figure 1.1.). Of the two materials, CsI(Na) exhibits the highest light output, approaching 85% of NaI(Tl). CsI(Tl) commonly exhibits a light output nearing 45% of NaI(Tl). The high density of both materials (4.51 g/cm^3) gives them particularly high gamma stopping cross sections.

In gamma spectrometry applications below 5 MeV, the escape of

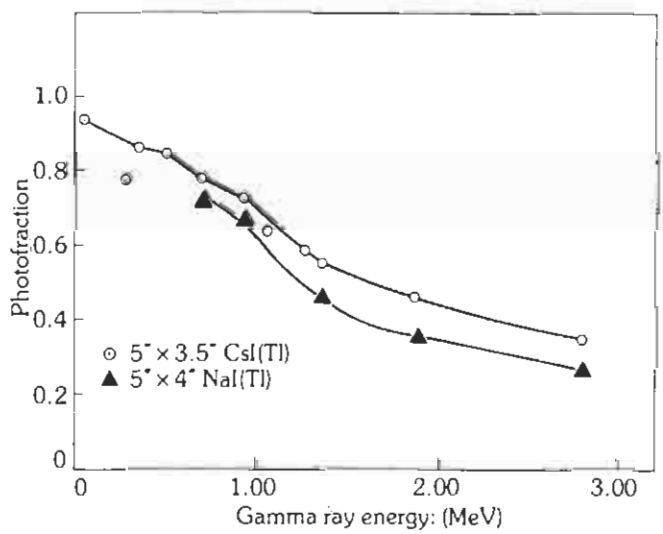

Fig. II.4. CsI(Tl) and NaI(Tl) Photofractions, for similar crystal geometries.

Table II.3. CsI(Tl) and CsI(Na) data.

	CsI(Tl)	CsI(Na)
Light output relative to NaI(Tl)	45%	85%
Wavelength of maximum emission	550 nm	420 nm
Decay constant	1 μs	0.63 μs
Afterglow (after 6 ms)	0.5—5%	0.5—5%
Index of refraction at max emission	1.80	1.84
Temperature coefficient of the light output at 300 K (negative)	0.24—0.67%/K	Same
Thermal coefficient of linear expansion	54×10^{-6}/K	Same
Cleavage plane	None	None
Hardness (Mho)	2	2
Density	4.51 g/cm^3	4.51 g/cm^3
Melting point	894 K	894 K
Hygroscopic	Slightly	Yes

scattered or annihilation photons from the crystal produce an undesirable continuum below the photopeak. These escape events become increasingly probable at higher gamma energies and complicate the analysis of high energy spectra. In these instances CsI(Tl) or CsI(Na) are suitable alternatives to NaI(Tl) crystals since for equal sized crystals a larger photofraction can be obtained, or conversely, an equivalent photofraction can be obtained with smaller crystals.

The advantage of high stopping power is illustrated in figure II.4. where photofractions as a function of gamma ray energy are plotted for CsI(Tl) and NaI(Tl) crystals of similar geometry.

The effects of the higher stopping power of CsI(Tl) are evident - the improvement of photofraction increases with gamma ray energy. The ratio of CsI(Tl) to NaI(Tl) is 1.25 at 2.76 MeV even though the CsI(Tl) crystal is 13 mm shorter in length.

Both CsI(Tl) and CsI(Na) are damaged by moisture. CsI(Tl) crystals will suffer local surface damage upon direct contact with water or exposure to 90% atomospheric humidity. Resurfacing the crystal will generally restore original performance. CsI(Na) is hygroscopic and must be hermetically sealed at all times. Exposure to humidity levels as low as 30% will degrade scintillation performance through the interaction of water with the sodium activator. Prolonged exposure will produce drastic loss of scintillation performance and internal damage to the crystal.

The advantages of the CsI(Tl) and CsI(Na) for gamma spectrometry are due to their high photofraction, detection efficiency and rugged physical character. The energy resolution of both materials-approaches that of NaI(Tl) when electronics with suitable shaping times are used (approximately 6 μs). However, this limits the maximum counting rates and timing ability of both materials.

3. High Z materials

High Z materials are of special interest since they combine a high stopping power to good scintillation characteristics.

Weight and size limitations are important considerations in the design of detectors for high energy applications. High Z scintillators are particularly desirable for reducing detector volume requirements and simplifying related system equipment such as photomultiplier tube arrays and support structures. The high absorption coefficient for gamma rays does not only have a positive influence on the size of the detector, but also improves the spatial resolution of a system.

At low and intermediate gamma ray energies, the larger photofraction of a high Z material (relative to a NaI(Tl) crystal of comparable size) may be advantageous despite the lower light output and poorer resolution that characterize some of these materials. High energy total absorption counters and small, low energy detectors are two applications where high Z scintillators are particularly useful.

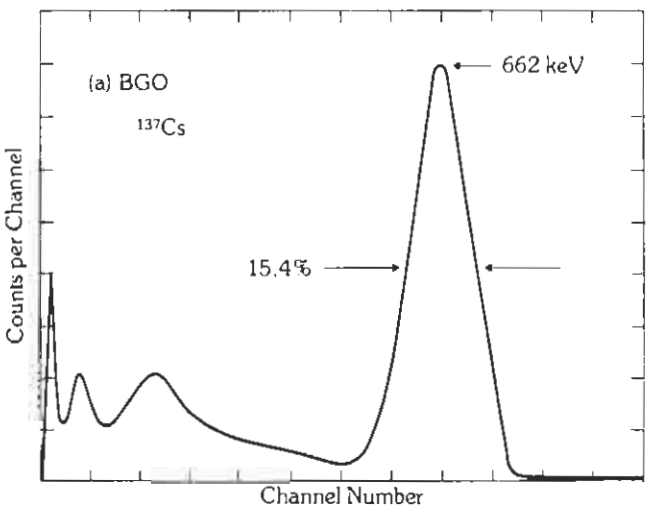

Fig. II.5. Response of a BGO detector to a ^{137}Cs source.

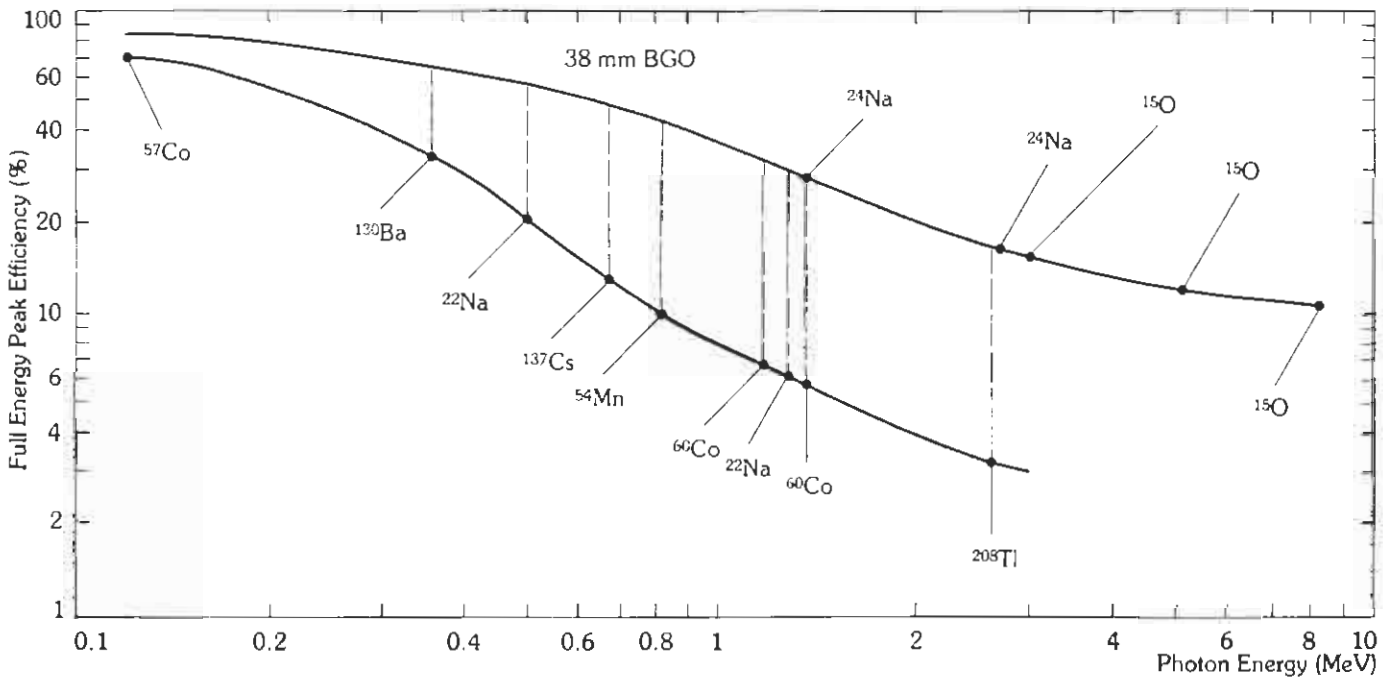

Fig. II.6. Full energy peak efficiencies of a BGO and a NaI(Tl) detector (1). Size of the detectors: 1½" × 1½".

3a. $Bi_4Ge_3O_{12}$

Bismuth germanate, usually abbreviated as BGO, is a pure intrinsic scintillator developed by Harshaw/Filtrol, which has some attractive properties as a scintillator. It has a high stopping power, a short decay constant and a very low afterglow.
Furthermore, the chemical inertness and the rugged physical properties of BGO makes it suitable for several applications.

Scintillation characteristics

BGO is suitable for many pulse counting applications.
Since the decay constant of 0.3 μs as well as the wavelength of maximum emission of 480 nm are comparable to those of NaI(Tl), similar photomultiplier tubes and electronic chains can be used.
Bismuth germanate is an intrinsic scintillator. The light emitted in fluorescence and now observed has been identified with the $^3P_1 \rightarrow {}^1S_0$ electronic transition within the Bi^{3+} ion. This means that it is free of problems associated with non-uniform dopant distributions.
The response of BGO to γ radiation is shown in fig. II.5. This figure also illustrates the reduced backscatter and compton effects possible with a high Z scintillator.

Fig. II.6. illustrates the full energy peak efficiency for a BGO and a NaI(Tl) crystal of equal sizes at different energies.

Charged particle detection

The scintillation characteristics of BGO can also be used for detection of charged particles. E.g. the response of BGO to 5.5 MeV α particles from ^{241}Am is shown in fig. II.7.
The peak appears at the pulse height position for 1 MeV γ-rays, duplicating the performance of CaF_2(Eu).

High stopping power

The γ-ray absorption coefficient of BGO is impressive. It finds its origin in the high atomic number of bismuth (Z = 83) and the density of the bismuth germanate (7.13 g/cm³).
The ratio of the total absorption coefficient of BGO compared to NaI(Tl) is about 2.5. This means a reduction in size of a factor of 2.5 in one linear dimension, which may lead to a 16-fold volume reduction in the finished geometry.

BGO is useful in any application where space is limited and optimum stopping power is required.

Chemical inertness

BGO is a non-hygroscopic, inert crystal which can be easily handled in most environments. The detector size may be reduced and the housing simplified, because hermetically sealed hardware is not required.

This simplifies design parameters for both Integral Line type assemblies and for unique systems where multiple crystals must be assembled in a tightly packed array.

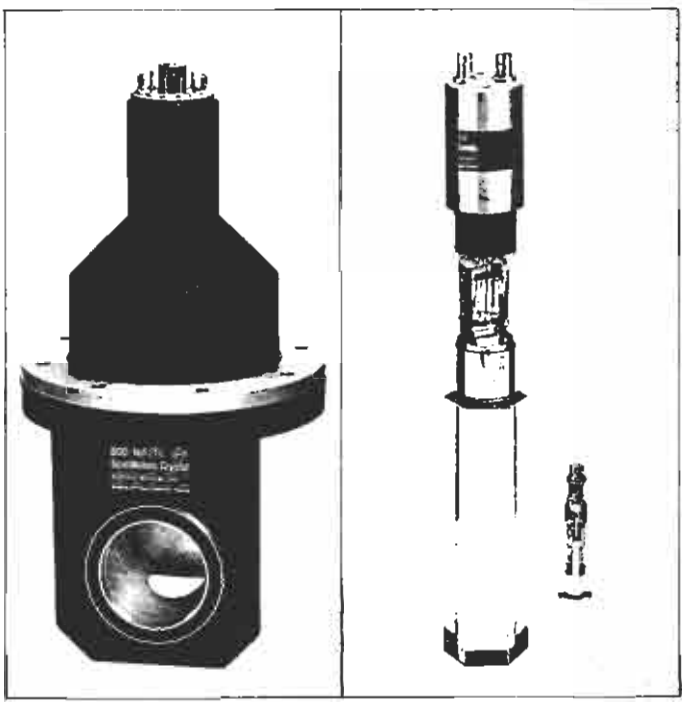

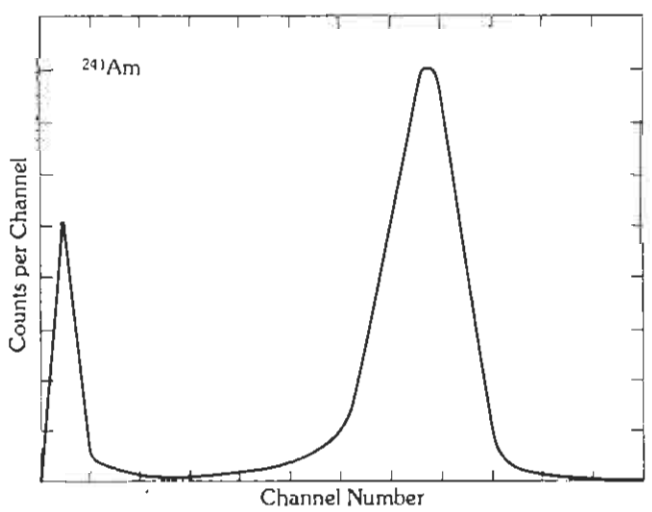

Fig. II.7. Response of a BGO detector to the α radiation of ^{241}Am.

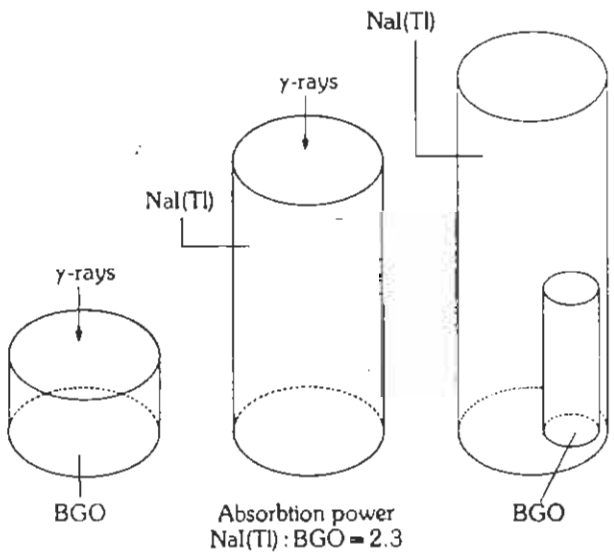

Fig. II.8. Comparable absorption power.

BGO is very useful at high energies because of its short radiation length (cf fig. II.9.). The scintillation performance of BGO approaches that of NaI(Tl) at very high energies.
Also for anti coincidence shields the reduction in volume can be a very important factor. See also fig. II.10. and Chapter V.1.

Because of the high absorption coefficient and low afterglow, BGO is well suited for use in computer tomography, industrial density gauging and well logging.

Table II.4. $Bi_4Ge_3O_{12}$ data

Light output relatve to NaI(Tl)	12—14%
Wavelength of maximum emission	480 nm
Decay constant	0.3 μs
Afterglow (after 3 ms)	0.1%
Index of refraction at 480 nm	2.15
Temperature coefficient of the light output at 300 K (negative)	1.5—1.7%/K
Thermal coefficient of linear expansion	7×10^{-6}/K
Cleavage Plane	None
Hardness (Mho)	5
Density	7.13 g/cm³
Melting point	1323 K
Hygroscopic	No

3b. $CdWO_4$

$CdWO_4$ is a scintillator which combines a high stopping power with good scintillation properties. The light output is about 40% of that of NaI(Tl). The emitted light reaches its maximum at 540 nm and the afterglow is very low. The thickness to stop 90% of 150 keV gamma's is only 3 mm for $CdWO_4$.

The wavelength and the relatively high light output makes $CdWO_4$ an attractive scintillator to use in combination with silicon photodiodes. Also since the lateral loss of the radiation is low because of the high absorption power, such units are ideal for use in devices where a good spatial resolution must be obtained.

Table II.5. $CdWO_4$ data

Light output relative to NaI(Tl)	40%
Wavelength of maximum emission	540 nm
Decay constant	5 μs → 13 μs
Afterglow (after 3 ms)	0.1%
Index of refraction at 540 nm	2.2—2.3
Temperature coefficient of the light output at 300 K (negative)	0%/K
Thermal coefficient of linear expansion	10.2×10^{-6}/K
Cleavage plane	<010>
Hardness (Mho)	4.0—4.5
Density	7.9 g/cm³
Melting point	1598 K
Hygroscopic	No

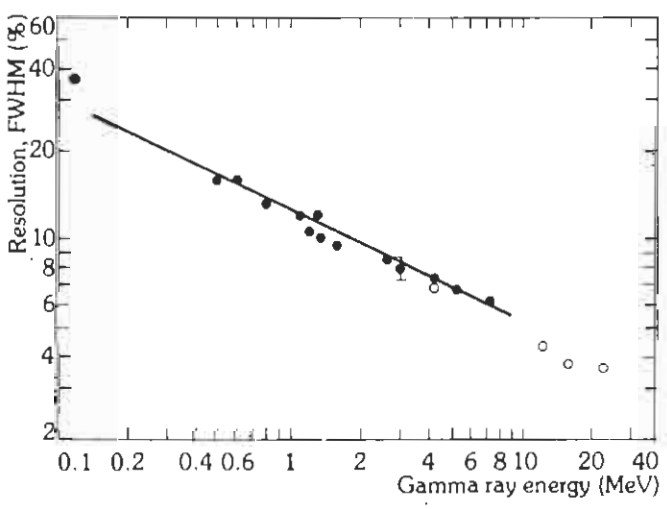

Fig. II.9. Energy resolution of the BGO detector vs gamma-ray energy.

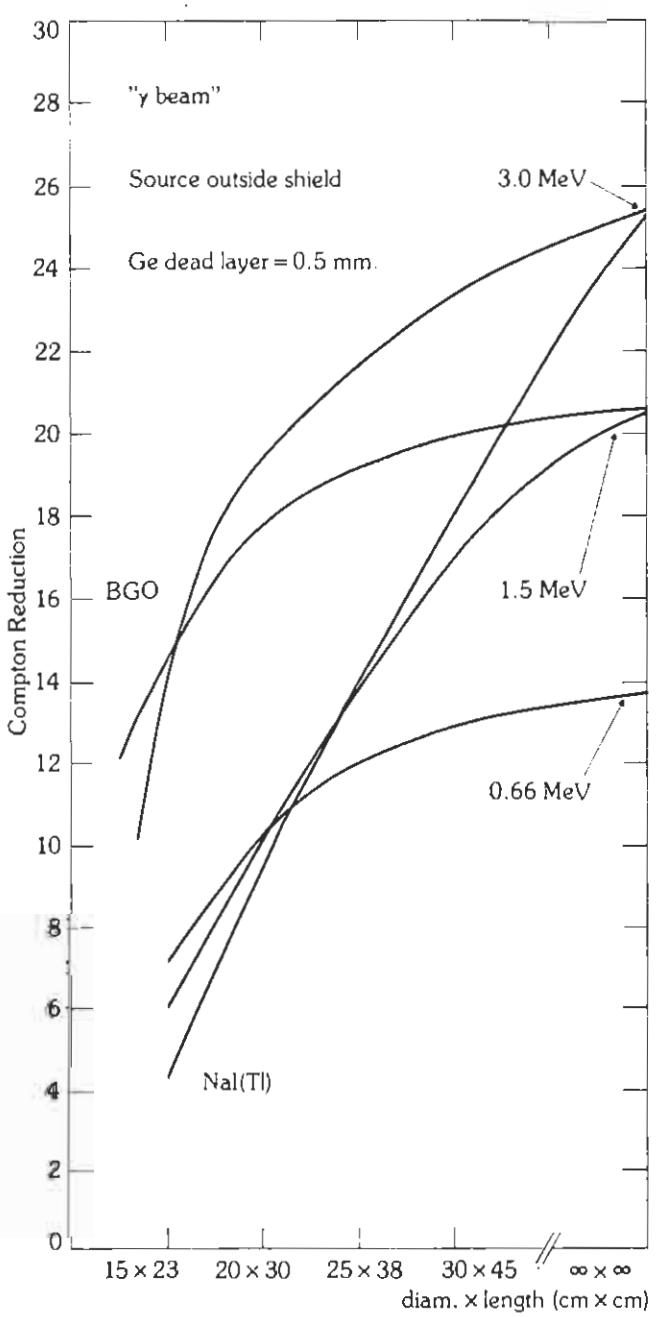

Fig. II.10. Compton reduction of BGO and NaI(Tl). Calculated!

4a. $CaF_2(Eu)$

$CaF_2(Eu)$ is a transparent, hard material useful for detecting gamma rays up to several hundred keV and charged particles in the MeV region.
Unlike many scintillation crystals, $CaF_2(Eu)$ is nonhygroscopic and relatively inert. It has sufficiently high resistance to thermal and mechanical shock for most applications and is easily fabricated into a variety of detector geometries. CaF_2 has a very low vapor pressure, allowing it to be used in a wide range of vacuum applications. It is insoluble in water and most organic solvents, permitting radioactive samples in solution to be placed in direct contact with the crystal. It is nontoxic and requires no special safety precautions in handling or packaging.
The optical properties of $CaF_2(Eu)$ contribute to its usefulness as a scintillation detector. The refractive index at emission maximum is 1.44 which closely matches the index of many optical coupling materials and photomultiplier tube face plates.
This close match in refractive index results in high light collection efficiency at the photomultiplier tube cathode. The maximum emission wavelength of 435 nm is well suited for use with S-11 or bialkali photocathode response. $CaF_2(Eu)$ transmits visible light well, but it has a sharp absorption band at 400 nm. In applications where optimum energy resolution is required, crystal lengths of less than one inch are recommended due to the self absorption of $CaF_2(Eu)$.
A gamma ray spectrum is illustrated in figure II.11. This spectrum was obtained using a $CaF_2(Eu)$ crystal coupled to a selected photomultiplier tube.

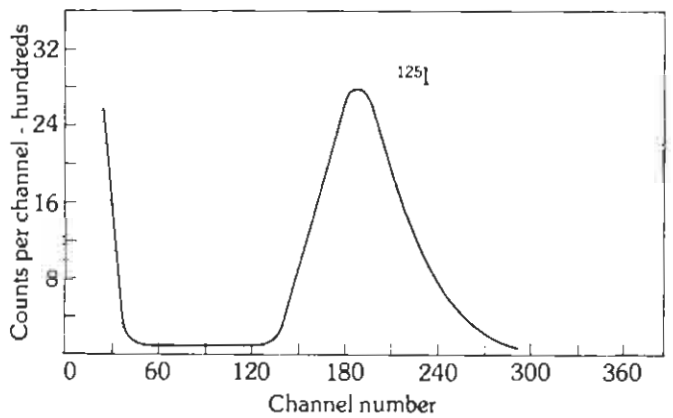

Fig. II.11. Response of $CaF_2(Eu)$ to ^{125}I gamma rays.

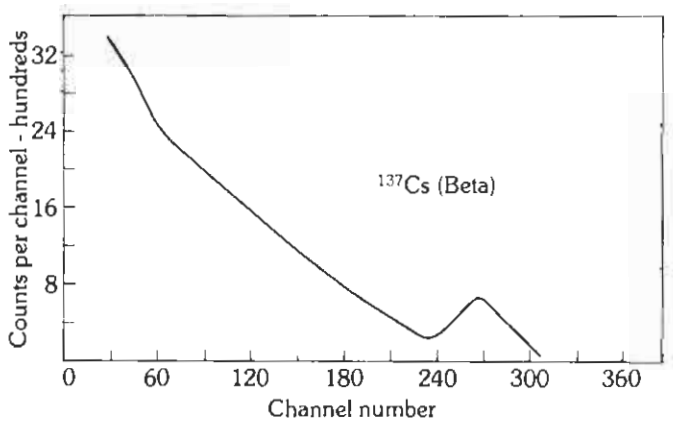

Fig. II.12. Response of $CaF_2(Eu)$ to ^{137}Cs beta particles.

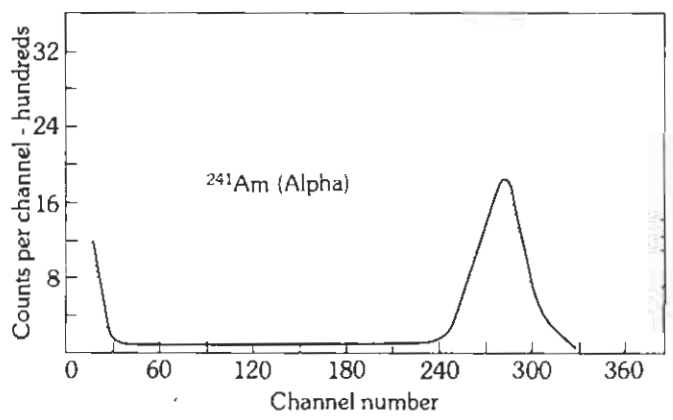

Fig. II.13. Response of $CaF_2(Eu)$ to ^{241}Am alpha particles.

Figure II.12. illustrates the ^{137}Cs internal conversion beta spectrum and figure II.13. the alpha spectrum of ^{241}Am observed in $CaF_2(Eu)$. The 5.5 MeV alpha peak appears at 1 MeV in a gamma calibrated spectrum indicating approximately 20% light output for alpha absorption relative to beta.

A notable characteristic of $CaF_2(Eu)$ is the lack of long term light decay following intense excitation, often referred to as "afterglow". This property is particularly valuable in both steady state and pulsed X-ray applications where high intensity fluxes are encountered. The decay constant of $CaF_2(Eu)$ is 0.94 μs $\pm$ 0.01 μs for gamma ray excitation. For space applications and others where it is impossible to control the environment, a parameter of considerable interest is the response of scintillation crystal to temperature. The relation of light output as a function of temperature for $CaF_2(Eu)$ is decreasing with increasing temperature at approximately ½%/°C in the range of 0 to 60°C.

Table II.6. $CaF_2(Eu)$ data

Light output relative to NaI(Tl)	50%
Wavelength of maximum emission	435 nm
Decay constant	0.94 μs
Afterglow (after 3 ms)	≤0.3%
Index of refraction at 435 nm	1.44
Temperature coefficient of the light output at 300 K (negative)	0.3—0.5%/K
Thermal coefficient of linear expansion	19.5×10^{-6}/K
Cleavage plane	<111>
Hardness (Mho)	4.0
Density	3.18 g/cm^3
Melting point	1691 K
Hygroscopic	No

4b. BaF_2

Pure BaF_2 crystals have been found to scintillate to alpha and beta particles and to gamma rays. The low solability, non-hygroscopic nature and good absorption for gamma rays make it an attractive scintillator for specific applications. BaF_2 exhibits at least two decay constants a very fast one with a low intensity at about 220 nm and another higher intensity, longer decay component at 320 nm. The linearity of response with gamma rays appears to be acceptable for most practical purposes. BaF_2 responds to alpha and beta particles

in a manner similar to $CaF_2(Eu)$. BaF_2 exhibits little self absorption of its scintillation.

Table II.7. BaF_2 data

Light output relative to NaI(Tl)	fast component	4%
	slow component	20%
Wavelength of maximum emission	slow comp.	310 nm
	fast comp.	225 nm
Decay constant	slow comp.	620 ns
	fast comp.	0.8 ns
Index of refraction at 325 nm		1.49
Thermal coefficient of linear expansion		18.4×10^{-6}/K
Cleavage plane		<111>
Hardness (Mho)		3
Density		4.88 g/cm^3
Melting point		1627 K
Hygroscopic		No

4c. CsF

Caesium Fluoride is unique among the inorganic crystals due to its time constant of ~5 ns which is comparable to that of plastic scintillators. It is the only known phosphor exhibiting both high stopping power and high count rate capability (~10 MHz).

The emission spectrum of CsF at room temperature is centered at 425 nm. Its light output is calculated to be only 5% of that of NaI(Tl). This relatively low light emission accounts for an energy resolution of 20—30% for 662 keV. CsF is used in applications where count rates are very high or where fast timing is important.

CsF is extremely hygroscopic and requires hermetic packaging and low humidity handling at all times.

Table II.8. CsF data

Light output relative to NaI(Tl)	5%
Wavelength of maximum emission	390 nm
Decay constant	5 ns
Afterglow (after 6 ms)	0.003—0.03%
Index of refraction at 589 nm	1.478
Thermal coefficient of lienear expansion	31.7×10^{-6}/K
Cleavage plane	<100>
Hardness (Mho)	2
Density	4.64 g/cm^3
Melting point	955
Hygroscopic	Yes

5. LiI(Eu)

Europium activated lithium iodide is a scintillator with several characteristics useful for neutron counting. Neutrons are detected in LiI(Eu) through their interaction with the ^{6}Li component of the crystal as given by: $n + {}^6Li \rightarrow {}^4He + {}^3H + Q$.
This reaction is particularly desirable since no gamma ray is released. For interaction with thermal neutrons, the energy division between the alpha (^{4}He) and triton (^{3}H) is uniquely defined and a rather narrow line is obtained. The alpha and triton share the Q (reaction energy) of 4.78 MeV inversely to their respective masses. Thus, the triton receives 4/7 of the total energy while the alpha receives 3/7. The neutron peak appears at approximately 3 MeV permitting effective discrimination against all natural gamma rays.
LiI(Eu) can be supplied with either the natural isotopic abundance of ^{6}Li (7.5%) or with the ^{6}Li component enriched to 96%.

The neutron stopping power of ^{6}LiI(Eu) is calculated in the following manner. Collimated neutrons incident normal to the surface of the crystal are absorbed depending upon the number of absorbing atoms present and their neutron cross section. Of the incident neutrons (I_0) the number transmitted (I) is:

$$I = I_0 e^{-\Sigma_i N_i \sigma_i X} = I_0 e^{-\mu X}$$

where μ is the linear absorption coefficient per centimeter thickness and X is the thickness in centimeters of the crystal.
For each type of atom present, there is a corresponding absorption coefficient $N.\sigma$, which quantitatively is the reaction cross section σ times N, the number atoms/cm^3 of each type.
Thus, μ represents the summation of absorption coefficients for the different types of atoms present. These atoms are ^{6}Li, ^{7}Li, iodine and the europium activator (assumed to be of constant and natural isotopic abundance)

The effect of neutron capture in iodine (6.3 barns per atom) and in europium (4300 barns per atom) is not negligible. In fact, the competition of these reactions limits the efficiency of both normal and enriched lithium iodide. This capture in iodine produces another isotope with release of neutron capture gamma rays which usually escape the crystal or produce pulses that are not counted by the electronic circuitry.
The fraction of all neutrons which liberate 4.8. MeV in the crystal is given by:

$$\frac{(N.\sigma)_{^6Li}}{\mu}$$

It follows that for normal LiI(Eu), $\mu = 1.47$ cm^{-1}, so that a thickness of 2 cm to 4 cm is required for total absorption of thermal neutrons. For ^{6}LiI(Eu), $\mu = 16.7$ cm^{-1}, a thickness of 0.2 cm to 0.3 cm gives total absorption of thermal neutrons.

Table II.9. LiI(Eu) data

Light output relative to NaI(Tl)		35%
Wavelength of maximum emission		470 nm
Decay constant	γ radiation	0.6 μs
	n-radiation	1.4 μs
Index of refraction at 470 nm		
Thermal coefficient of linear expansion		40×10^{-6}/K
Cleavage plane		<100>
Hardness (Mho)		2
Density		4.08 g/cm^3
Melting point		719 K
Hygroscopic		Yes

III. HARSHAW MOUNTINGS OF SCINTILLATION PHOSPHORS

Contents

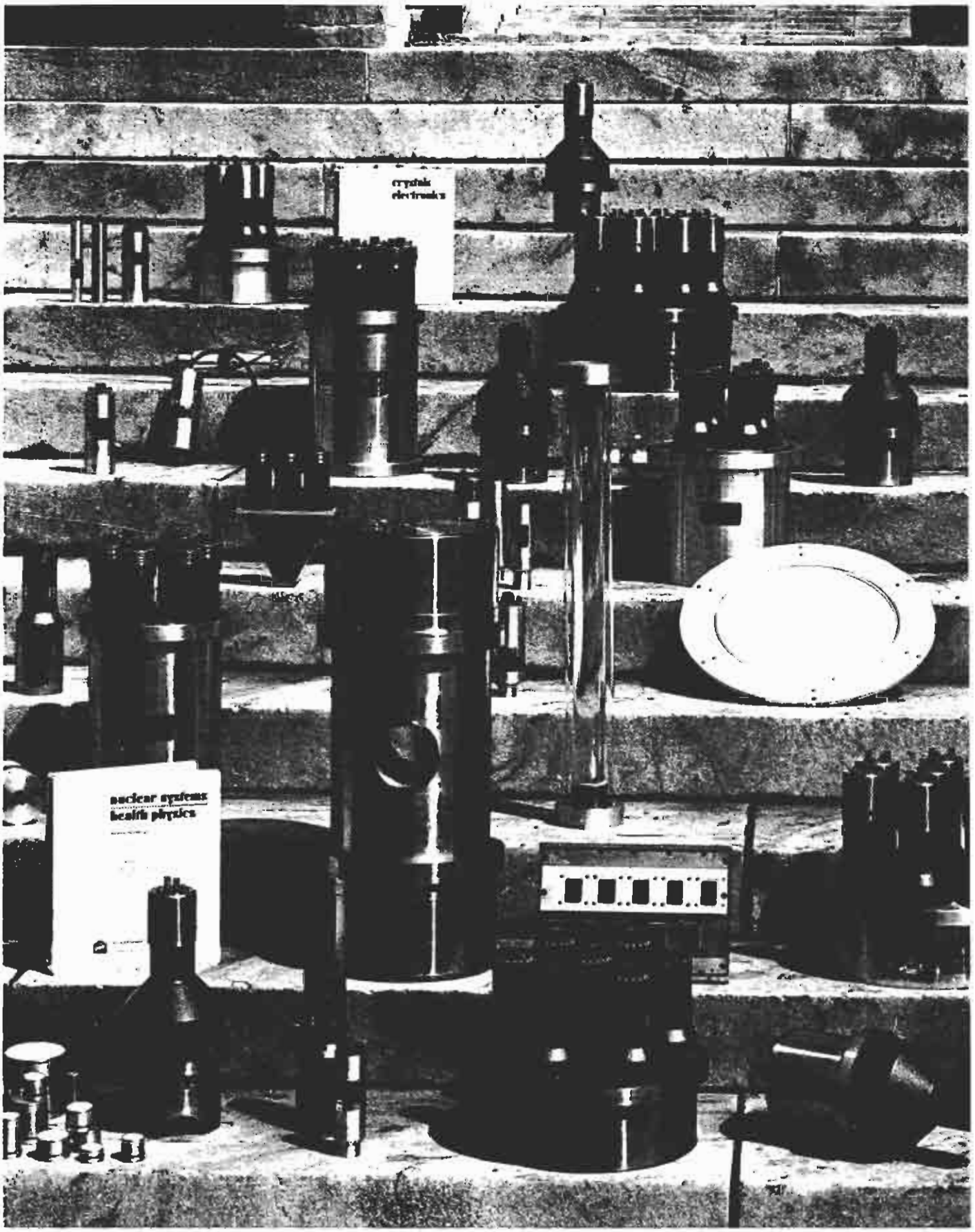

Harshaw mounted scintillation crystals.

III. HARSHAW MOUNTINGS OF SCINTILLATION PHOSPHORS

1a. Introduction

The proper mounting of scintillation crystals is a science combining advanced design and engineering skills with proven assembly techniques and materials to produce stable, high resolution radiation detectors. Of critical importance is the packaging of hygroscopic crystals which require hermetic sealing at all times. All Harshaw assemblies incorporate proven design, materials and manufacturing techniques to ensure the reliability of each hermetic seal over extended periods of time and operating conditions. Additionally, each welded seal and optical interface is carefully constructed to attain the high standards of performance and durability demanded by the nuclear industry.
Since 1950, the company has pioneered the design and production techniques that have become accepted as standards throughout the detector industry. The company was the first manufacturer to commit large-scale research and development to scintillation crystal technology.
The following pages contain useful information and detailed specifications for the various types of Harshaw mounted scintillation phosphors.

STANDARD LINE, INTEGRAL LINE AND MATCHED WINDOW LINE assemblies are designs pioneered by Harshaw/Filtrol to fulfill most radiation counting requirements. Examples of special assemblies are also included to demonstrate the unique crystal geometries and housings available for specialized applications.

1b. General conditions

Harshaw detectors can be stored at temperatures from −15°C to +45°C. Care has to be taken however that the temperature gradient is not more than 5°C per hour. This is also valid while unpacking the crystals after arrival.
Typical operating temperatures for Harshaw scintillation detectors are between 5°C and 45°C.

The mechanical shock resistance of a detector depends on the scintillation material selected, the dimensions of the scintillator and the mechanical strength of the encapsulating hardware. This resistance can range from a few g's to 50 g with specially built units. If special temperature or shock requirements are needed, Harshaw/Filtrol's expert technical staff can assist in designing detectors which meet your requirements, you should put these requirements to the Harshaw/Filtrol experts for a solution.

1c. Warranty

Each Harshaw scintillation detector is manufactured from high quality crystals, treated with skills necessary to obtain the best possible resolution and assembled and packaged in accordance with advanced design and engineering techniques.

When used in a normal laboratory environment, all Harshaw scintillation detector assemblies carry a two year warranty against detector malfunction due to faulty construction or failure of the hermetic seal(s).
Photomultiplier tubes carry the manufacturer's warranty extended from date of shipment from Harshaw/Filtrol. Each detector assembly is tested prior to shipment and is accompanied by a "Harshaw/Filtrol Test Report" bearing the performance specifications of the detector at the time of shipment. These records are permanently maintained by Harshaw/Filtrol for future reference.
Detector assemblies designed for use in field applications where severe thermal and mechanical shock conditions may be encountered carry a specific warranty under terms agreed upon by Harshaw/Filtrol and the customer.
Scintillation detectors designed for use in a normal laboratory environment will operate reliably between 5°C and 45°C provided the rate of temperature change does not exceed 5°C/hour.
With reasonable handling and care your detector will provide you with many years of satisfactory service. In the event you have any questions concerning your unit, please feel free to contact your local Harshaw/Filtrol representative.

1d. Explanation drawing of Nomenclature.

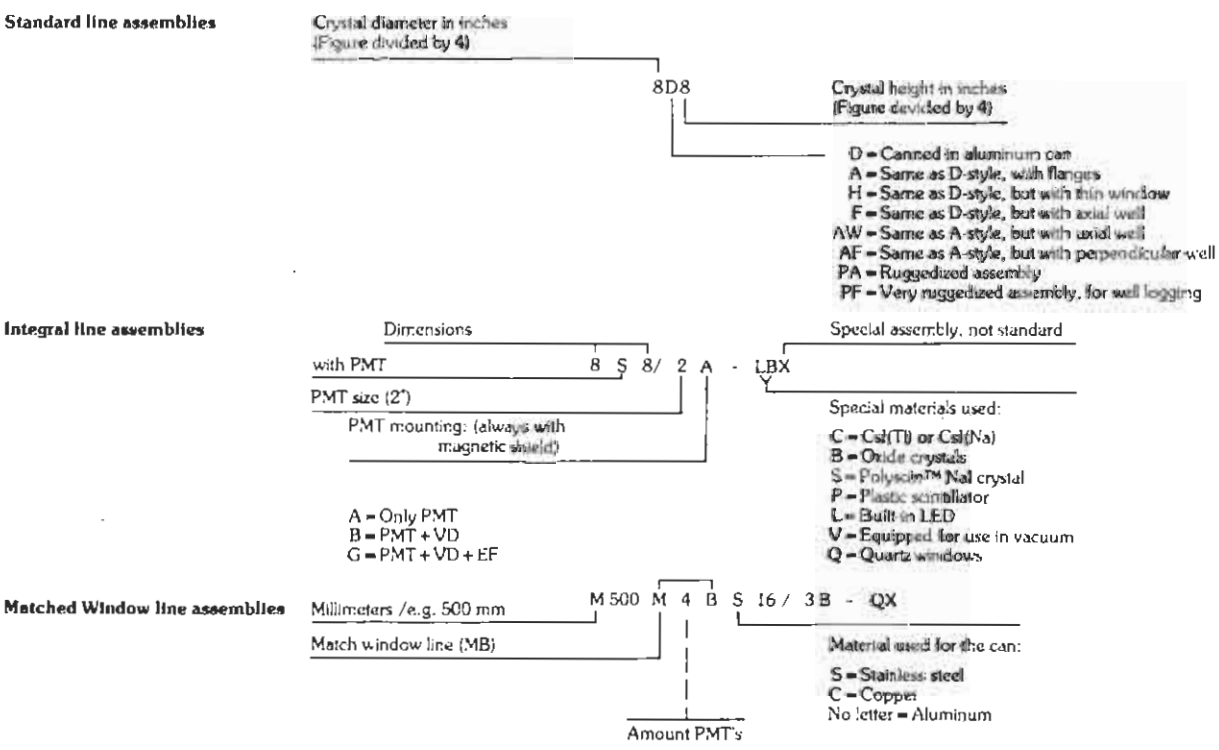

2a. Standard Line assemblies

The housings for all of the STANDARD LINE assemblies can be fabricated from aluminum or from low background material such as stainless steel or electrolytic copper.

The units can also be provided with lightpipes of quartz or pure sodium iodide when it is desirable to provide a beta and/or gamma-ray filter between the ^{40}K of the phototube and the scintillator. Where stainless steel background well-type assemblies are requested we advise that the well component of the low background assembly is fabricated with thin aluminium.

Some geometries may require light pipes to enhance the energy resolution.

D

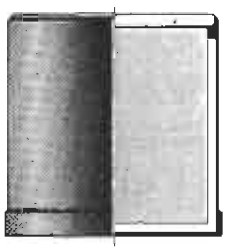

Fig. III.1.

A

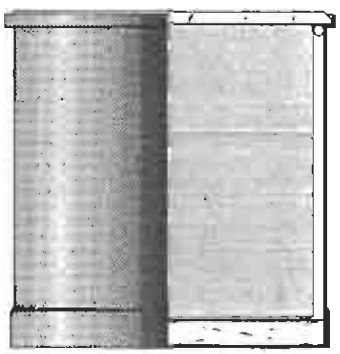

Fig. III.2.

H

Fig. III.3.

F

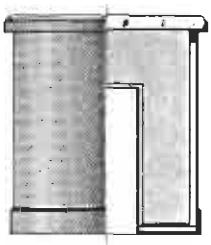

Fig. III.4.

AW

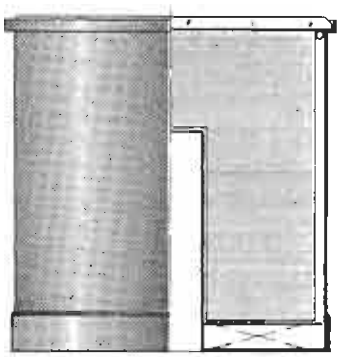

Fig. III.5.

AF

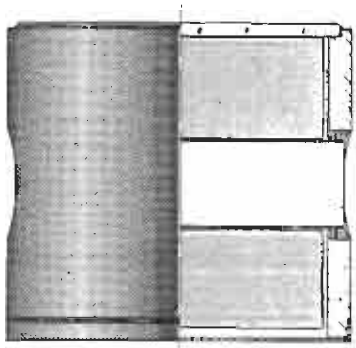

Fig. III.6.

PA

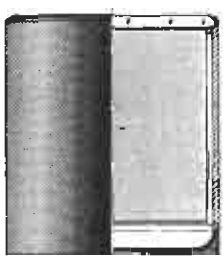

Fig. III.7.

PF

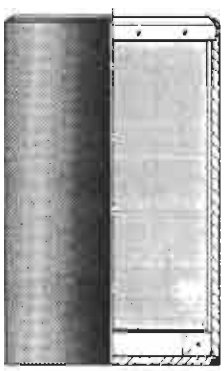

Fig. III.8.

2b. Integral Line assemblies

The Integral Line Assembly has been widely accepted by scientists dealing with ionizing radiation in all kinds of institutes. A number of advantages of this kind of assembly have been mentioned in the introduction above.

Phototubes most often used are listed in table I.2. (chapter I). One of the most standardized integral units is the 3" × 3" Integral Line assembly. This detector has been widely accepted by scientists all over the world because of its excellent resolution and efficiency. Harshaw standard 3" × 3" Integral Line assemblies have energy resolutions at 662 keV of 7.0% or better.

S

Fig. III.10.

S

Fig. III.11.

S

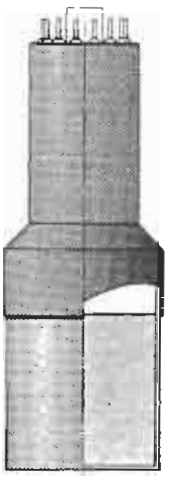

Fig. III.12.

SW

Fig. III.13.

SAF

Fig. III.14.

2c. Matched Window Line assemblies
Harshaw MATCHED WINDOW LINE detector assemblies can be described as demountable crystal/tube combinations, incorporating crystals of 5" diameter and larger and photomultiplier tubes of 3" to 5" diameter. Each of the P.M. tubes is coupled to a window of glass, Vycor or quartz of the same diameter by means of a silicon grease optical interface. The area of the crystal not viewed by the photomultiplier tube(s) is covered with highly reflective material, assuring maximum light collection efficiency in each MATCHED WINDOW LINE detector.
MATCHED WINDOW LINE assemblies incorporating NaI(Tl) crystals up to 81 cm diameter are presently available from Harshaw/Filtrol.

MATCHED WINDOW LINE detectors are generally more rugged than STANDARD LINE TYPE-D-assemblies and INTEGRAL LINE detectors. Proper shock mounting hardware and thermal insulation should be employed before using MATCHED WINDOW LINE detectors in field applications.

As the diameter and the length of a crystal increases, the number of PMT's recommended also increases. In some cases it is desirable to "close-pack" the tube array because of interference between individual magnetic shields. In these instances a common magnetic shielding dome is often employed.

MB

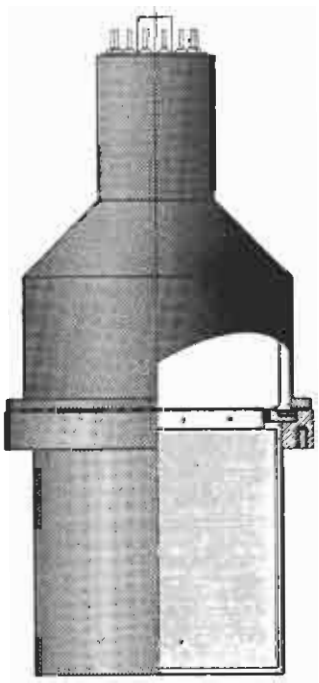

Fig. III.15.

MB

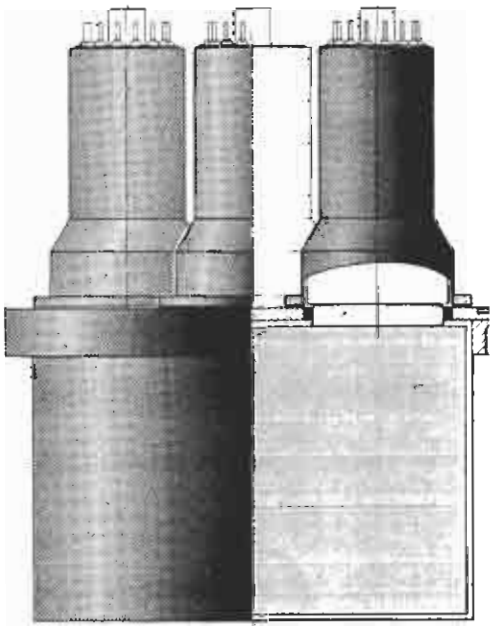

Fig. III.16.

2d. Special assemblies

Harshaw/Filtrol produces several lines of special detectors to fulfil particular application requirements. These assemblies are noted for unique crystal and housing geometries and the special materials and assembly techniques used in their construction.

Several examples of special detectors are described and illustrated in the following sections.

The routine production of these assemblies is based on new and increasing applications for designs that until recently were considered "one-of-a-kind" and limited to the research laboratory.

To keep pace with the rapid growth of the nuclear industry, an important share of Harshaw/Filtrol personnel and facilities are committed to designing and developing custom assemblies. These detectors are instrumental in obtaining new data from experimental studies and previously inaccessable environments. The results are ultimately seen in the creation of new applications and technologies.

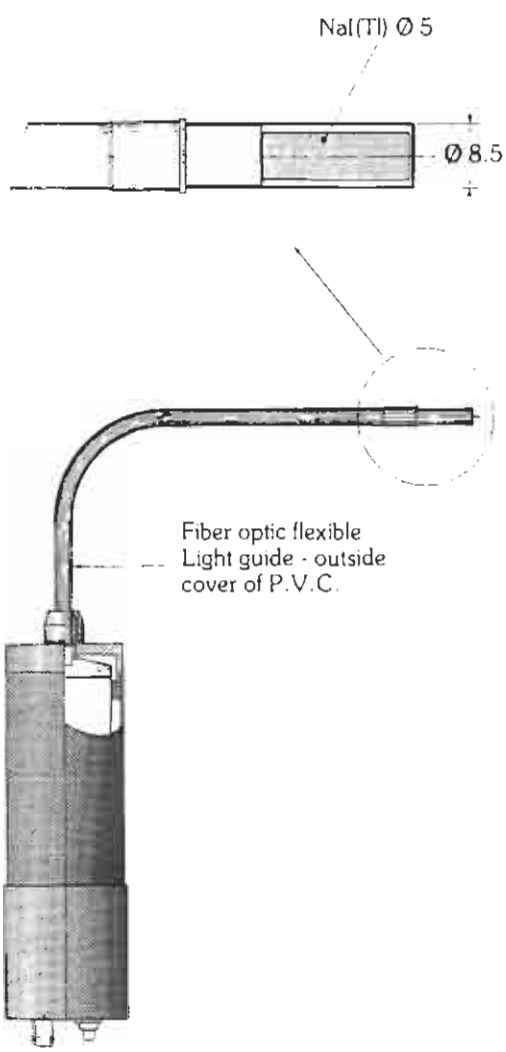

Fig. III.17. Flexible light guide probe

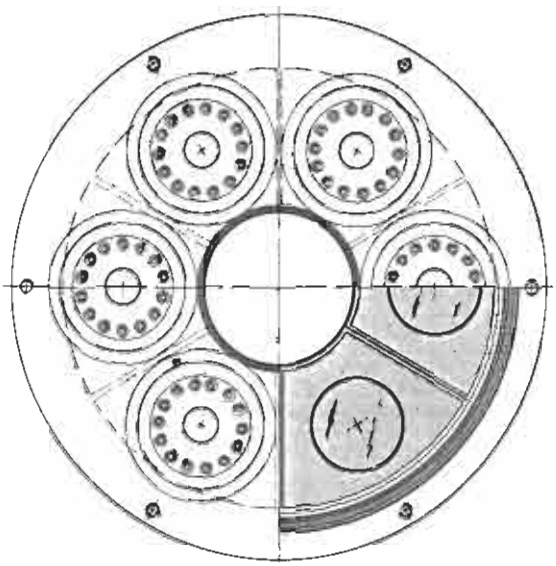

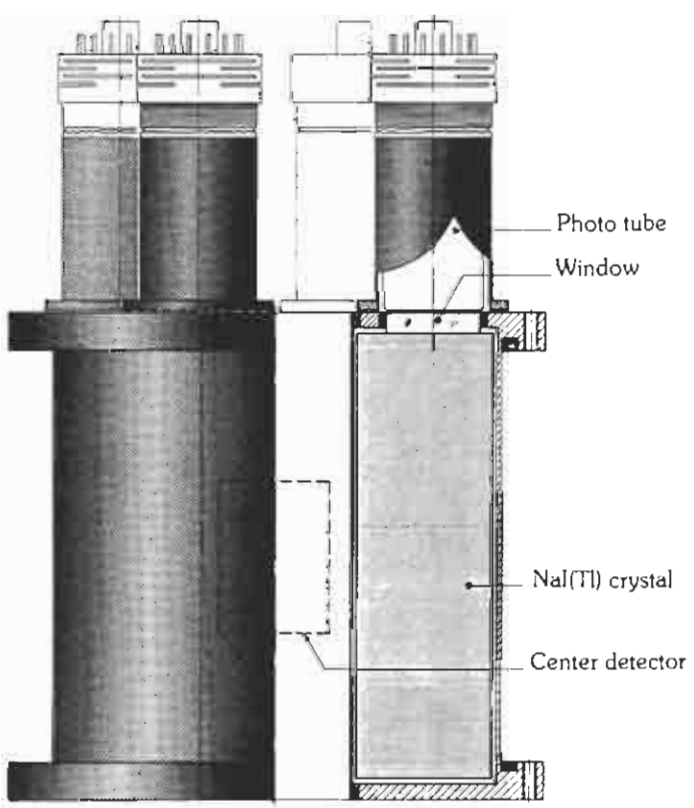

Fig. III.18. Sum spectrometer

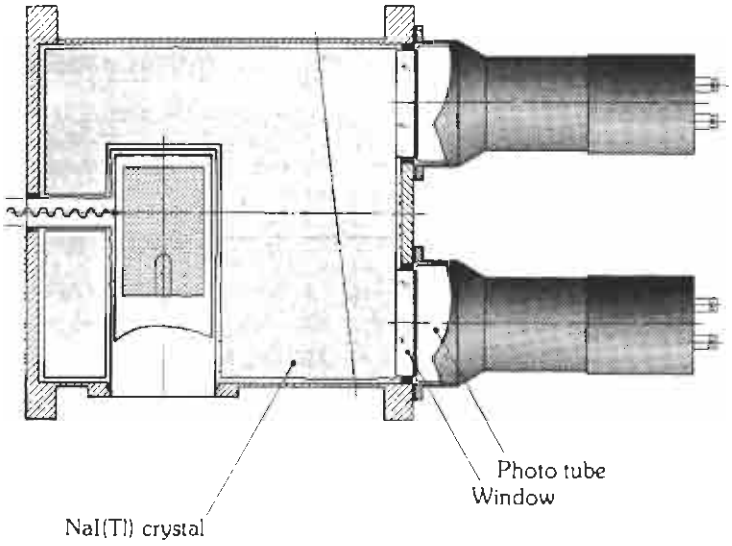

Fig. III.19. NaI(Tl) Anti Compton shield

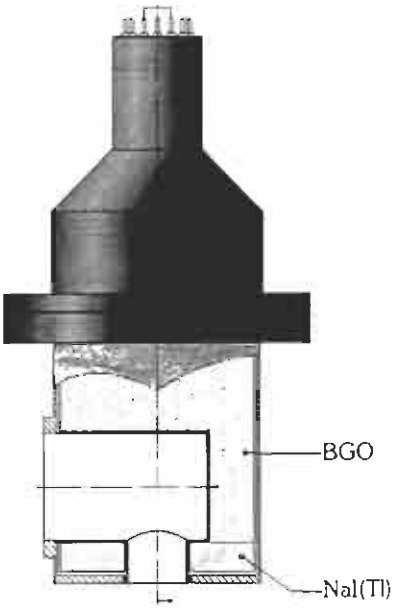

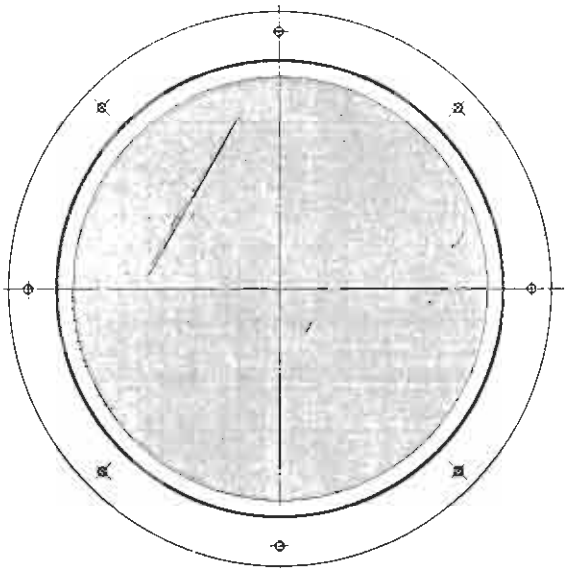

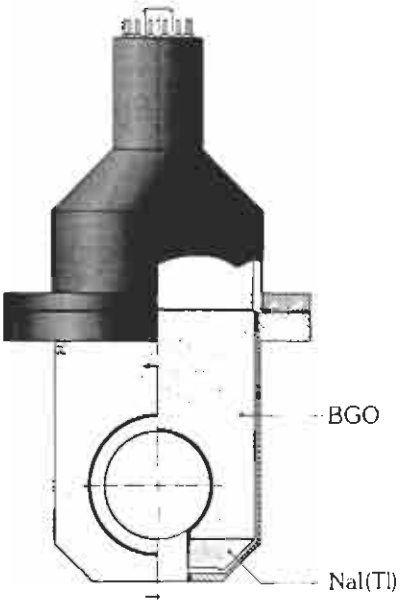

Fig. III.20. BGO Anti Compton shield

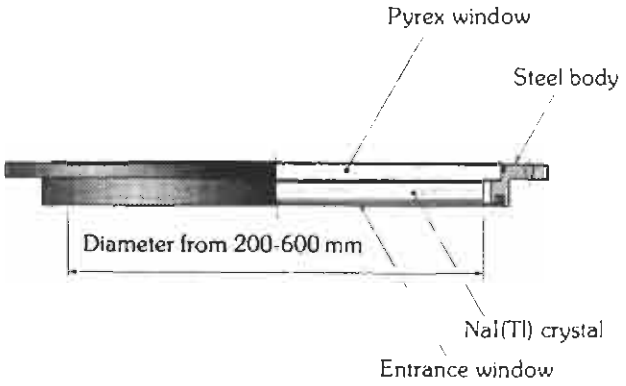

Fig. III.21. Gamma camera crystals

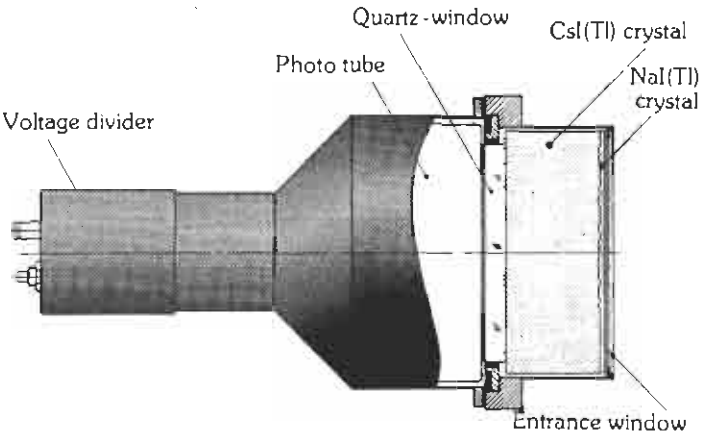

Fig. III.22. Phoswich detectors

2e. Accessories

2e.1. Photomultipliers

In principle Harshaw/Filtrol can use any photomultiplier available. In practice PMT's are usually selected for application or for special customer requirements.
For special applications, photodiodes can be mounted. (see also table I.2.)

2e.2. PMT bases

a. "Plug-on" base

The "plug-on" base contains the voltage divider network necessary for a proper functioning of the photomultiplier tubes.
It is made of aluminium and incorporates the socket of the photomultiplier tube.

The standard "plug-on" base has a gain potentiometer, MHV high voltage connector and BNC signal connector.

The following options are available:
1. An extra dynode output for fast timing applications.
2. A focus potentiometer adjustable for optimum resolution.
3. An emitter follower can also be supplied. In this case two extra leads for 12 to 20 V supply are provided.
4. A SHV high voltage connector.
5. A stainless steel housing.

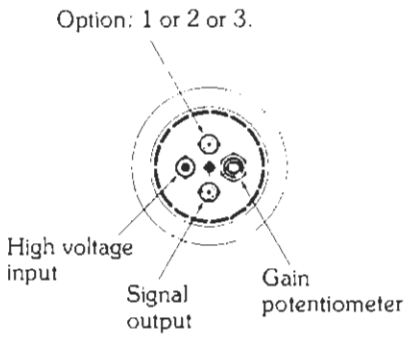

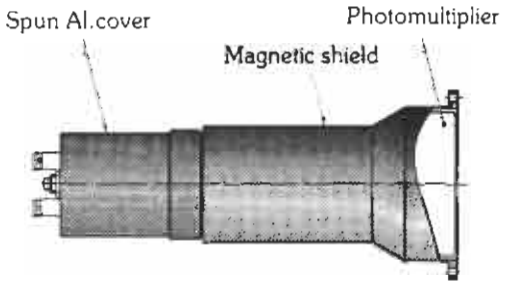

Fig. III.23. Outline of standard "plug-on" base.

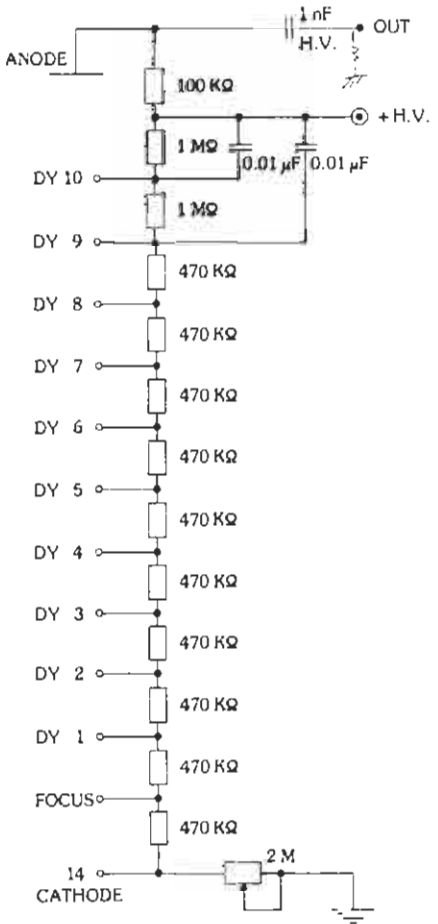

Fig. III.24. Standard voltage divider network.

2e.2b. "Low-background" tube base

All Harshaw INTEGRAL LINE and MATCHED WINDOW LINE assemblies can be equipped with so called "low-background" tube bases. The low-background base replaces the normal tube base, which may contain very faint traces of thorium contributing to the background of the assembly.

The low-background base consists of a stainless steel cap incorporating the voltage divider and if necessary also the emitter follower circuitry.

The low-background base cannot be removed from the assembly since the voltage divider resistors are directly soldered to the wires of the photomultiplier tube.

2e.3. Electronics

Besides the detectors with their voltage dividers/emitter followers, Harshaw/Filtrol also supplies a range of NIM electronics to operate these detectors:

NB-11:	Charge sensitive preamplifier
NB-15X:	Same as NB-11, but in a plug-on version
NA-17:	Amplifier
NA-23:	Stabilized amplifier/analyzer, used for detectors with ^{241}Am pulsers
NV-32A:	High voltage supply
NV-25A:	High voltage supply for more PMT's
NHD:	High voltage distributor box for 2—6 outputs, individually adjustable
NC-26R:	Time analyzer for use in an anticompton gamma spectrometer
NC-25A:	Pulse shape analyzer
NH-85:	NIM bin and power supply for 12 one width modules
NR-25, NR-30:	Logarithmic and linear ratemeters
NS-12, NS-30:	Scalers
NT-27:	Timer

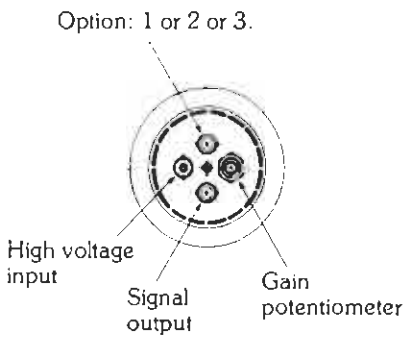

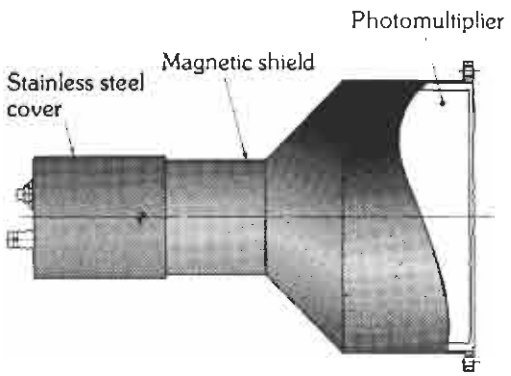

Fig. III.25. Low-background base.

IV. GENERAL TECHNICAL INFORMATION

Contents:

Periodic Table of the Elements

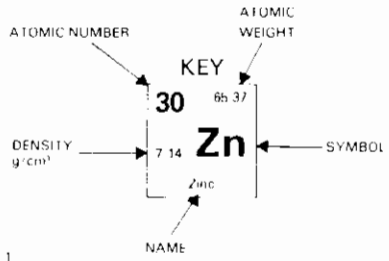

GROUP IA	IIA	IIIB	IVB	VB	VIB	VIIB	VIII			IB	IIB	IIIA	IVA	VA	VIA	VIIA	VIIIA
1 1.00797																	2 4.0026
0.071 H																	0.126 He
Hydrogen																	Helium
3 6.939	4 9.0122											5 10.811	6 12.01115	7 14.0067	8 15.9994	9 18.9984	10 20.183
0.53 Li	1.85 Be											2.34 B	2.26 C	0.81 N	1.14 O	1.505 F	1.20 Ne
Lithium	Beryllium											Boron	Carbon	Nitrogen	Oxygen	Fluorine	Neon
11 22.9898	12 24.312											13 26.9815	14 28.086	15 30.9738	16 32.064	17 35.453	18 39.948
0.97 Na	1.74 Mg											2.70 Al	2.33 Si	1.82w P	2.07 S	1.56 Cl	1.40 Ar
Sodium	Magnesium											Aluminum	Silicon	Phosphorus	Sulfur	Chlorine	Argon
19 39.102	20 40.08	21 44.956	22 47.90	23 50.942	24 51.996	25 54.938	26 54.938	27 58.933	28 58.71	29 63.54	30 65.37	31 69.72	32 72.59	33 74.96	34 78.96	35 79.909	36 83.80
0.86 K	1.55 Ca	2.0 Sc	4.51 Ti	6.1 V	7.19 Cr	7.43 Mn	7.86 Fe	8.9 Co	8.9 Ni	8.96 Cu	7.14 Zn	5.91 Ga	5.32 Ge	5.72 As	4.79 Se	3.12 Br	2.6 Kr
Potassium	Calcium	Scandium	Titanium	Vanadium	Chromium	Manganese	Iron	Cobalt	Nickel	Copper	Zinc	Gallium	Germanium	Arsenic	Selenium	Bromine	Krypton
37 85.47	38 87.62	39 88.905	40 91.22	41 92.906	42 95.94	43 (98)	44 101.07	45 102.905	46 106.4	47 107.870	48 112.40	49 114.82	50 118.69	51 121.75	52 127.60	53 126.904	54 131.30
1.53 Rb	2.6 Sr	4.47 Y	6.49 Zr	8.4 Nb	10.2 Mo	11.5 Tc	12.2 Ru	12.4 Rh	12.0 Pd	10.5 Ag	8.65 Cd	7.31 In	7.30 Sn	6.62 Sb	6.24 Te	4.94 I	3.06 Xe
Rubidium	Strontium	Yttrium	Zirconium	Niobium	Molybdenum	Technetium	Ruthenium	Rhodium	Palladium	Silver	Cadmium	Indium	Tin	Antimony	Tellurium	Iodine	Xenon
55 132.905	56 137.34	57 138.91 *	72 178.49	73 180.948	74 183.85	75 186.2	76 190.2	77 192.2	78 195.09	79 196.967	80 200.59	81 207.37	82 204.37	84 208.980	84 (210)	85 (210)	86 (222)
1.90 Cs	3.5 Ba	6.17 La	13.1 Hf	16.6 Ta	19.3 W	21.0 Re	22.6 Os	22.5 Ir	21.4 Pt	19.3 Au	13.6 Hg	11.85 Tl	11.4 Pb	9.8 Bi	(9.2) Po	(302) At	Rn
Cesium	Barium	Lanthanum	Hafnium	Tantalum	Wolfram	Rhenium	Osmium	Iridium	Platinum	Gold	Mercury	Thallium	Lead	Bismuth	Polonium	Astatine	Radon
87 (223)	88 (226)	89 (227) **	104 (261)														
– Fr	5.0 Ra	Ac															
Francium	Radium	Actinium															

*	58 140.12	59 140.907	60 144.24	61 (147)	62 150.35	63 151.96	64 157.25	65 158.924	66 162.50	67 164.930	68 167.26	69 168.934	70 173.04	71 174.97
	6.67 Ce	6.77 Pr	7.00 Nd	Pm	7.54 Sm	5.26 Eu	7.89 Gd	8.27 Tb	8.54 Dy	8.80 Ho	9.05 Tm	6.98 Yb	9.84 Lu	7.89 Gd
	Cerium	Praseodymium	Neodymium	Promethium	Samarium	Europium	Gadolinium	Terbium	Dysprosium	Holmium	Erbium	Thulium	Ytterbium	Lutetium
**	90 232.038	91 (231)	92 238.03	93 (237)	94 (242)	95 (243)	96 (247)	97 (247)	98 (249)	99 (254)	100 (253)	101 (256)	102 (254)	103 (257)
	11.7 Th	15.4 Pa	19.07 U	19.5 Np	Pu	Am	Cm	Bk	Cf	Es	Fm	Md	No	Lw
	Thorium	Protactinium	Uranium	Neptunium	Plutonium	Americium	Curium	Berkelium	Californium	Einsteinium	Fermium	Mendelevium	Nobelium	Lawrencium

Note: Density values for gaseous elements are for liquids at the boiling point.

IV. GENERAL TECHNICAL INFORMATION

1. Interaction of gamma radiation with matter

Scintillation counters are most frequently used in the field of gamma detection and gamma spectroscopy. In these applications it is often useful to know the mode of interaction and the probability that interaction will occur.
The principal modes of interaction are the Compton effect, the photoelectric effect and pair production. These interactions occur independently from each other and comprise the total attenuation coefficient.

$$\mu = \tau_{photo} + \sigma_{Compton} + \pi_{pair}$$

(In this way additional effects as nuclear photoabsorption, Rayleigh-, Delbrück- and nuclear scattering are neglected).
In chapter I. a brief description of these three basic interactions of gamma radiation with matter is already given. Some more information about Compton scattering is given in chapter V., paragraph "Anti-Compton assemblies".
According to kinematics involved in the three dominating interactions of gamma quanta with matter, the corresponding attenuation coefficients (in cm^2/g) depend on the gamma energy and on the atomic number Z of the target as indicated in figure IV.1.

Interaction	Cross section (cm^2/g)	Depends on atomic numbers	Energy
Photoelectric absorption	τ	Z^4 to Z^5	$E^{-3.5}$ to E^{-1}
Compton scattering	σ	Z	approx. E^{-1}
Pair production	π	Z^2	ln E

In the curves given on the following pages these cross sections (in cm^2/g) are multiplied by the specific mass (in g/cm^3) for obtaining linear attenuation coefficients (in cm^{-1}). The intensity I_o of a gamma beam incident on an absorbing layer of thickness d is reduced to the transmitted intensity according to:

$$I(E) = I_o(E) \exp(-\mu(E)d)$$

The absorbed intensity is given by:

$$I_o(E) - I(E) = I_o(E)\ (1 - \exp -\mu(E)d))$$

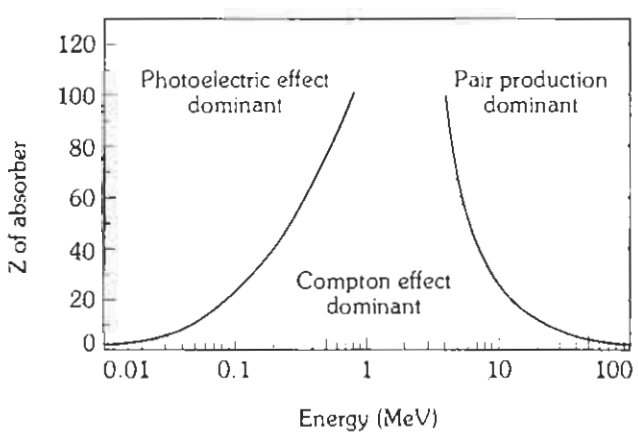

Fig. IV.1. Relative importance of the three major types of gamma ray interaction with matter.

2. Use and misuse of linear attenuation curves

The proper way to use the absorption curves displayed on the following pages is eg. to find an answer to the question: "what fraction of gamma's are left in a small diameter beam with a certain energy after passing an absorbing layer". The answer is given by the formula $I(E) = I_o(E) \exp(-\mu d)$.
Another piece of information given by the curves is: "what is the relative chance for a gamma ray to interact through Compton effect, photoelectric effect and pair production while passing through a certain medium".
What curves do not tell is: "what is the photopeak content compared to the Compton spectrum content obtained with a NaI(Tl) detector". This is not simply the values of $\tau_{photo}/\sigma_{Compton}$. The reason for this is: a lot of Compton scattered gamma's do exhibit a second photoelectric absorption within a short time and thus contribute to the photopeak content.
Another question the curves do not solve is: "what gamma intensity is left after passing a shielding layer".
The answer found through the transmission formula gives only information about gamma's of the same energy as the initial gamma's. A lot of gamma's did exhibit Compton scattering and are present behind the shielding layer with lower energy. Especially with low Z absorbers this effect is very pronounced.
These few examples make clear that one should be alert in the use of the attenuation curves.

3. Nomogram

This nomogram is a graphic display of the formula
$I/I_o = e^{-\mu d}$
and
$(I_o - I)/I_o = (1 - e^{-\mu d})$
for transmitted and absorbed gamma ray intensity. Given μ (cm^{-1}) and d (cm) one can find I/I_o and $(I_o - I)/I_o$.

In essentially the same way as for these two figures the third can be found with the nomogram.
Procedure:
1. Find the total attenuation coefficient of the relevant material at the defined energy ($\mu(E)$ in cm^{-1}).
2. Mark this data point on the μ-line.
3. Mark the thickness (d in cm) point on the d-line.
4. Draw a straight line through these two points and find the intersection with the absorption/transmission line.

The relative importance of these three processes as a function of the Z of the absorbing material and the energy of the incident gamma ray can also be plotted as illustrated in fig. IV.1.

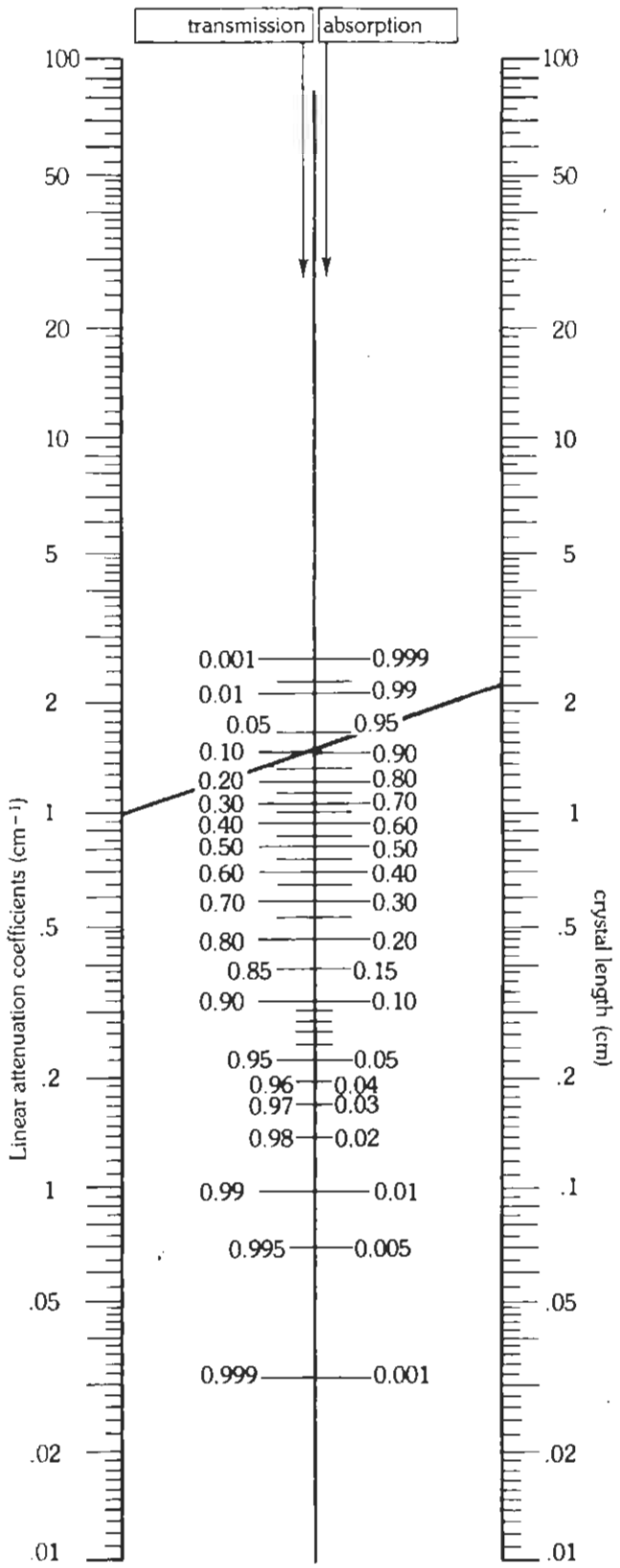

Fig. IV.2. Nomogram.
Absorption/transmission of gamma rays.

NaI

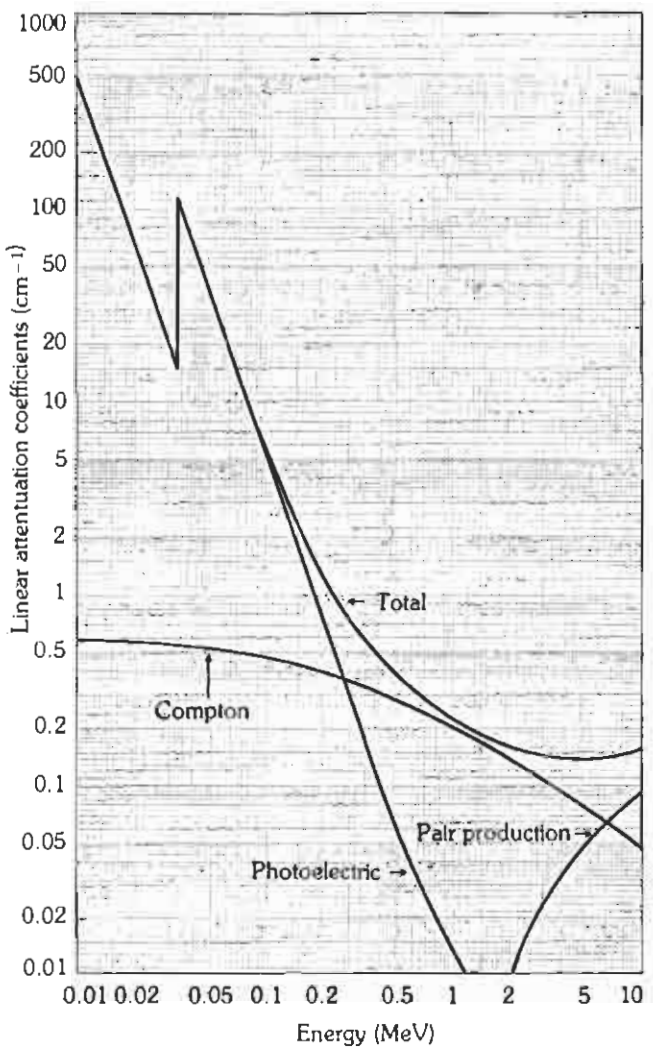

Specific mass = 3670 kg/m³
Atomic Number: Z(I) = 53
Z(Na) = 11
Electron Binding Energies:
K-edge (I) = 33.17 keV
L_I-edge (I) = 5.19 keV
L_{II}-edge (I) = 4.85 keV
L_{III}-edge (I) = 4.56 keV
Average K X-Ray Energy (I) = 29.2 keV

CsI

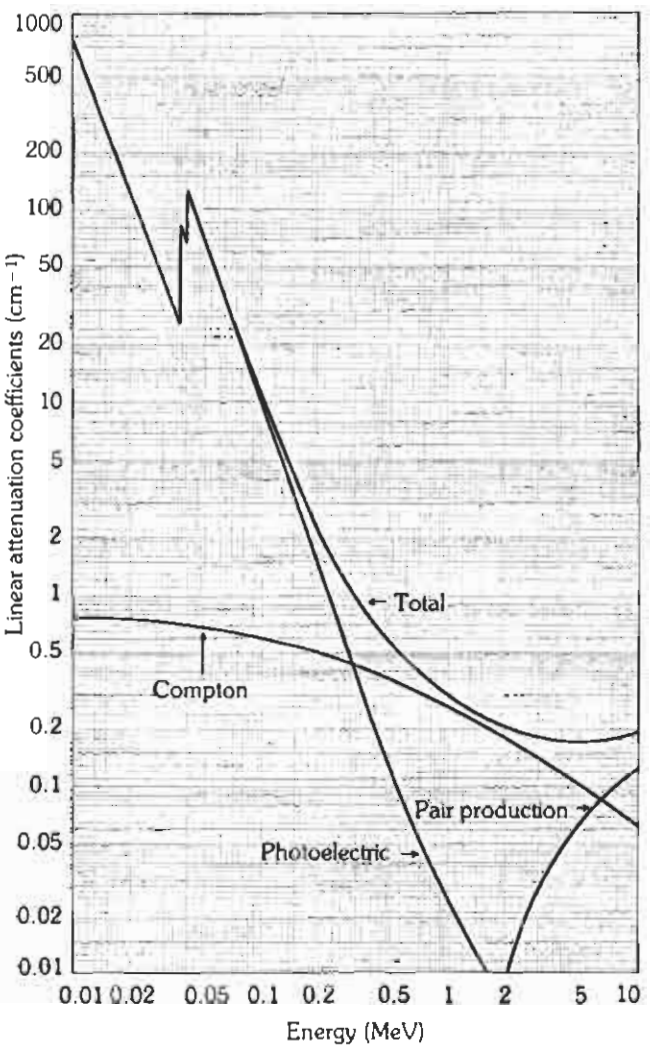

Specific mass = 4510 kg/m³
Atomic number: Z (I) = 53
Z (Cs) = 55
Electron Binding Energies:
K-edge (I) = 33.17 keV
K-edge (Cs) = 35.98 keV
L_I-edge (Cs) = 5.72 keV
L_{II}-edge (Cs) = 5.36 keV
L_{III}-edge (Cs) = 5.01 keV
Average K X-Ray Energy (Cs) = 31.6

BGO

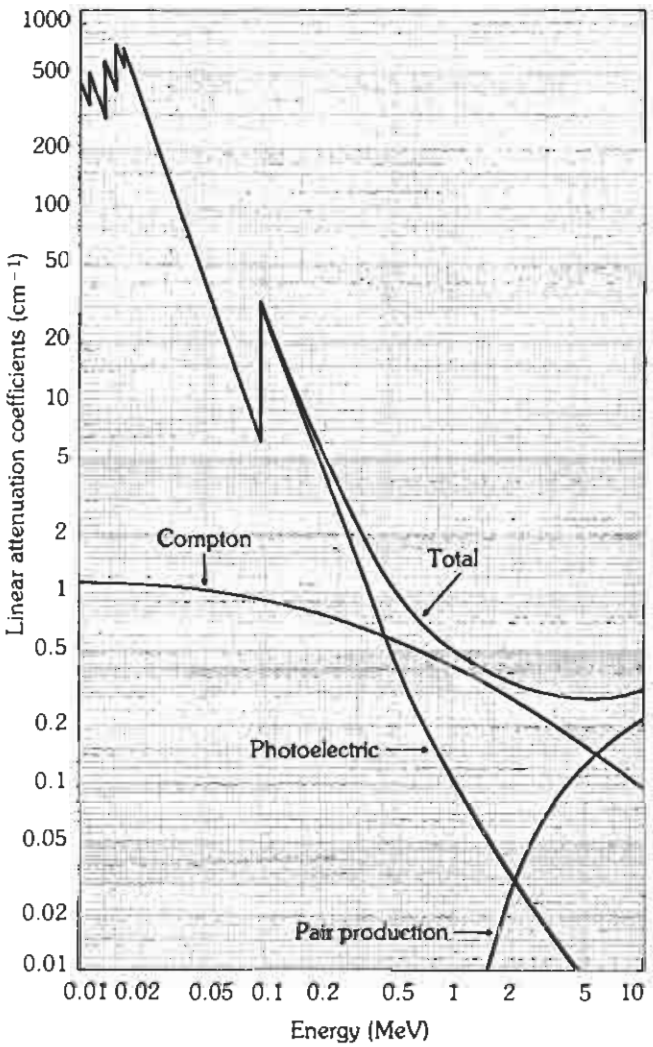

Specific mass = 7130 kg/m³
Atomic number: Z (Bi) = 83
Z (Ge) = 32
Electron Binding Energies:
K-edge (Bi) = 90.53 keV
L_I-edge (Bi) = 16.39 keV
L_{II}-edge (Bi) = 15.71 keV
L_{III}-edge (Bi) = 13.42 keV
K-edge (Ge) = 11.10 keV
Average K X-Ray Energy (Bi) = 78.9 keV

$CdWO_4$

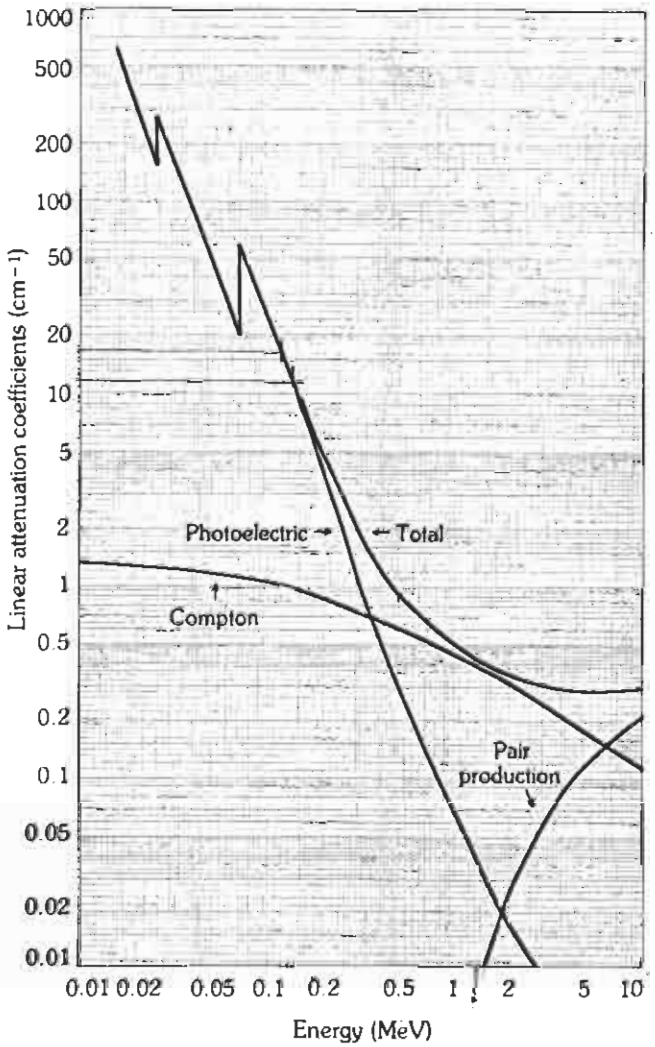

Specific mass = 7900 kg/m³
Atomic number: Z(Cd) = 48
Z(W) = 74
Electron Binding Energies:
K-edge (W) = 69.5 keV
L_I-edge (W) = 12.1 keV
L_{II}-edge (W) = 11.5 keV
L_{III}-edge (W) = 10.2 keV
K-edge (Cd) = 26.7 keV

CaF_2

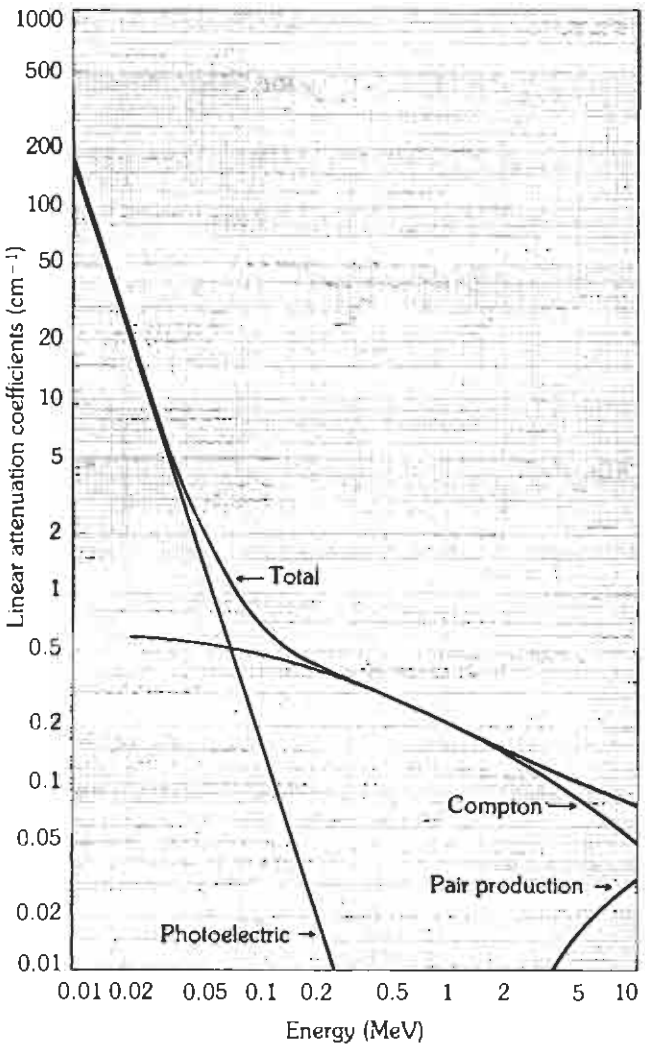

Specific mass = 3190 kg/m³
Atomic number: Z (Ca) = 20
Z (F) = 9
Electron Binding Energies:
K-edge (Ca) = 4.04 keV
K-edge (F) = 0.69 keV
Average K X-Ray Energy (Ca) = 3.7 keV

BaF_2

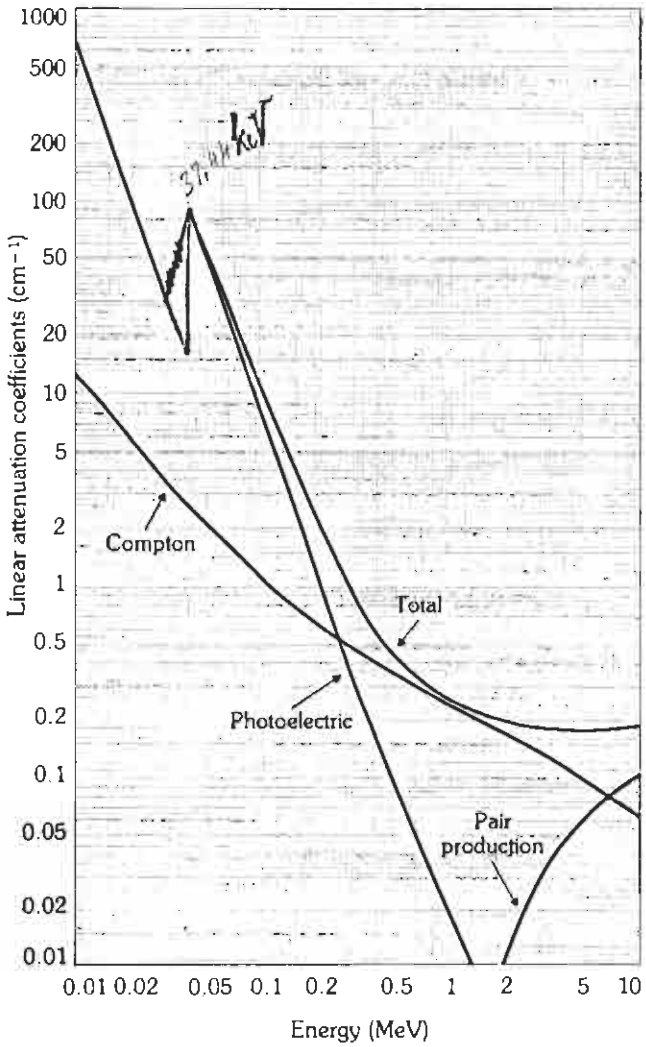

Specific mass = 4880 kg/m³
Atomic number: Z(Ba) = 56
Z(F) = 9
Electron Binding Energies:
K-edge (Ba) = 37.44 keV
L_I-edge (Ba) = 5.99 keV
L_{II}-edge (Ba) = 5.62 keV
L_{III}-edge (Ba) = 5.25 keV
K-edge (F) = 0.69keV

CsF

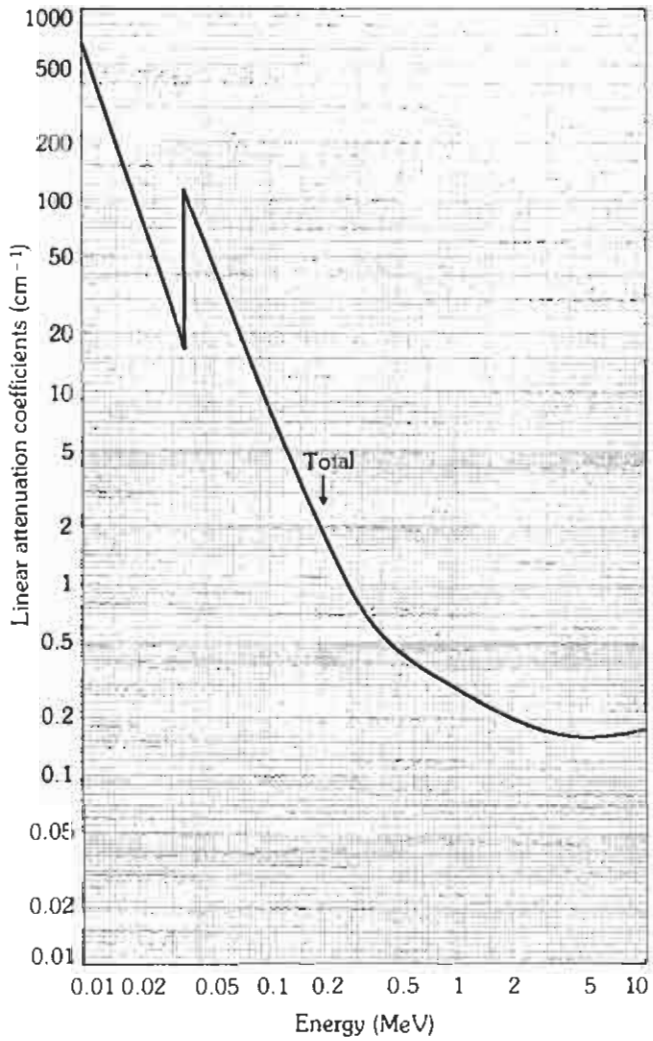

Specific mass = 4640 kg/m³
Atomic number: Z(Cs) = 55
Z(F) = 9
Electron Binding Energies:
K-edge (Cs) = 35.98 keV
L_I-edge (Cs) = 5.72 keV
L_{II}-edge (Cs) = 5.36 keV
L_{III}-edge (Cs) = 5.01 keV
K-edge (F) = 0.69 keV
Average K X-ray energy (Cs) = 31.6 keV

Plastic Scintillator

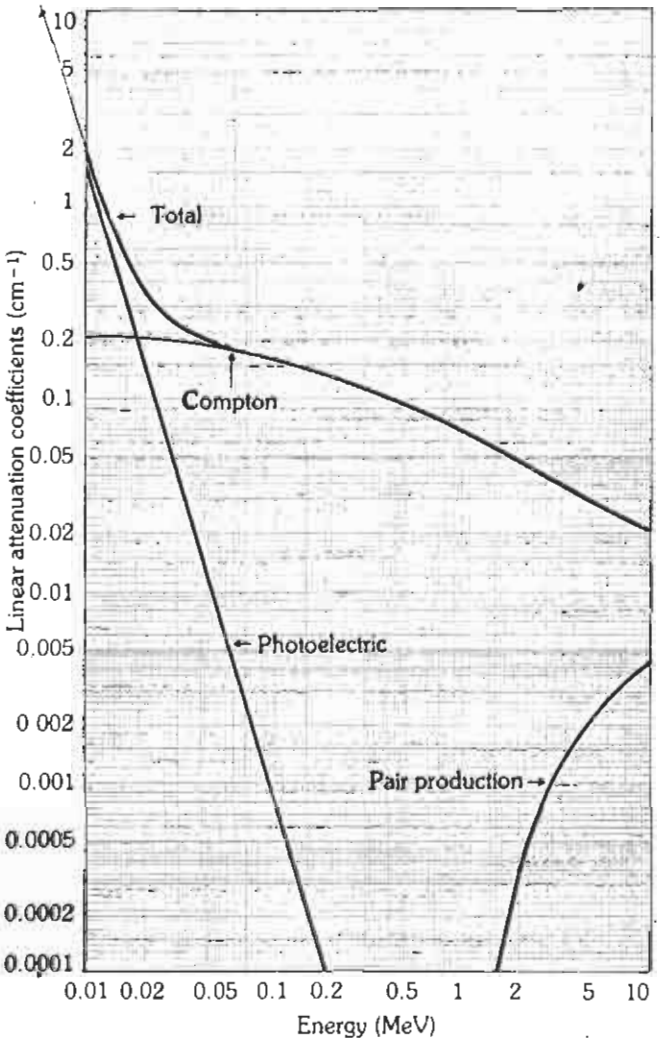

Specific mass = 1050 kg/m³
No atoms per cm³
H: 5.25×10^{22}; C: 4.75×10^{22}
N: 1.8×10^{18}; O: 1.8×10^{18}
Atomic number: Z (C) = 6
K-edge (C) = 0.28 keV

Si

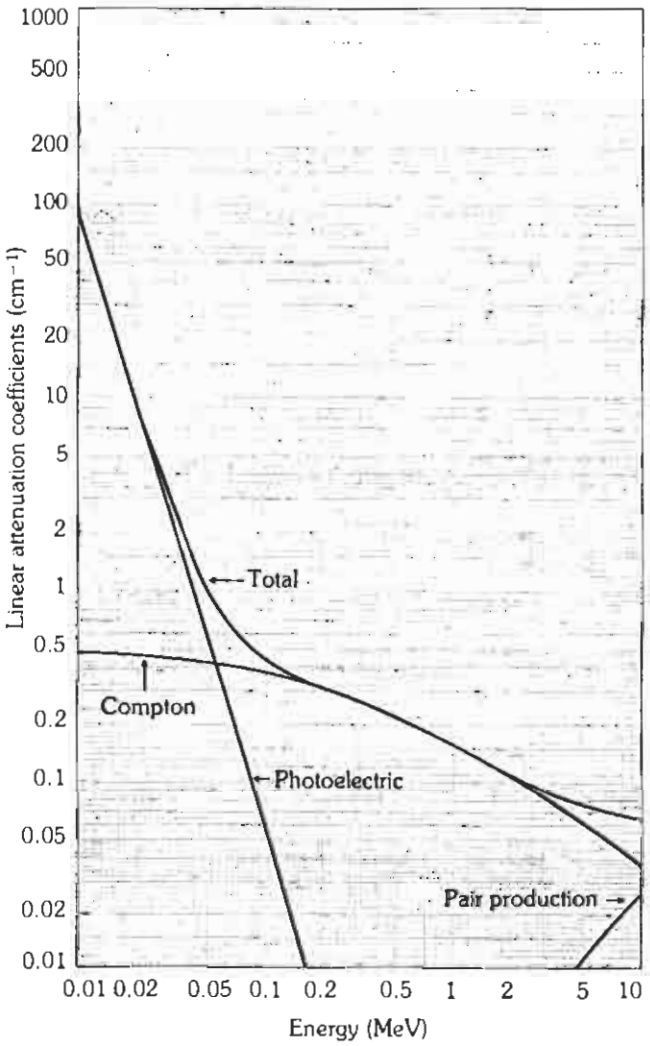

Specific mass = 2420 kg/m³
Atomic number: Z = 14
Electron Binding Energy:
K-edge = 1.84 keV
Average K X-Ray Energy: 1.75 keV

Ge

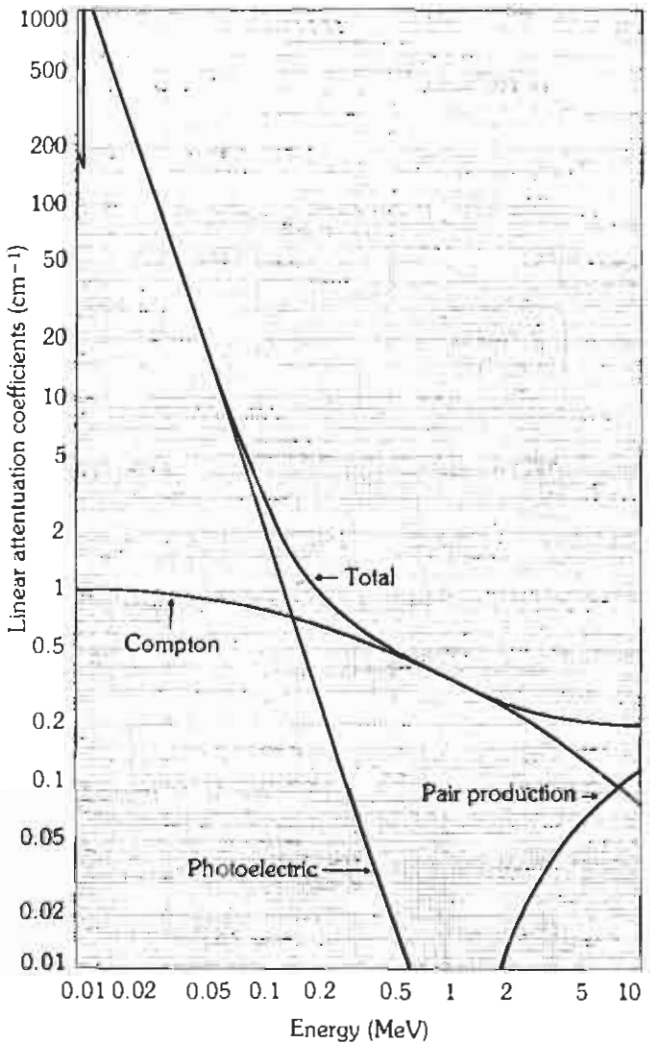

Specific mass = 5350 kg/m³
Atomic number: Z = 32
Electron Binding Energy:
K-edge = 11.1 keV
Average K X-Ray Energy = 10 keV

Be

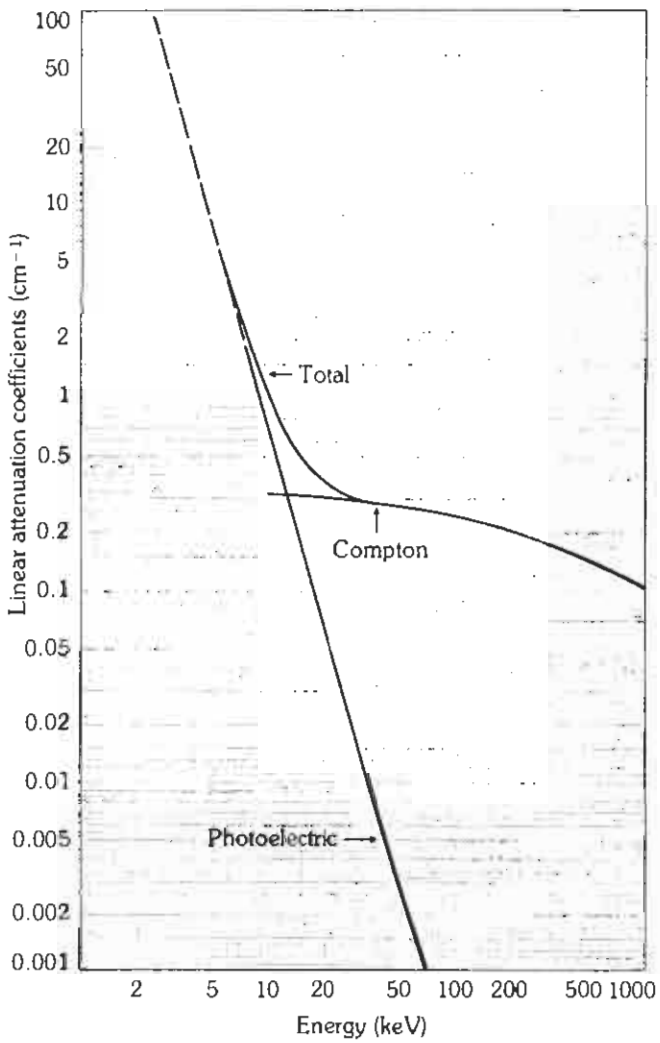

Specific mass = 1850 kg/m³
Atomic number: Z = 4
K-Binding Energy = 0.116 keV

Al

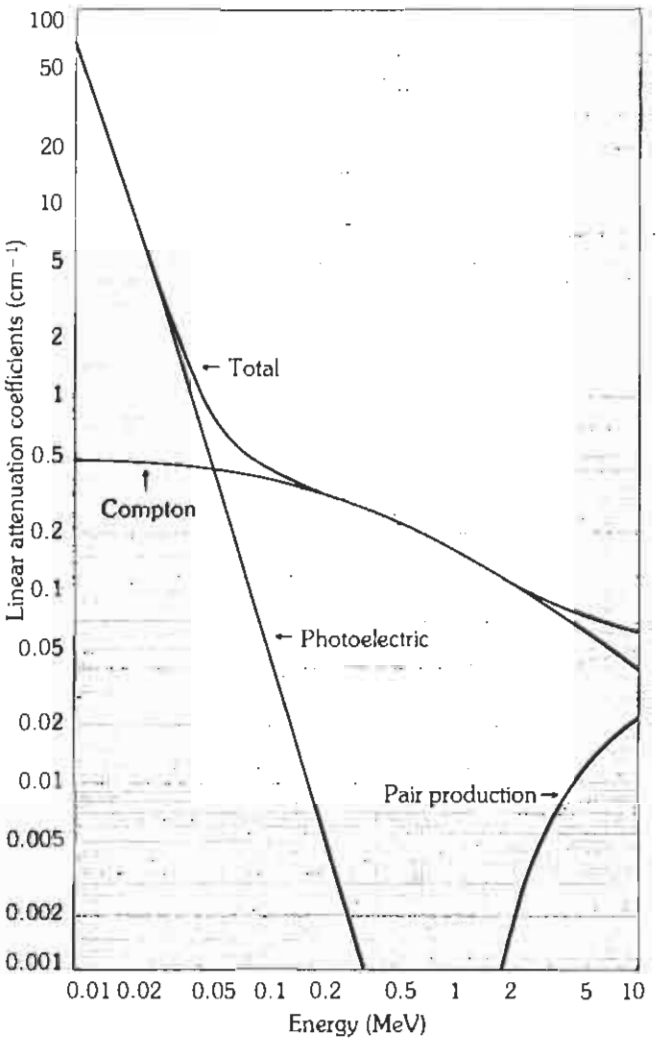

Specific mass = 2700 kg/m³
Atomic number: Z = 13
Electron Binding Energies:
K-edge = 1.56 keV
Average K X-Ray Energy = 1.45 keV

Al_2O_3

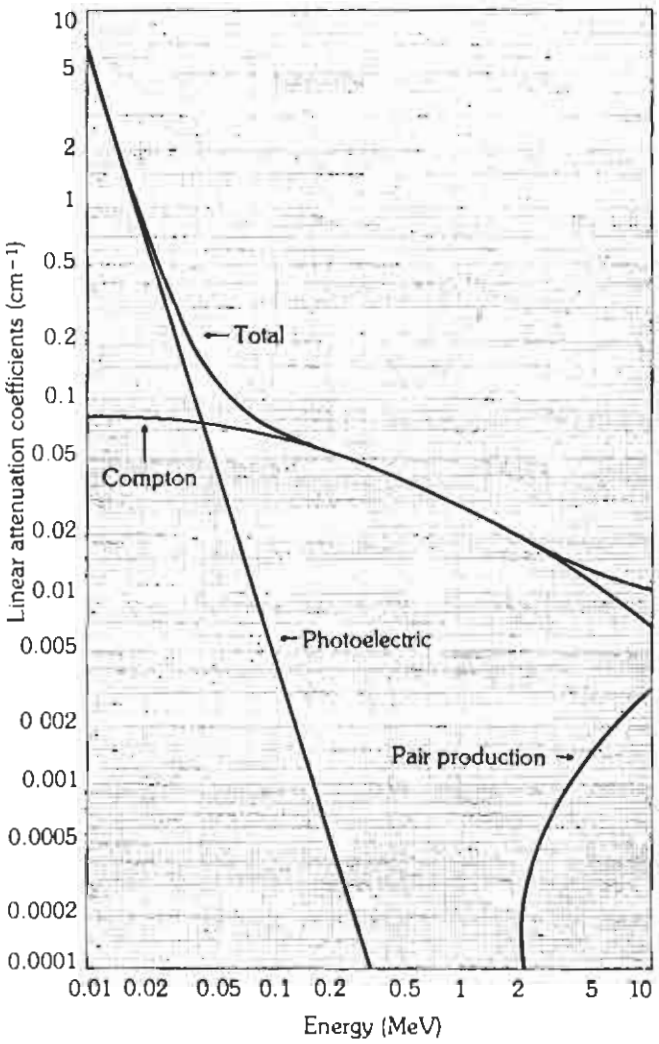

Specific mass
Depends upon packing density, about 450 kg/m³
Atomic number: Z (Al) = 13
Z (O) = 8
K-edge (Al) = 1.56 keV

W

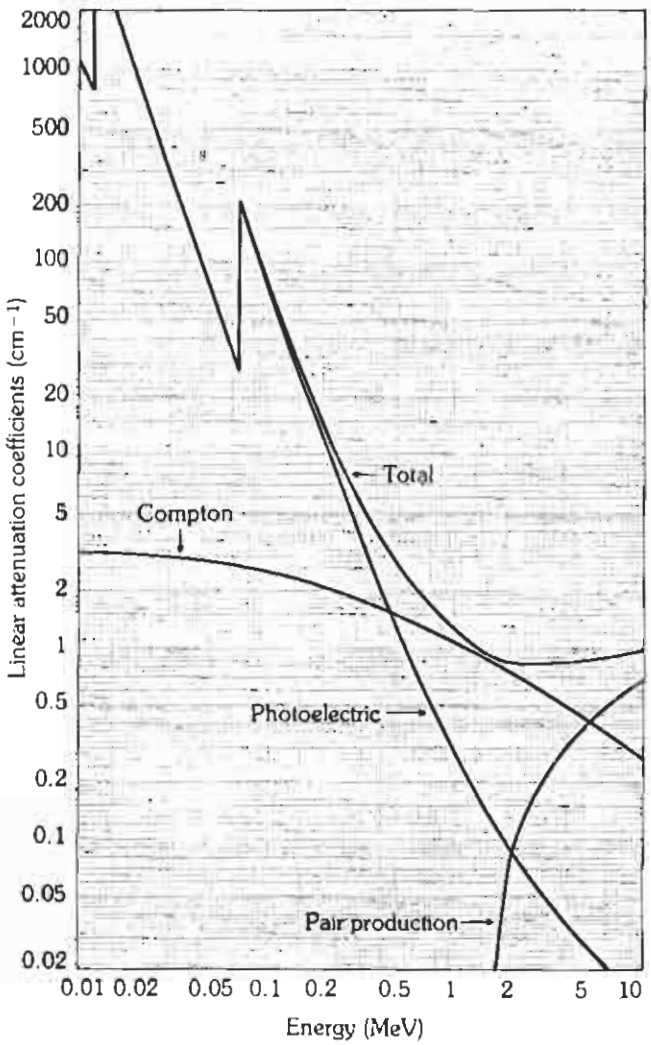

Specific mass = 19350 kg/m³
Atomic number: Z = 74
Electron Binding Energies:
K-edge = 69.53 keV
L_I-edge = 12.10 keV
L_{II}-edge = 11.54 keV
L_{III}-edge = 10.21 keV
Average K X-Ray Energy = 60.7 keV

Pb

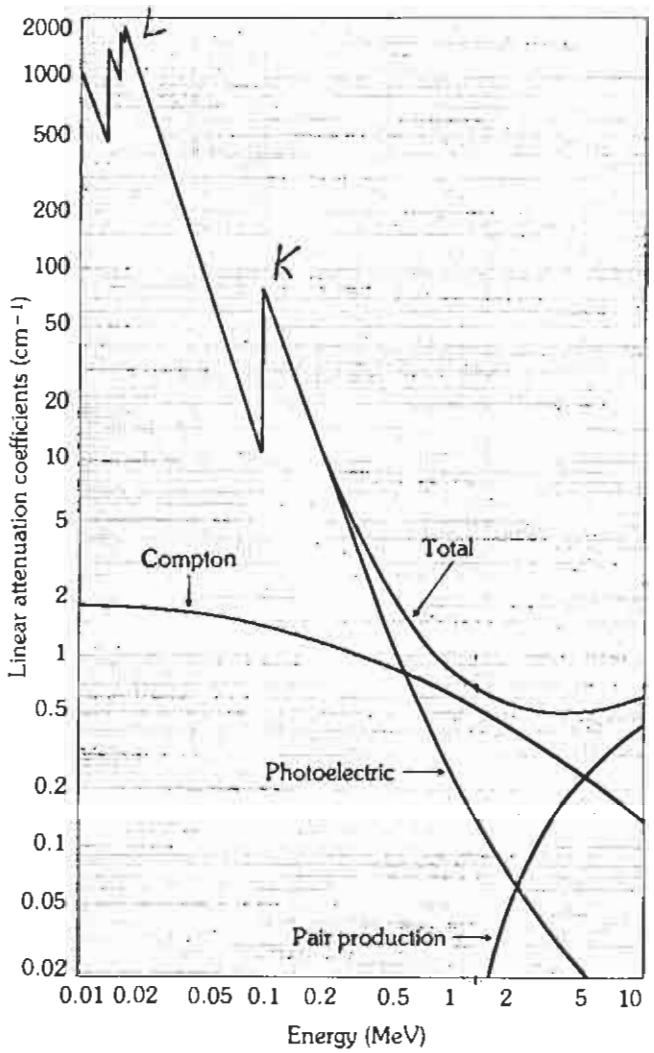

Specific mass = 11350 kg/m³
Atomic number: Z = 82
Electron Binding Energies:
K-edge = 88.02 keV
L_I-edge = 15.87 keV
L_{II}-edge = 15.21 keV
L_{III}-edge = 13.05 keV
Average K X-Ray Energy = 76.74 keV

Cu

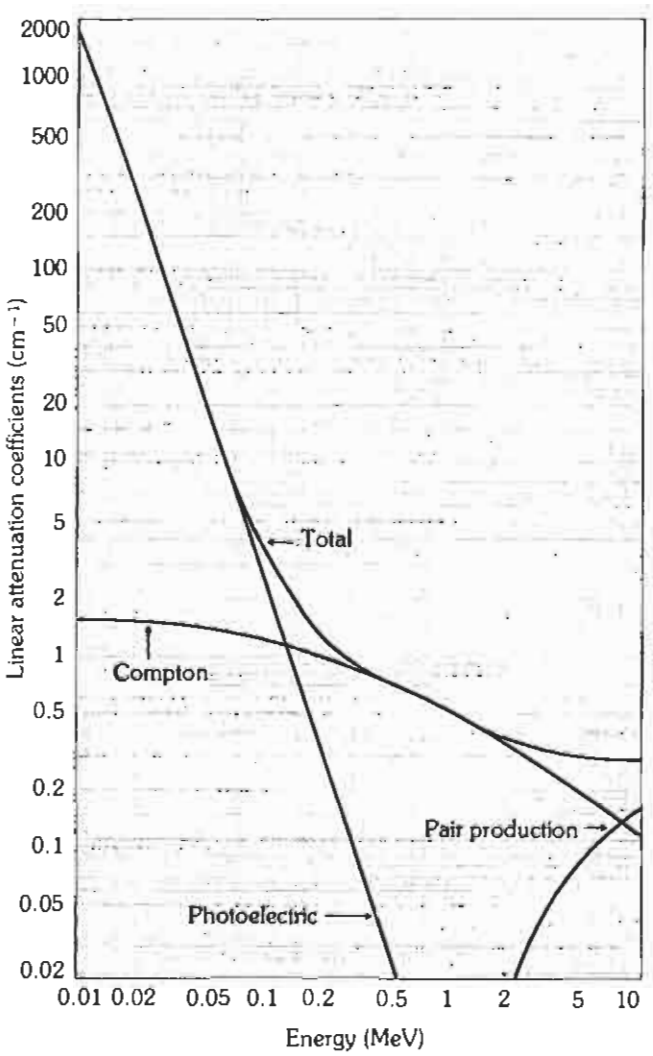

Specific mass = 8920 kg/m³
Atomic number: Z = 29
Electron Binding Energies:
K-edge = 8.98 keV
L_I-edge = 1.10 keV
L_{II}-edge = 0.95 keV
L_{III}-edge = 0.93 keV
Average K X-Ray Energy = 8.11 keV

Fe

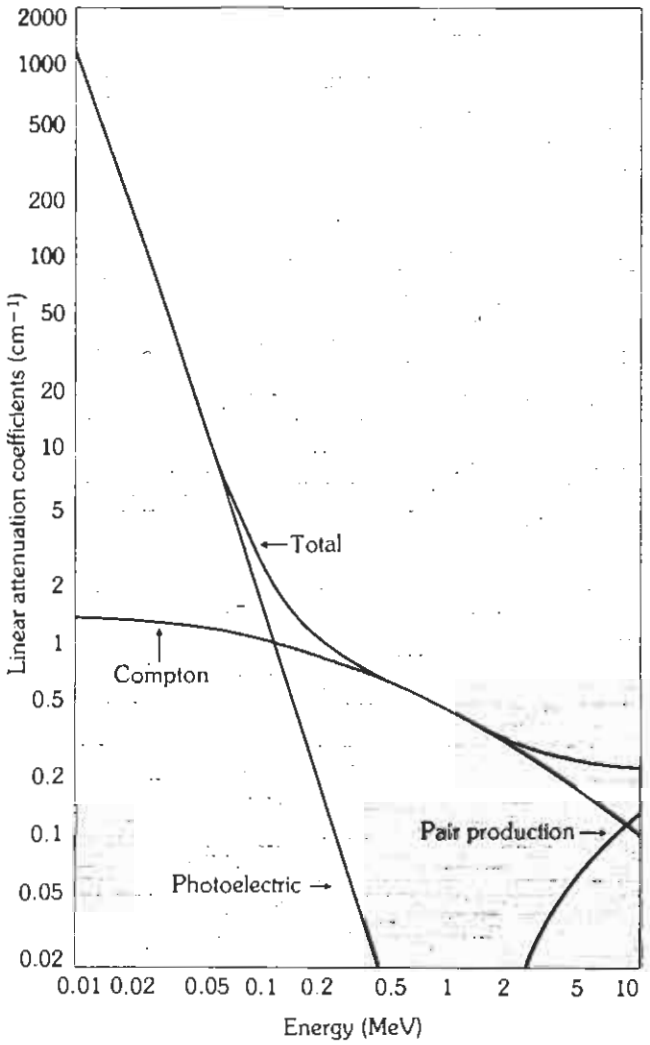

Specific mass = 7860 kg/cm³
Atomic Number: Z = 26
Electron Binding Energies:
K-edge = 7.11 keV
L_I-edge = 0.84 keV
L_{II}-edge = 0.72 keV
L_{III}-edge = 0.71 keV
Average K X-Ray Energy = 6.47 keV

Sn

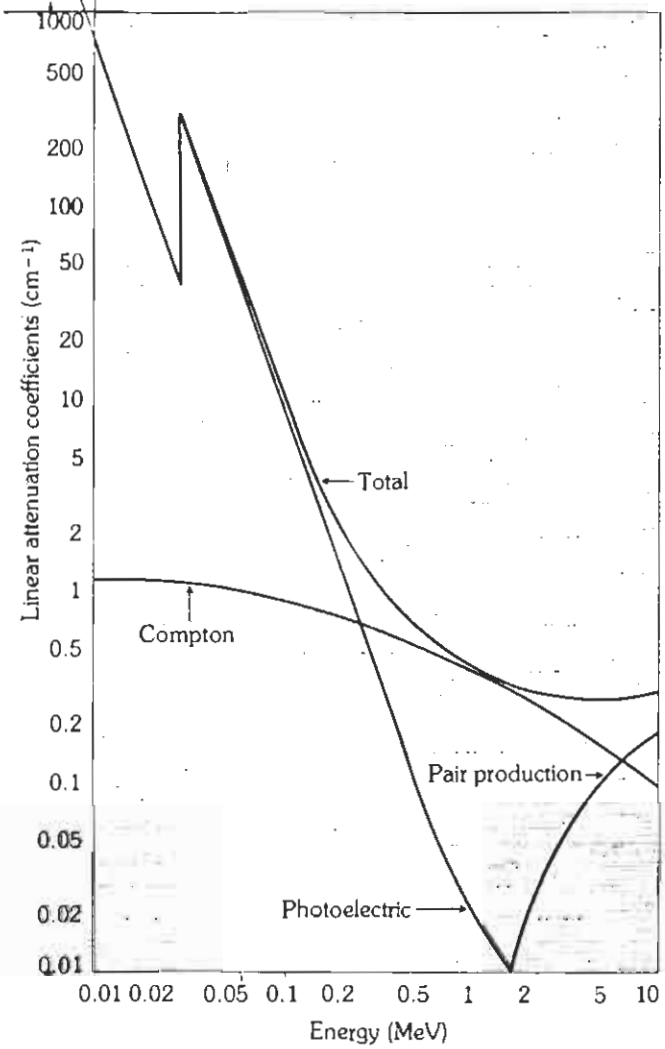

Specific mass = 7280 kg/m³
Atomic number: Z = 50
Electron Binding Energies:
K-edge = 29.20 keV
L_I-edge = 4.47 keV
L_{II}-edge = 4.16 keV
L_{III}-edge = 3.93 keV
Average K X-Ray Energy = 25.8 keV

$\lambda(6\,keV) = 260 \times 10^{-4}\ cm^{-1} = 2.6 \times 10^{-2}\ cm^{-1}$

dopo 5 cm $\quad I \sim e^{-5 \times 2.6 \times 10^{-2}} \sim 0.88$

H_2O

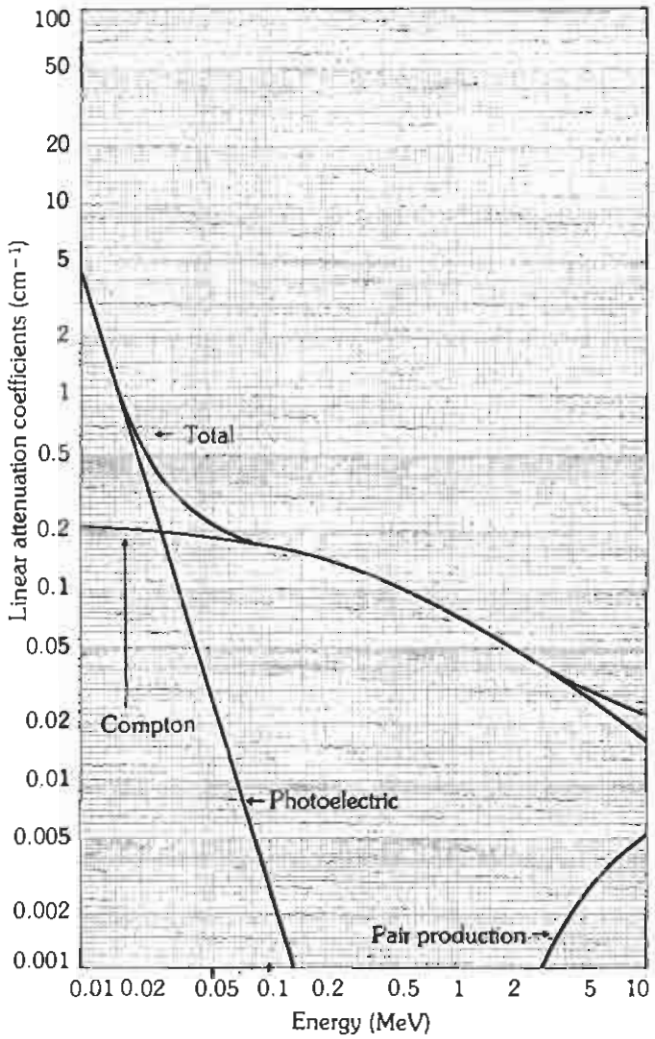

Specific mass = 1000 kg/m³

Air

x 10⁻⁴

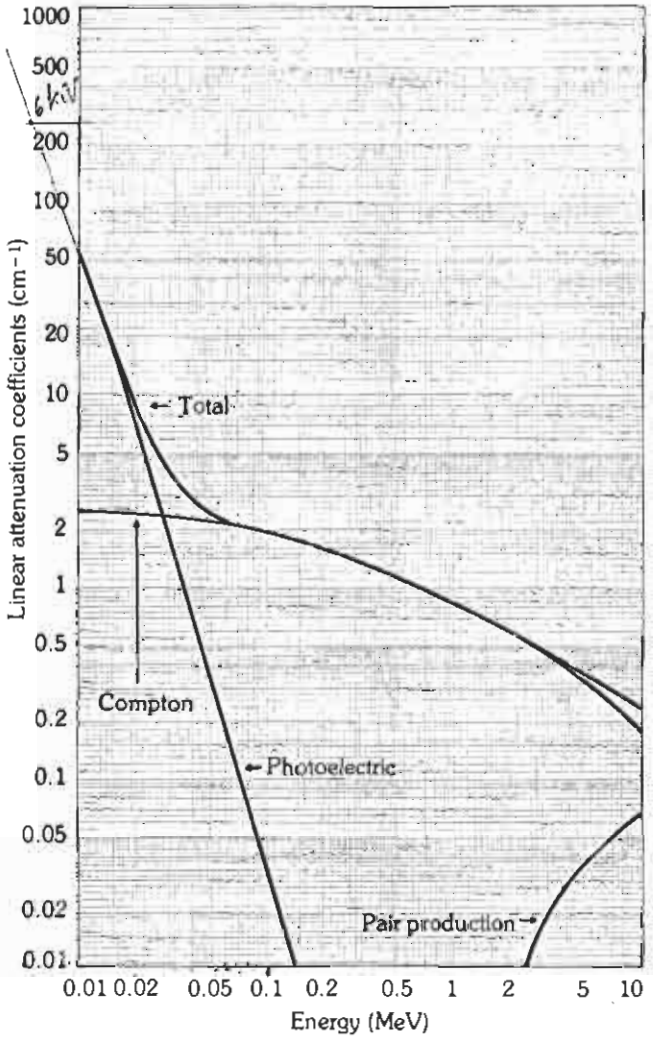

Specific mass = 1.293 kg/m³
Composition of "air"
78.04 volume percent nitrogen
21.02 volume percent oxygen
0.94 volume percent argon

5. Transmission through windows

The choice of the entrance window material and dimensions depends strongly on the gamma ray energy to be detected and on the end use for the detector.

Especially at gamma ray energies below 100 keV the actual detection efficiency depends strongly upon absorption in the detector entrance window. A large variety of window materials are used for Harshaw Nuclear Detectors. Fig. IV.22. gives transmission curves for the window materials most commonly used. From this figure it is clear that for detecting Röntgen or gamma ray energies below 5 keV a Beryllium window can best be used as an entrance window.

6. Radionuclides used for calibration in spectrometry

γ Sources

Nuclide	Gamma ray energy (keV)	Half life (years)
^{55}Fe	5.9	2.69
^{129}I	30	1.7×10^{7}
^{241}Am	60	458
^{57}Co	122	0.74
^{133}Ba	356; 32	10.8
^{22}Na	511; 1275	2.6
^{137}Cs	662	30.17
^{54}Mn	835	0.86
^{65}Zn	1115	0.67
^{60}Co	1333; 1173	5.27
^{228}Th	2614	1.91

β Sources

Nuclide	Maximum beta energy (MeV)	Half life (years)
^{63}Ni	0.066	100
^{14}C	0.156	5730
^{147}Pm	0.225	2.62
^{90}Sr	0.546; 2.274	28.6
^{204}Tl	0.764	3.85

α Sources

Nuclide	Alpha energy (MeV)	Half life (years)
^{233}U	4.8	1.6×10^{5}
^{210}Po	5.3	0.38
^{241}Am	5.5	458

7. SI Units and other units used in radiation detection

Throughout the world the International systems of Units (SI) has been accepted and is commonly used, although historically used units are still handled. Especially in the field of the radioactivity measurements both old and new units are used.

The basic units of the SI

Unit	Name	Symbol
Length	meter	m
Mass	kilogram	kg
Time	second	s
Electrical current	Ampère	A
Temperature	Kelvin	K
Luminous intensity	candela	cd
Amount of substance	mol	mol

Below are some units derived from the SI:

Unit	Name	Symbol	SI units
Energy	Joule	J	kgm^2s^{-2}
Activity of a radioactive source	Becquerel	Bq	s^{-1}
Absorbed dose	Gray	Gy	$J.kg^{-1}$
Dose equivalent	Sievert	Sv	$J.kg^{-1}$

Relation between other units and SI-units

Unit	Name	Symbol	Conversion
Mass	atomic mass	u	$1\ u = 1.66057\ 10^{-27}$ kg
Energy	electron volt	eV	$1\ eV = 1.60219\ 10^{-19}$J
Activity of a radioactive source	Curie	Ci	$1\ Ci = 3.7\ 10^{10}$ Bq
Absorbed dose	rad	rad	$1\ rad = 10^{-2}$ Gy
Equivalent absorbed dose	rem	rem	$1\ rem = 10^{-2}$ Sv
Exposure	Röntgen	R	$1\ R = 2.58\ 10^{-4}\ Ckg^{-1}$
Length	Ångström	Å	$1\ Å = 0.1\ nm = 10^{-10}$ m

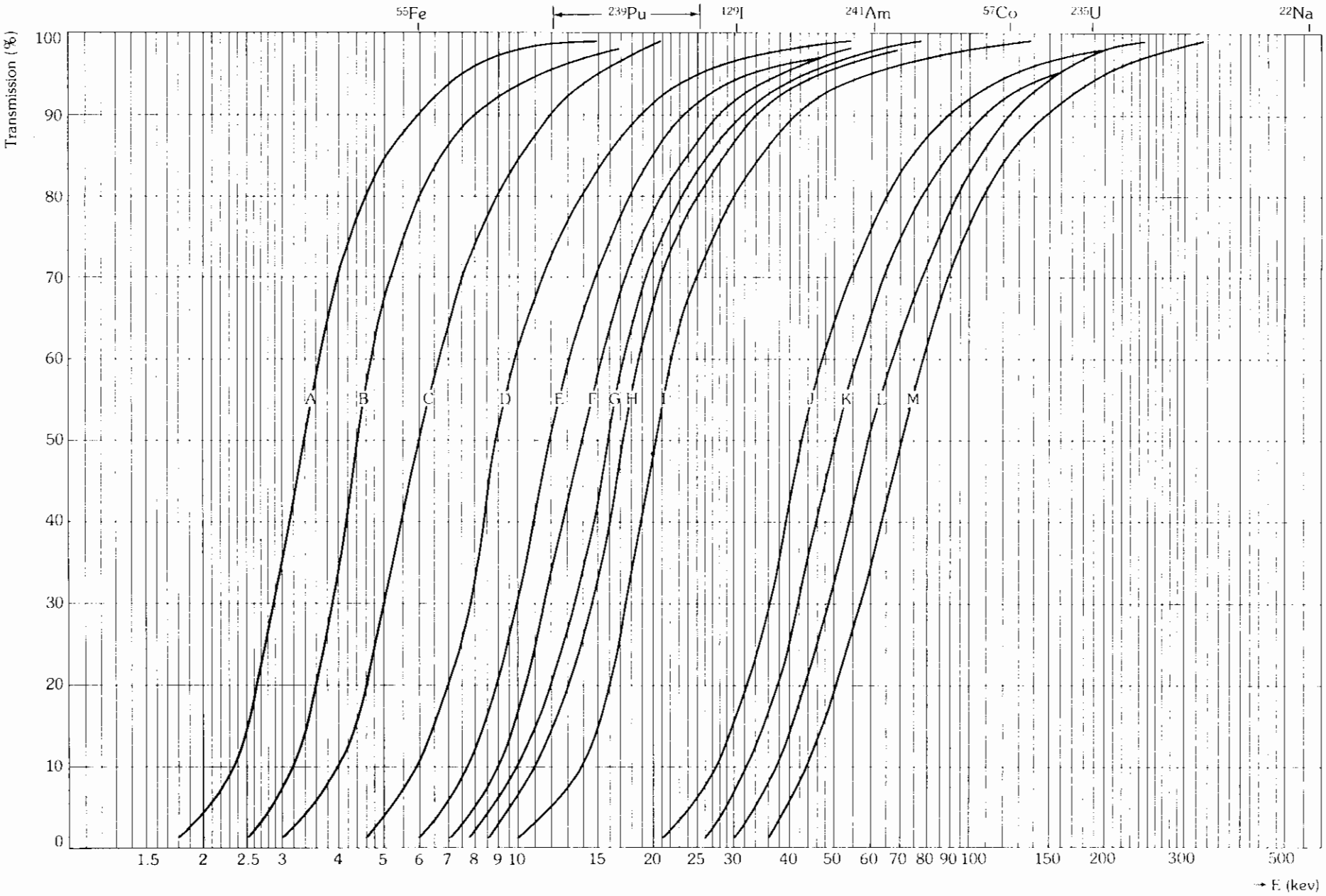

Fig. IV.22. Percent transmission through windows of various materials.

A = 0.2 Be.	C = 0.025 Al.	E = 0.2 Al.	G = 0.4 Al.	I = 0.8 Al.	K = 0.8 Cu.	M = 0.5 S.S.
B = 0.5 Be.	D = 0.1 Al	F = 0.3 Al.	H = 0.5 Al.	J = 0.5 Cu.	L = 0.3 S.S.	

Thikness in mm.

V. SPECIAL APPLICATIONS

Contents:

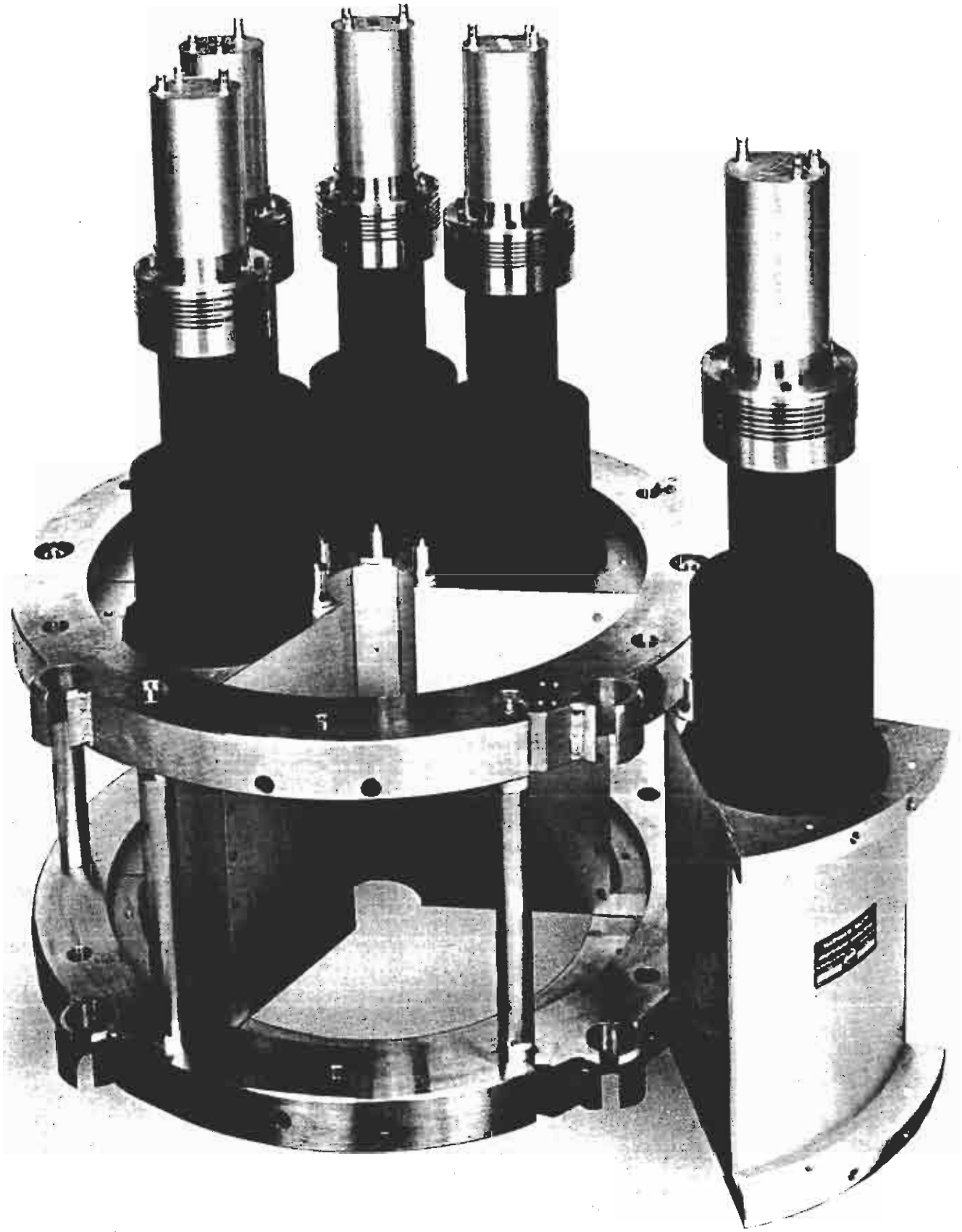

Sum spectrometer.

V. SPECIAL APPLICATIONS

In this section some units are described for special purposes. In most cases the optimum dimensions of these units depend very much on the specific applications. Therefore only a few typical examples are given for each item.
For many years Harshaw/Filtrol specialists advised their customers on the optimum configurations of these special units. This resulted in the development of units that found general application in the Nuclear Research Institutes and in the Health Physics Departments. Compton-suppression systems, low level gamma spectrometers and low energy phoswich systems were very popular.
To avoid the necessity of a large number of separated NIM modules with complicated control settings, Harshaw/Filtrol developed NIM modules for these special units combining the various functions necessary for proper functioning of the detectors as a system.

For performing anti-coincidence timing with large NaI(Tl) shields and central Ge(Li) detectors the **Anti-Compton Analyzer NC-26R** was designed to contain fast timing amplifiers, constant fraction discriminators and coincidence/anti-coincidence units.
The Phoswich system functioning on the different decay times of different scintillation materials makes use of the specially designed **Pulse Shape Discrimination System NC-25A.**
These highly sophisticated electronic modules make it possible to easily obtain the best characteristics of the Compton suppression spectrometer and the Phoswich system.

1. Compton suppression spectrometer

In gamma spectroscopy performed with Ge(Li) detectors the detection of low intensity peaks is often complicated by the presence of Compton scattering of gamma radiation of higher energy.
In the energy range from 200 keV to 5 MeV, the interaction between gamma quanta and a Ge(Li) detector takes place mainly through Compton scattering. Fig. V.1. shows the scattering of a gamma quantum with energy E on an electron of the scattering medium.

The electron with energy T is counted in the Ge(Li) detector and the scattered gamma with energy E' is leaving the Ge(Li) detector. (In fact this process is more complicated through the multiple Compton scattering in the Ge(Li) detector).

This compton scattering process is governed by the formula:

$$E' = \frac{E}{1+\frac{E}{0.511}(1-\cos\Theta)},$$

E and E' in MeV.

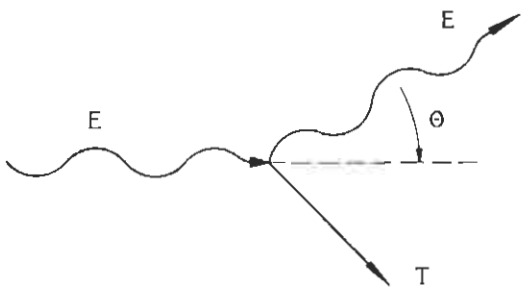

Fig. V.1. Compton scattering process.

The kinetic energy which is transferred to the recoil electron and absorbed in the Ge(Li) detector is given by:

$$T = \frac{E^2(1-\cos\Theta)}{E(1-\cos\Theta)+0.511}.$$

This Compton spectrum extends from 0 keV up to the Compton edge. The Compton edge is caused by backward scattering of the incident gamma quanta. The energy is given by:

$$\text{Compton edge: } \frac{E}{1+0.511/2E}$$

The escape of the Compton scattered gamma ray makes it possible to suppress the detected Compton electron in the Ge(Li) detector by absorbing the scattered gamma in a large NaI(Tl) or CsI(Tl) crystal and observing a coincidence signal in the central Ge(Li) detector and the surrounding guard detector. Proper gating of the multi-channel analyzer makes it possible to suppress the Compton continuum to a large extent.

In a separate Harshaw/Filtrol report called "Low Level Counting Compton Suppression", various characteristics of the Compton process are shown. One of these is that above 200 keV the scattering occurs predominantly in the forward direction. The best suppression therefore is achieved with asymmetric position of the Ge(Li) detector.

Fig. V.2. is an illustration of such an asymmetrical external source Compton suppression spectrometer.
Harshaw/Filtrol now offers several Compton suppression spectrometer designs using BGO instead of NaI or CsI. These are illustrated in the figure below. Hardware design is simplified because BGO is nonhygroscopic and the overall detector size is reduced because of BGO high Z and resultant enhanced stopping power.

2. Low level system

The detection of samples containing only traces of radioactive materials is often troublesome through the presence of background radiation from walls, other surroundings and cosmic quanta.
In a Ge(Li) detector this ambient radiation can cause a substantial background level. The use of a good lead shielding is of course essential in this case.

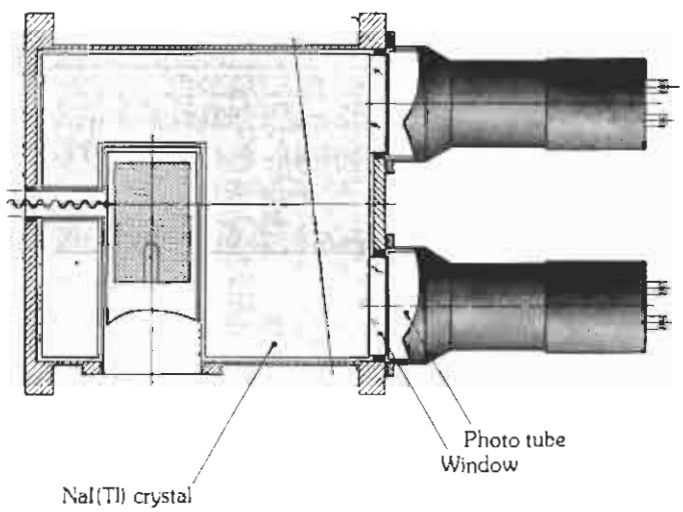

Fig. V.2. Asymmetric Compton suppression spectrometer.

For a further reduction of background, active shielding, i.e. a shield of scintillation material used as a reto detector, can be used. A NaI(Tl) shield surrounding the Ge(Li) central detector will diminish the background radiation to a large extent.
Figure V.3. gives an illustration of the effect of passive lead shielding together with active shielding with a 30 x 30 cm NaI(Tl) detector on the background spectrum of a Ge(Li) detector.

The selection of low background materials makes it possible to achieve very low detection limits.

Fig. V.4. gives an example of a low level system consisting of a central Ge(Li) detector, guard NaI(Tl) shield and NaI(Tl) plug crystal.

The configuration in fig. V.4. with a sample inside the NaI(Tl) shield can be used with sources emitting no coincident gamma radiation. In this case normal anti-coincidence techniques can be used to obtain background and Compton suppressed Ge(Li) spectra. If the source emits coincident gamma radiation this can be used to obtain even lower background radiation (as shown in fig. V.3., d) by setting an energy window on a NaI(Tl) gamma line and observing the Ge(Li) spectrum coincident with this line. A special application of this coincidence spectrometer is "Pair Spectrometry".

3. Pair Spectrometer

When samples emit gamma rays with energies large enough for pair production (see fig. IV.1.) it is possible to use this pair production effect in obtaining the ultimate in suppression of the disturbing Compton effect as well as the undesired background radiation.

By means of the pair production effect the gamma energy E is transferred into kinetic energy for the simultaneously created positron-electron pair. Apart from this kinetic energy the rest energy of the created particles (1.022 MeV) must be realized. This rest energy is again emitted in the form of two annihilation quanta when the positron interacts with an electron, which results in the complete

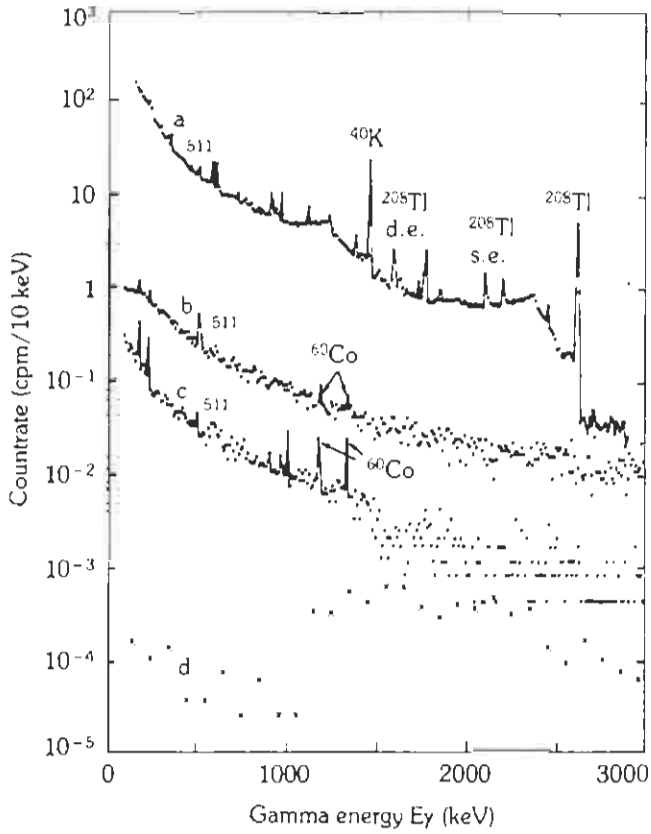

Fig. V.3. Background spectra of a Ge(Li) detector

a Without shielding.
b With shielding, 10 cm lead, 2 cm iron, 1 cm copper
c With Anti coincidence, 30 x 30 cm NaI(Tl) guard detector.
d Coincident with 1.02 MeV of NaI(Tl) detector

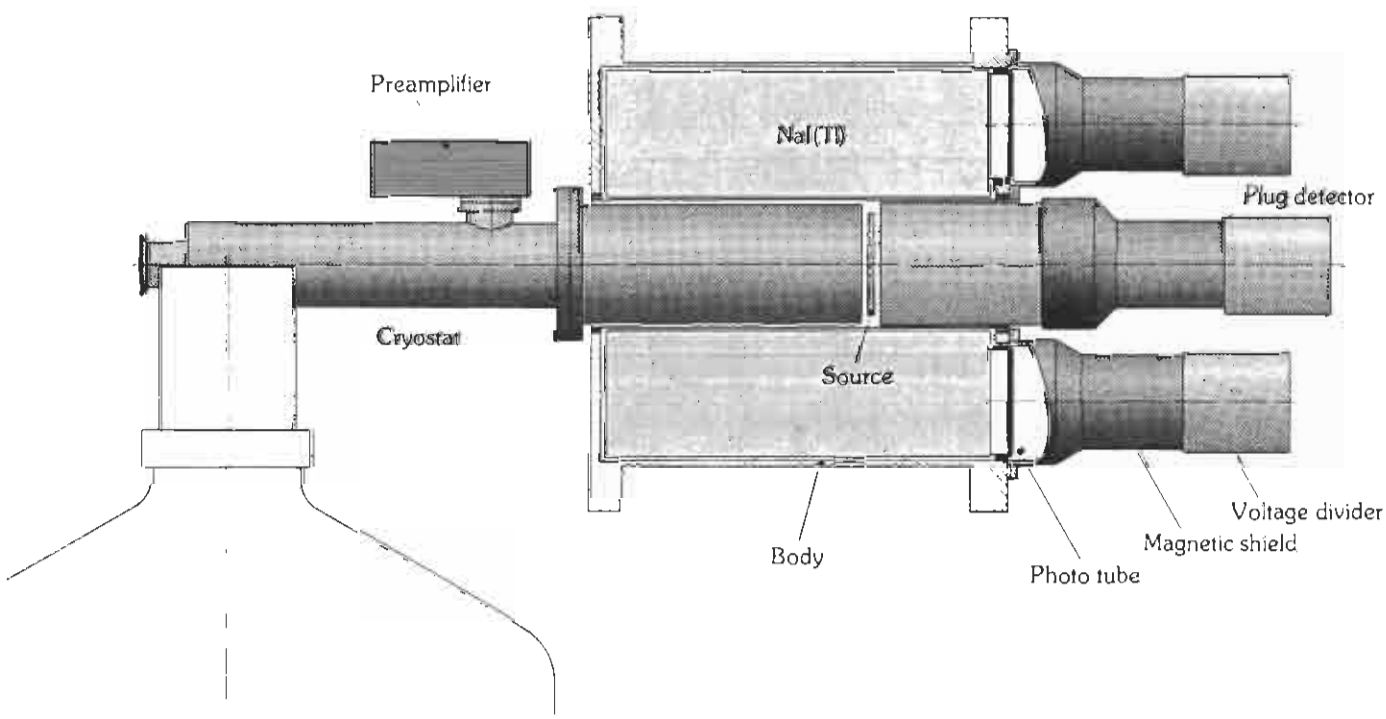

Fig. V.4. Low level system.

annihilation of both particles. The two 511 keV quanta are diametrically emitted. This interaction permits the detection of pair events by means of a coincidence requirement between the positron-electron pair created in a center crystal and the annihilation quanta absorbed in an annular crystal arrangement.

Such a center crystal can be a high efficiency NaI(Tl) crystal or a Ge(Li) detector with very good energy resolution.
Obviously it will be comparatively easy to use a pair spectrometer as an Anti-Compton spectrometer by simply connecting the annulus in anti-coincidence with the center crystal. Normally, however, it is recommended to use a bigger center crystal for this application.

Positron emitters
A large number artificially produced radio-active samples emit gamma rays in coincidence with positron particles (β^+ decay). In such a case the positron can annihilate into two 511 keV gammas. Again these gammas can be detected in a crystal surrounding a central detector and if a coincidence requirement is met between the 511 keV gammas and the events detected in the central detector, the gammas emitted after β^+ decay can be detected with a very low background.

4. Sum spectrometers / multiplicity filter

Information about high angular momentum nuclear states can be obtained through the study of gamma radiation following heavy-ion compound-nucleus reactions. Since the evaporation residues are produced in a wide range of angular momenta and reaction channels high selectivity is required to exacerbate the transitions from the high spin domain.
An approach to select the high spin region is to use a detector with close to 4 π geometry to observe the total energy dissipated in the gamma cascade.

At high spin the excitation energy of the evaporation residues is mainly rotational energy. In this situation high total gamma decay energy corresponds to high total angular momentum.
Presently large segmented crystal balls are in use for this application. The number of segments varies from small (e.g. 6) to very large (over 150). Many of these units are made out of NaI(Tl) scintillation crystals. BGO offers some advantages over NaI(Tl) for this type of detectors. These advantages are due to its nonhygroscopic nature and good photopeak efficiency at high energies. These benefits combine to form a compact, high resolution 4 π spectrometer well suited for most high energy physics experiments.

5. Phoswich detection system

High efficiency detection of low level radiation in the presence of an ambient background required special design technique. A unique method of pulse shape analysis stressing good performance and simple operation is available using phoswich detectors developed by Harshaw/Filtrol.

The Phoswich detector is composed of a thin front NaI(Tl) section optically coupled to a larger section of a different scintillation material (usually CsI(Tl) or CsI(Na)). The entire detector package is optically coupled to a photomultiplier tube whose output is composed of signals originating within either one or both of the scintillators.

Operating principle
The two scintillation crystals viewed by the photomultiplier tube operate as an efficient low background detector for the radiation of

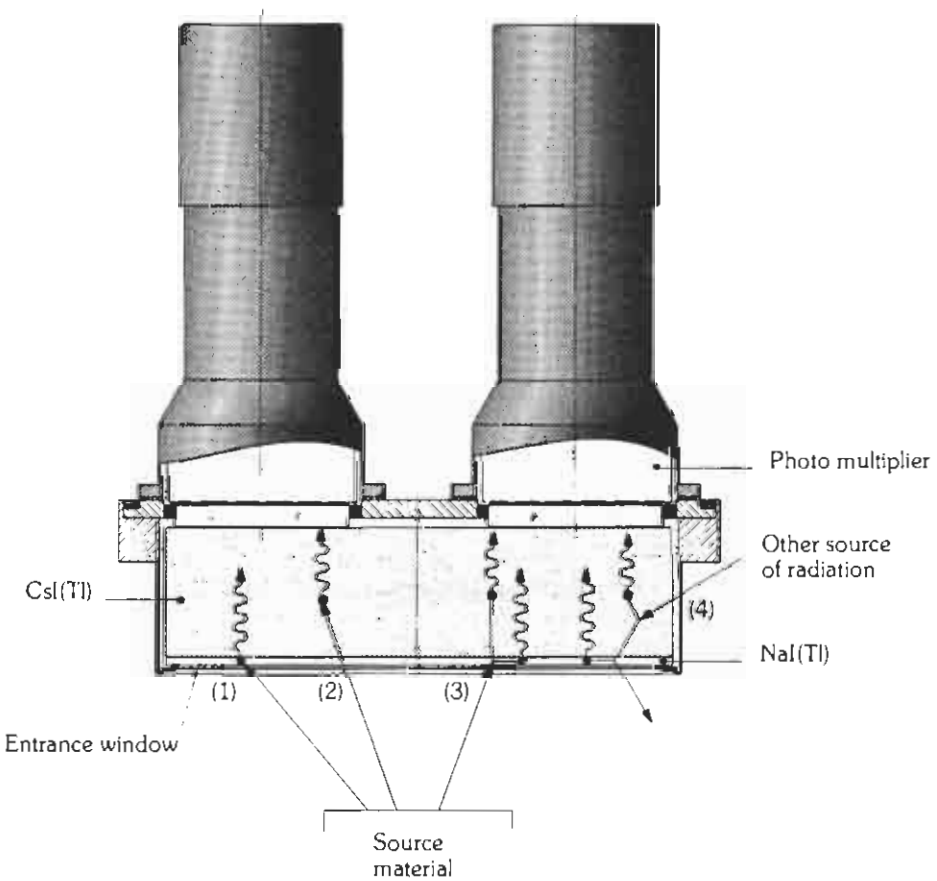

Fig. V.5. Typical interaction in Phoswich detectors.

interest. The larger section acts as an anti-coincidence shield while the thin section transmits the unwanted high energy radiation, but has sufficient thickness to be essentially 100% efficient (refer to Fig. V-5 (event 1)) for the radiation of interest. With this configuration, any high energy radiation will either pass through without interaction as illustrated in figure V-5 (as event 2) or a Compton scattering (event 3) will occur in the thin section. If the Compton scattering event occurs, the larger CsI(Tl) or CsI(Na) scintillator absorbs the scattered photon and supplies an anti-coincidence signal to allow electronic rejection of the event.
Radiation entering from the rear or sides of the detector (event 4) will be viewed by the anti-coincidence scintillator. If it should undergo Compton scattering into the thin detector, the event will still be recognized as spurious.

Electronics
To ensure optimum performance in the system, the associated electronics must be able to separate the different signals arising from the two scintillation crystals. Separation is determined by the phosphor decay time of each material. Various techniques are employed to separate these times. With "pure" signals (those originating in one or the other of the two crystals but NOT in both simultaneously) separation is relatively simple. However, a significant proportion of the events that should be rejected are composed of mixed signals originating from both crystals. Accordingly, the electronics must be capable of rejecting an event even if just a small fraction of the energy is scattered into the anti-coincidence crystal. At the same time, the electronics must accept events of the desired energy that originate from total absorption in the primary NaI(Tl) crystals.
The specially designed NC-25A is a highly sophisticated module capable of separating pulses originating from the two crystals at the same time. In this way the large secondary crystal can be used to measure the high energy spectrum while the low energy spectrum is collected from the thin primary detector. An application note describing the principles of this module is available.
The phoswich principle may be expanded to facilitate the detection of alpha and beta particles in the presence of a gamma ray background by utilizing a CaF_2 (Eu) scintillator coupled to a larger NaI(Tl) anti-coincidence crystal. An application note on this system is also available.

Applications
A possible application of the Phoswich principle is low level alpha-beta-gamma counting with an extreme thin CaF_2 (Eu) primary detector.
Counting efficiency for these detectors is determined essentially by the geometry, since radiation entrance windows are not required (CaF_2 (Eu) is not hygroscopic). Another application is in low level plutonium, americium and uranium detection.

A 20 cm diameter Phoswich detector with 3 mm NaI(Tl) primary detector and 5 cm CsI(Tl) secondary detector is capable of measuring background count rates of only some counts per minute in the plutonium X-ray region (12-25 keV), which makes such a unit a very sensitive tool for detection of small plutonium contaminations.

5. Whole Body Counting

In this text whole body counting refers to surveying people with gamma detectors in order to trace radioactive isotopes incorporated in their bodies. This technique has mainly two applications, one is to monitor radioactive contamination of people and the other deals with diagnostic tracerwork. It is obvious that the sensitivity of this technique mainly depends on the signal to noise ratio of the detector installation.

Therefore, high absolute gamma detection efficiency, low background radiation and good energy resolution of the detector are required to achieve reliable results.

Four different geometries are commonly used in whole body counting:

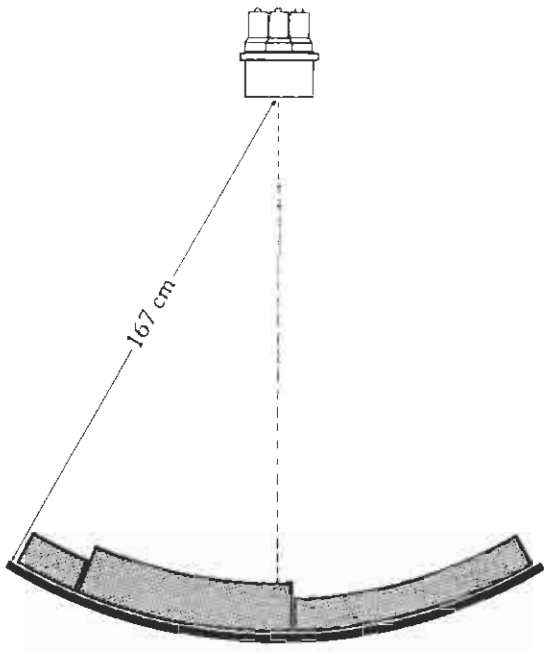

Fig. V.6a. The arc geometry.

The advantage of having approximately equal distances between different source regions and the detector, and therefore uniform geometrical response, is partly offset by the low detection efficiency of this arrangement.

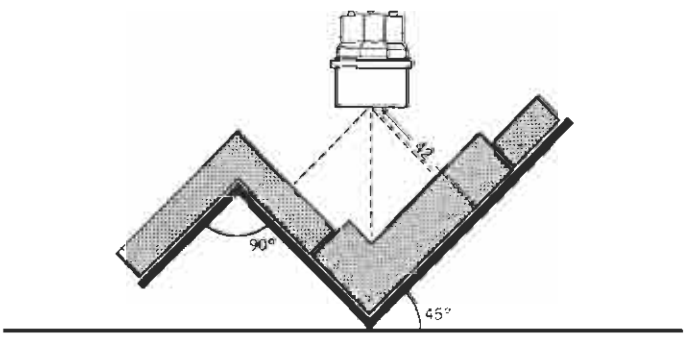

Fig. V.6b. The chair geometry.

In this arrangement the subjects are much closer to the detector. This results in higher absolute counting efficiencies. This advantage, however, must be paid for with non uniform geometrical response.

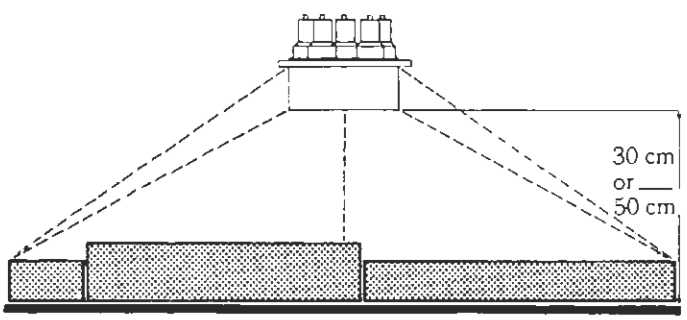

Fig. V.6c. Single detector stretcher geometry.

One detector is fixed in a position above the stretcher at distances between 30 and 70 cm. Increasing the detector distance reduces the detection efficiency but improves the uniformity of the geometrical response.

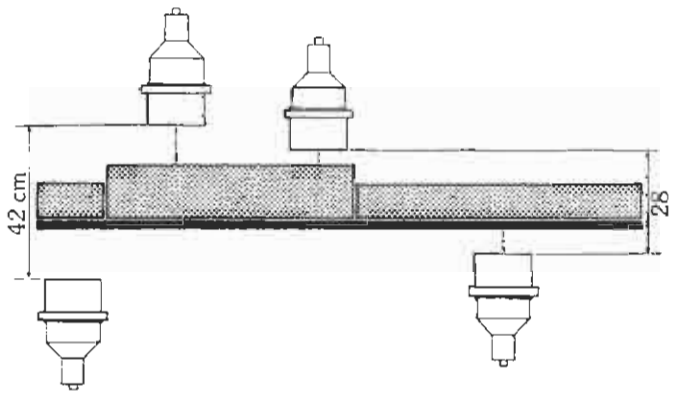

Fig. V.6d. Multi detector stretcher geometry.

Two detectors are mounted above and two below a stretcher at positions as indicated in fig. V.6d.
Uniformity of geometrical response is considerably improved in this arrangement.

A good compromise between high detection efficiency and uniform geometrical response is to scan the object by moving one or more detectors relative to the body with fixed or variable speed.
Calibration measurements and calculation models must be applied to analyze the results obtained by this scanning method.

To compare the merits of different crystal sizes calculations were made for photo peak detection efficiencies for the shown whole body counter geometries.
In fig. V.7. the results are plotted versus the incident gamma energy. Uniform isotope distribution in a "standard Phantom" was assumed.
Absorption and scattering effects of the gamma quanta in the phantom were disregarded. The NaI(Tl)-crystals were not shielded.

Fig. V.8. shows the ratio of counting time versus gamma energy for different NaI(Tl)-crystal sizes and counting geometries:

$$\frac{t_x}{t_r} = \left(\frac{P_x}{P_r}\right)^2 \frac{B_x}{B_r}$$

P and B refer to peak and background counting rates per unit energy in the same energy interval, respectively. The different detector units (x) were compared with the 38 × 15 cm reference unit (r) by taking the counting times t_x and t_r, which are necessary to obtain the same statistical counting errors for the rates P_x and P_r.
The four 15 × 10 cm crystals are compared with the 38 × 15 cm unit at 30 cm distance (stretcher). It is interesting to note that for high gamma energies the 38 × 15 cm unit requires a counting time which is an order of magnitude smaller than that for the 20 × 10 cm unit.

Of increasing interest in whole body counting is the use of a large number of 4" × 4" × 16" Polyscin NaI(Tl) bars. E.g. 16 to 20 detectors, both above and underneath the stretcher, increase the geometric response and the efficiency to an extremely high level.

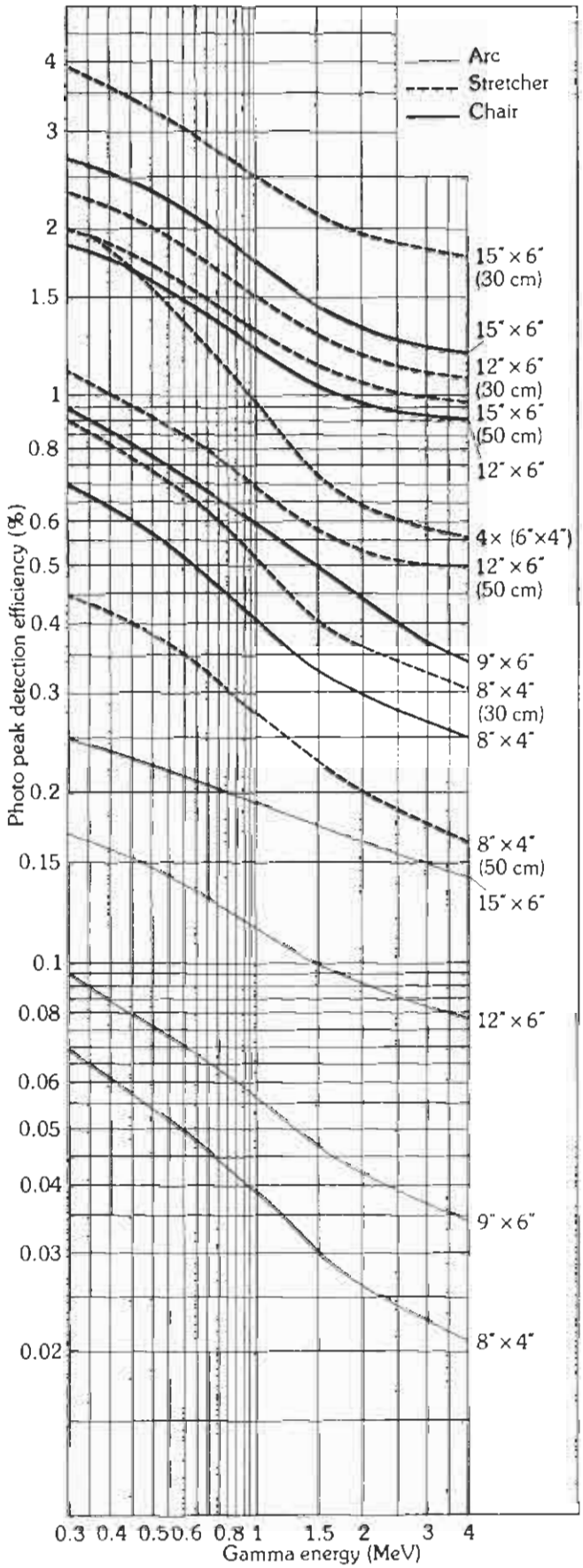

Fig. V.7. Photo peak detection efficiency for different crystal sizes and various body counter geometries.

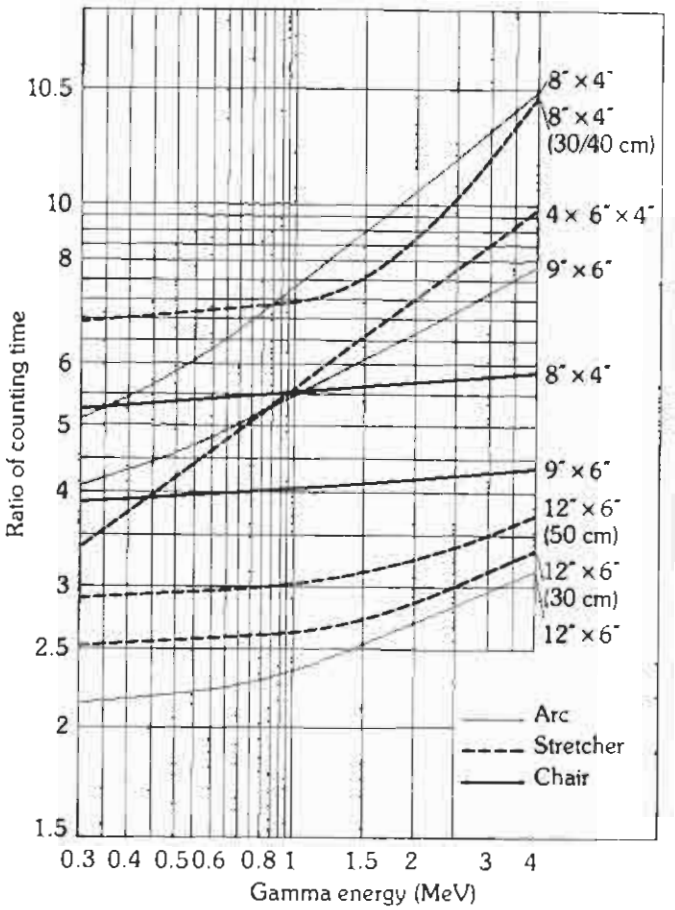

Fig. V.8. Comparison of different detectors with the 15" × 6" reference unit.

Computed Tomography (CT, PET)

Computed Tomography (CT) has provided a great improvement in X-ray diagnostics. Advances in CT technology have come through advances in computer technology and X-ray detectors.
The spatial resolution for some of these imaging devices is obtained by using many small scintillation detector devices.
In the types of machines available, several different crystal materials are in use: NaI(Tl), CaF_2(Eu), BGO, $CdWO_4$ and CsI(Tl).

Positron Emission Tomography (PET) is an imaging modality which employs the detection of positron emitting isotopes to image well defined areas or "slices" of the body. Detectors for this application should have good photopeak efficiency at 511 keV and should exhibit fast coincident resolving time. BaF_2 and CsF are both well suited for this application, because of their fast timing properties.